DISRUPTIONS IN NEUROMUSCULAR TRANSMISSION AND COLONIC MOTILITY IN DIET-INDUCED OBESITY

By

Yogesh Bhattarai

A DISSERTATION

Submitted to
Michigan State University
in partial fulfillment of the requirements
for the degree of

Neuroscience – Doctor of Philosophy

2015

ABSTRACT

DISRUPTIONS IN NEUROMUSCULAR TRANSMISSION AND COLONIC MOTILITY IN DIET-INDUCED OBESITY

By

Yogesh Bhattarai

Diet-induced obesity (DIO) is primarily driven by the consumption of a high fat (HF) diet and is recognized as a major risk factor for the development of gastrointestinal (GI) motility complications, especially in the colon. Colonic motility is regulated by the division of the autonomic nervous system called the enteric nervous system (ENS). Despite high incidences of GI motility disorders in HF DIO, the role of enteric nervous system (ENS) in the development of these complications is unclear. The ultimate goal of this translational project was to understand how the consumption of a HF diet leads to impaired colon motility through effects on the cells controlling neuromuscular transmission.

The etiology of obesity–induced colon motility disorders is multi-factorial and includes alterations to multiple cell types including enteric nerves and the GI smooth muscles. These cells communicate to control contraction and relaxation of smooth muscle via series of coordinated inhibitory and excitatory signaling mechanisms. Disturbances in these signaling mechanisms contribute to colon motility disorders. Therefore, it is crucial to identify in detail how neuromuscular transmission and smooth muscle excitability are regulated before the pathogenesis of HF diet associated colonic dysmotility can be studied.

In the first part of this dissertation I studied the etiology of inhibitory neuromuscular transmission and smooth muscle excitability in the mouse distal colon. I found that inhibitory neuromuscular transmission is primarily mediated by ATP acting on P2Y1 receptors and nitric oxide (NO) diffusion on to the GI smooth muscle. These neurotransmitters act on the small

conductance Ca^{2+}-activated K^+ (SK) channels and the Ca^{2+}-activated Cl^- (CaCCs) channels to produce IJPs in the mouse distal colon. In addition, I discovered that the large conductance Ca^{2+}-activated K^+ channels (β1BK channel) play a crucial role in regulation smooth muscle excitability by controlling smooth muscle action potential firing activity in the mouse distal colon. Next, I sought to determine how HF diet alters neuromuscular signaling and smooth muscle cell physiology. My results show that HF diet specifically disrupts NO mediated inhibitory neuromuscular transmission, SM relaxation and excitability leading to impaired colonic propulsive motility. Genetic KO of β1BK channel closely recapitulates HF diet induced impairments in the mouse distal colon. This suggests that compromised BK channel β1-subunit function/expression might play a role in mediating colonic dysmotility in obesity.

ACKNOWLEDGMENTS

I would like to express my sincere appreciation and gratitude to my advisor Dr. James Galligan for all the support and encouragement that he has provided over the years. He has been a phenomenal mentor who has stimulated with in me a sense of excitement for research, and provided critical insights and feedback when necessary. I would also to thank Dr. Brian Gulbransen and Dr. Mark Kadrofske for allowing me complete a significant portion of my dissertation work in their labs. I am sincerely grateful to Dr. Greg Swain for providing his guidance and support through out my PhD training. This dissertation would not have been possible without the constant supervision, guidance and constructive criticism of my committee members. It has been a real honor to work with all of them.

I owe my sincere gratitude to Dr. Hui Xu, Roxanne Fernandes, and Beth Lockwood for teaching me new techniques and helping me with non-technical aspects of the research. I would also like to thank my lab members and friends Marion France, Nadine El-Ayache, Eileen Rodriguez-Tapia, Ryan Mui, David Fried, Prafulla Regmi and Ujjwal karki who made my stay in MSU all the more fun and an enjoyable experience. I am indebted to the Neuroscience Program at MSU for providing me with funding and all other logistics to help me complete my graduate education.

I cannot thank my family enough for all their scarifies. They are inseparable part of my life and the greatest source of my inspiration. I would therefore like to dedicate this dissertation to my family members Manish Bhattarai (brother), Prerana Bastola (sister-in-law); Madhav Bhattarai (dad), and Pushpa Bhattarai (mom) for standing besides me and dealing with my absence for all these years.

TABLE OF CONTENTS

LIST OF TABLES

LIST OF FIGURES

KEY TO ABBREVIATIONS

ACh	Acetylcholine
ADP	Adenosine diphsphate
ADP-β-S	Adenosine 5′-[β-thio]diphosphate trilithium salt
AMP	Adenosine monophosphate
Ano1	Anoctamin-1
ANS	Autonomic nervous system
ATP	Adenosine triphosphate
β1BK	Large conductance Ca^{2+}-activated K^{+} channels
CaCC	Ca^{2+}-activated Cl^{-} channels
CaCM	Ca^{2+}-calmodulin complex
CMMC	Colonic migrating motor complex
CNS	Central nervous system
DAF-FM-DA	Diaminofluorophore 4-amino-5-methylamino-2′-7′-difluorofluorescein diacetate
DIO	Diet-induced obesity
DMSO	Dimethyl sulfoxide
EFS	Electrical field stimulation
ENS	Enteric nervous system
fIJP	Fast inhibitory junction potential
GI	Gastrointestinal
GSH	Reduced glutathione
GSSG	Glutathione disulphide

5-HT	5-Hydroxytryptamine
HF	High fat
H_2O_2	Hydrogen peroxide
IJP	Inhibitory junction potential
ICC	Interstitial cells of Cajal
IK	Intermediate conductance Ca^{2+}-activated K^+ channels
IPANS	Intrinsic primary afferent neurons
KO	Knock out
L-NNA	Nitro-L-arginine
LMMP	Longitudinal muscle myenteric plexus
MLCK	Myosin light chain kinase
MRS2179	2′-deoxy-N6-methyladenosine 3′, 5′-bisphosphate tetrasodium salt
NANC	Non-adrenergic, non-cholinergic
NEM	N-ethylmaleamide;
NO	Nitric oxide
nNOS	Neuronal nitric oxide synthase
NFA	Niflumic acid
NTPDase	Ecto-nucleotidases
β-NAD	β–nicotinamide adenine dinucleotide
NMT	Neuromuscular transmission
O_2^-	Superoxide anion
$ONOO^-$	Peroxynitrite
PA	Palmitic acid

PFA	Paraformaldehyde
PKG	Protein kinase g
PNS	Peripheral nervous system
POM-1	Sodium polyoxotungstate 1
PSNS	Parasympathetic nervous system
P2Y1	Purinergic receptor
RMP	Resting Membrane potential
ROS	Reactive oxygen species
SERCA	Smooth endoplasmic reticulum Ca^{2+} ATPase
sIJP	Slow inhibitory junction potential
SK	Small conductance Ca^{2+}-activated K^{+} channels
SMC	Smooth muscle cell
SNP	Sodium nitroprusside
SNS	Sympathetic nervous system
SOD	Superoxide dismutase
TTX	Tetrodotoxin
TEA	Tetra ethyl-ammonia
T2D	Type 2 diabetes
VIP	Vasoactive intestinal peptide
WB	Western blot
WT	Wild type

CHAPTER 1

GENERAL INTRODUCTION

1.1 Overview of the nervous system

The nervous system is a complex network of nerve cells and fibers that communicate electrochemical information back and forth between various regions of the body. The nervous system is divided into the central nervous system (CNS) and the peripheral nervous system (PNS). The CNS consists of the brain and the spinal cord, while the PNS consist of nerves and ganglia that lie outside the CNS. The PNS is further subdivided into the somatic and autonomic nervous systems. The somatic nervous system carries out various voluntary body functions like the movement of limbs and processing of sensory stimuli including hear, touch and sight, while the autonomic nervous system (ANS) maintains involuntary functions like controlling heart rate and digestion. The ANS comprises the enteric nervous system (ENS), the sympathetic nervous system (SNS) and the parasympathetic nervous system (PSNS) (Kandel *et al.*, 2000) The ENS is an autonomous entity, which regulates the gastrointestinal (GI) function (Furness, 2006). The SNS and the PSNS on the other hand have a modulatory role and are distributed mostly to internal organs (heart, lungs, and intestine), secretory glands (lachrymal, salivary gland sweat gland) and blood vessels. The SNS arises from the thoraco-lumbar region of the spinal cord and prepares the body for the "fight and flight" response by increasing blood supply to the skeletal muscles, increasing the heart rate, inhibiting GI functions and dilating the pupils. The PSNS arises from the cranio-sacral region of the spinal cord and prepares the body for "rest and digest" response by slowing heart rate, constricting pupils and promoting digestion (Kandel *et al.*, 2000).

Figure 1.1 Organization of the nervous system.

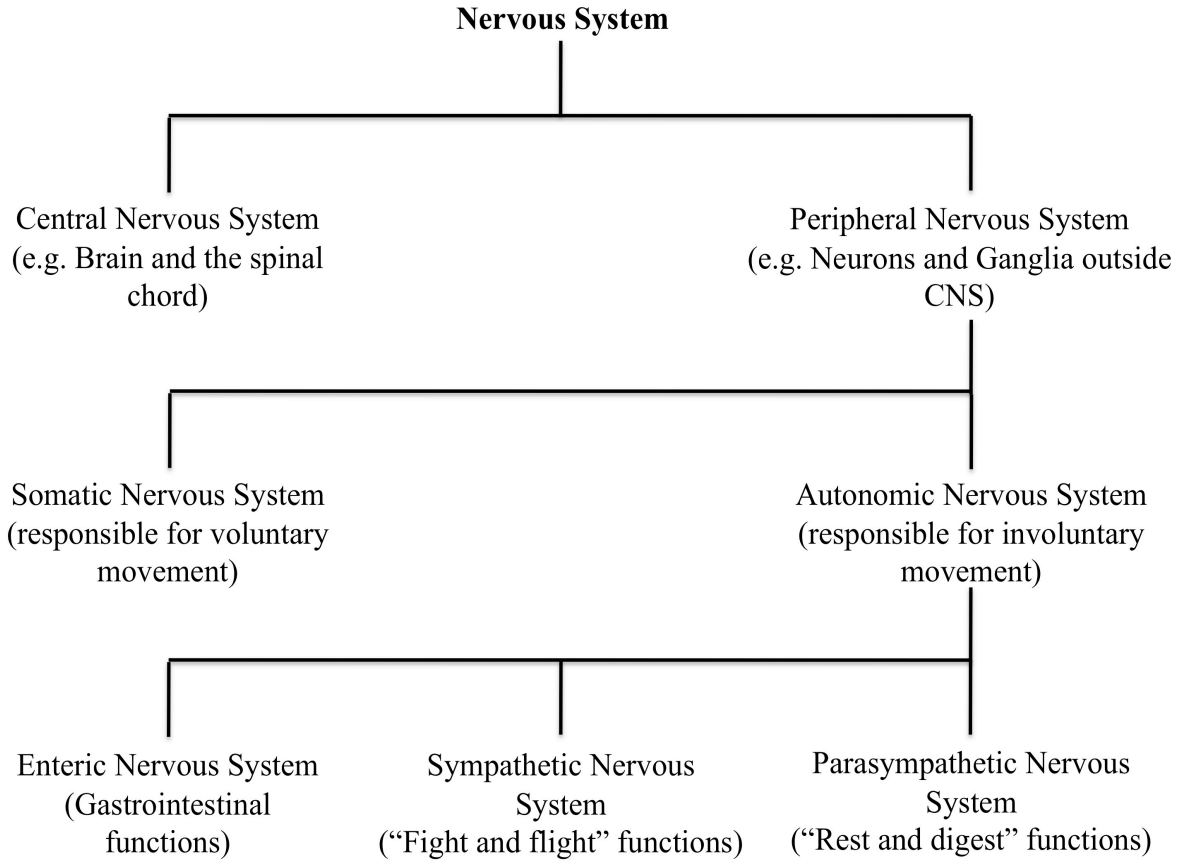

1.2 Overview of the gastrointestinal (GI) tract

The GI tract is an organ system that extends from the mouth to the anus. The primary function of the GI tract is to release digestive enzymes, absorb nutrients and excrete undigested waste. The GI tract is mesodermal in origin and is developmentally divided into the foregut, midgut and hindgut. The foregut consists of the esophagus, stomach and duodenum. Ligament of Treitz, a duodenojejunal flexure demarcates the boundary between the foregut and the midgut. The midgut consists of lower duodenum, jejunum, ileum, caecum, ascending colon and first two-third of the transverse colon. The hindgut consists of the remaining one third of the transverse colon, descending colon, rectum and the anal canal. Although different regions of the GI tract have structural and functional differences, the basic histology of the GI tract remains the same.

1.2.1 GI histology

Histologically, the GI tract is divided into four major layers namely: the mucosa, submucosa, muscularis and serosa. The architecture and the function of these layers are described below.

1.2.1.1 Mucosa

The surface architecture of the mucosa varies depending on the location and the function of the mucosa within the GI tract. The mucosa in the stomach and the small intestine increases the surface area by forming “rugae” (gastric folds) and “plicae circulares” (intestinal folds) respectively to help facilitate release of digestive enzymes and absorption of nutrients. Unlike the stomach and the small intestine, the mucosa in the large intestine are not involved in nutrient absorption and therefore does not contain any folds comparable to rugae or plicae (Sarna, 2010).

The mucosa consists of an epithelium and underlying lamina propia with the muscularis mucosa providing the demarcation between mucosa and submucosa. The epithelium in the

stomach consists of columnar epithelial cells including the glandular and the endocrine cells, which are responsible for secretion of alkaline mucous, gastric acids and enzymes. In the small intestine, the intestinal mucosa protrudes from the epithelial lining to form finger like projections called the "intestinal villi." The villus contains endocrine cells that release gastrin, somatostatin, cholecystokinin and secretin into the lumen of the small intestine. The major function of the villi is to increase the surface area of the intestine and serve as a site of absorption for fluids and nutrients. The mucosa of the large intestine on the other hand contains thin brush border layer of columnar epithelium with numerous 'mucin' producing goblet cells to help lubricate the stool (Sarna, 2010).

The middle layer of lamina propria contains loose connective tissues, nerves, blood vessels, fibroblasts and immune cells. In the small intestine, however, lymphocytes often invade the epithelium and form lymphoid nodules called the "peyer's patch." Peyer's patch in the lamina propria facilitates mucosal immune response.

Finally, a thin muscle layer of muscularis mucosa is found in the innermost portion of mucosa. Muscularis mucosa is more prominent in the large intestine compared to the small intestine where it influences absorptive and secretory functions of the epithelium via smooth muscle contractions and relaxations (Uchida & Kamikawa, 2007).

1.2.1.2 Submucosa

The submucosa of the large and the small intestine contains blood vessels, lymph vessels, connective tissues and the submucosa plexus. Besides this, the duodenal submucosa also contains 'Brunner's glands,' which release alkaline mucous secretion to protect small intestinal mucosa against the acidic environment. The submucosa plexus, also known as Meisssner's plexus, is located above the muscularis layer and contains nerves that control gastric and intestinal secretions.

1.2.1.3 Muscularis

The muscularis is a muscle layer that is located between the serosa and the submucosa. In the large and the small intestine, the muscularis contains the circular and the longitudinal muscle layer. In the stomach, however, an additional inner oblique muscle layer is also found. Between the circular and the longitudinal muscle layer, a layer longitudinal muscle myenteric plexus (LMMP) also known as the "Aurebach's plexus" is found. LMMP contains intrinsic primary afferent neurons (IPANS), interneurons and the excitatory and the inhibitory motor neurons which form local circuits to mediate GI motility (Furness, 2007c).

1.2.1.4 Serosa

The serosa consists of secretory epithelial cells, blood vessels and adipose tissues. The epithelial cells form a thin membranous sheath and encapsulate the GI tract. These epithelial cells secrete a serous fluid, which provides lubrication to reduce friction generated by the muscularis layer.

Figure 1.2 Histological layers of the gastrointestinal (GI) tract.

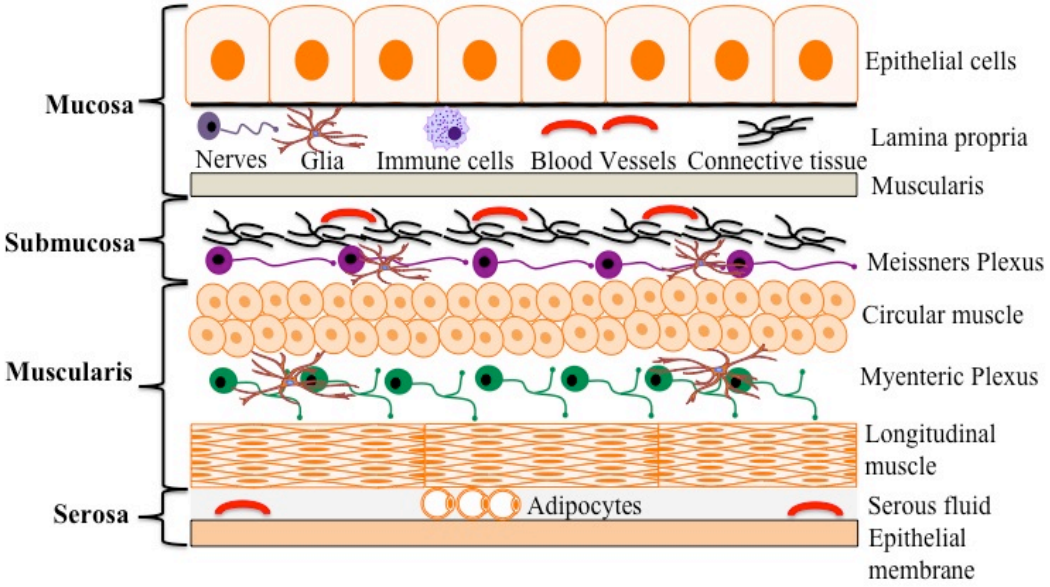

1.3 Intrinsic and Extrinsic innervations to the GI tract

1.3.1 Extrinsic innervations

The extrinsic innervations to the GI tract are provided via the SNS and the PSNS. In the SNS, the pre-ganglionic nerve fibers arise from the thoraco-lumbar region (T5-L2) of the spinal chord. The pre-ganglionic fibers from the thoracic region of spinal chord make a synaptic connection with the post-ganglionic nerve fibers in the celiac and the superior mesenteric ganglion to innervate the proximal colon, while the pre-ganglionic fibers from lumbar region extend to the inferior mesenteric ganglion and innervate the distal colon. The sympathetic pre-ganglionic nerve fibers releases acetylcholine (ACh), while the post-ganglionic nerve fibers release norepinephrine (NE) as the neurotransmitter. The sympathetic innervations through these pre-vertebral ganglia serves as an integration center between CNS and the ENS to decreases peristaltic speed (Gribovskaja-Rupp *et al.*, 2014), blood flow, and secretion during a "fight or flight" response (Anuras, 1992).

The PSNS on the other hand consists of the vagus and the pelvic nerves. These nerves arise from the cervical and the sacral (S2-S4) region of the spinal chord respectively. They have long pre-ganglionic fibers and make synaptic connections in or near the target organs. The vagus nerve provides parasympathetic innervations to the upper GI tract including the stomach, small intestine and proximal colon, while the pelvic nerves provide parasympathetic innervations to the distal colon, rectum and anus. Both the pre- and post-ganglionic neurons of the PSNS release ACh as the neurotransmitter. The PSNS modulates intrinsic innervations to increase peristaltic speed (Gribovskaja-Rupp *et al.*, 2014), blood flow and absorption during "rest and digest" response (Anuras, 1992).

1.3.2 Intrinsic innervations

The ENS mediates intrinsic innervations to the GI tract. The ENS is an semi-independent neural network that is found with in the walls of the GI tract, and controls GI motility and secretion (Costa, 2000). Although the sympathetic and the parasympathetic input to the GI tract plays a crucial role in modulating GI functions by acting as a relay center between ENS and the CNS, the ENS in itself is capable of integrating and processing GI functions (Anuras, 1992). It is therefore referred to as the "second brain" (M Costa, 2000).

The ENS comprises of neurons and glia. Developmentally, enteric neurons and glias are derived from vagal neural crest cells (Young & Newgreen, 2001) and ablation of these cells during development leads to loss of enteric ganglia (Yntema & Hammond, 1954). The ENS in an adult contains more than 400 million neurons (Furness, 2012), whereas enteric glia outnumber enteric neurons by a factor of 4-10 (Neunlist *et al.*, 2007). The enteric glia are irregular stellate shaped cells, which ensheath the neuronal cell bodies and provide regulatory signals for the development, survival and function of enteric neurons in the GI tract (Yu & Li, 2014).

Besides enteric neurons and glia, the ENS also contains dense network of interstitial cells of Cajal (ICC). ICC are pacemaker cells of the GI tract that are closely associated with the enteric neurons and the smooth muscles, where they not only modulate the rhythmic contractile activity via slow wave production, but also contributes to transportation, absorption and secretion of fluids in the GI tract (Anuras, 1992; Ordög *et al.*, 1999; Kunisawa & Komuro, 2008).

The majority of enteric neurons, glia and ICC in the ENS are arranged among submucosal (Meisssner's) and myenteric (Aurebach's) plexus (Furness, 2012), where they work together to regulate GI motility, local blood flow to the smooth muscles, gut barrier function and transmucosal movement of fluids for secretion of digestive enzymes and absorption of nutrients

(Furness, 2012; Yu & Li, 2014). Failure of either one of these component of the ENS to properly carry out it role leads to enteric neuropathies such as IBS, slow transit constipation, diabetic gastroparesis, achalasia, Chagas disease, pathogen induced diarrhea, Hirschsprung disease e.t.c (Furness, 2012).

Figure 1.3 Organization of the enteric nervous system (ENS). The ENS comprises of two major nerve plexuses, namely, the submucosal plexus (SMP) and the longitudinal muscle myenteric plexus (LMMP). The SMP controls GI secretion while the LMMP controls GI motility. Reprinted from Nature Reviews: Gastroenterol. Hepatology, volume 9, John B. Furness, The enteric nervous system and Neurogastroenterology, p286-294, copyright (2012) with permission from Macmillan. Abbreviations: ENS, enteric nervous system; SMP, submucosal plexus; LMMP, longitudinal muscle myenteric plexus.

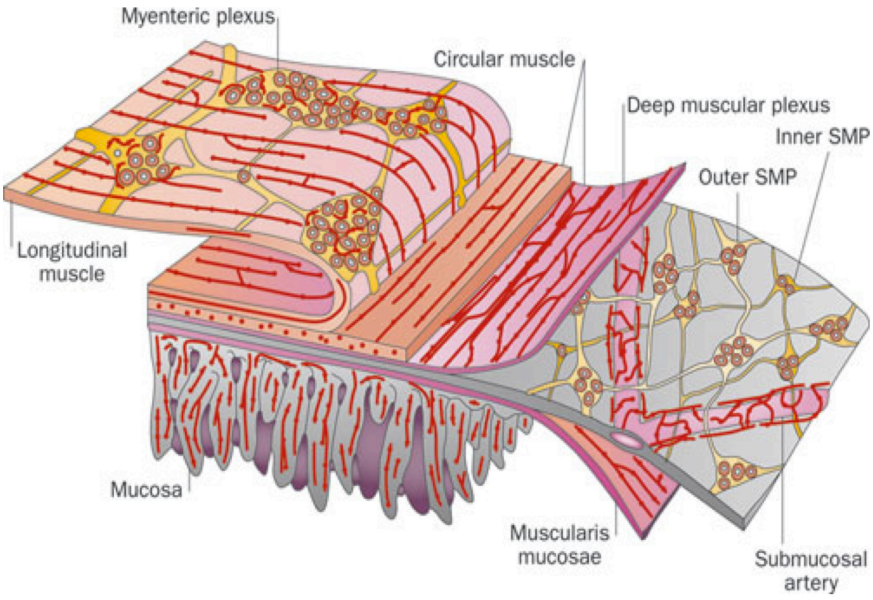

1.4 Morphological classification of enteric neurons

The enteric neurons have varying shapes and can be therefore be classified into three major types based on their morphology namely: Dogiel type I, Dogiel type II and Dogiel type III neurons (Brehmer *et al.*, 1999; Furness, 2007b).

1.4.1 Dogiel type I

Dogiel type I neurons have short, broad, and ~ 4-20 laminar dendrites. These dendrites are flattened in myenteric plane and have narrow field of influence, such that, they branch and end within the ganglion of origin (Brehmer *et al.*, 1999). Dogiel type I neurons are 13-35 μm long and 9-22 μm wide (Furness, 2006). They make up most of the inhibitory and excitatory motor neurons in the ENS. Dogiel type I neurons are mono-axonal and the axons continue up to four other ganglia before entering the circular muscle coat (Furness, 2006).

Figure 1.4 Schematic diagrams of Dogiel type I neurons example as classified by Dogiel. Reprinted: The enteric nervous system (Book) John B. Furness, copyright (2006).

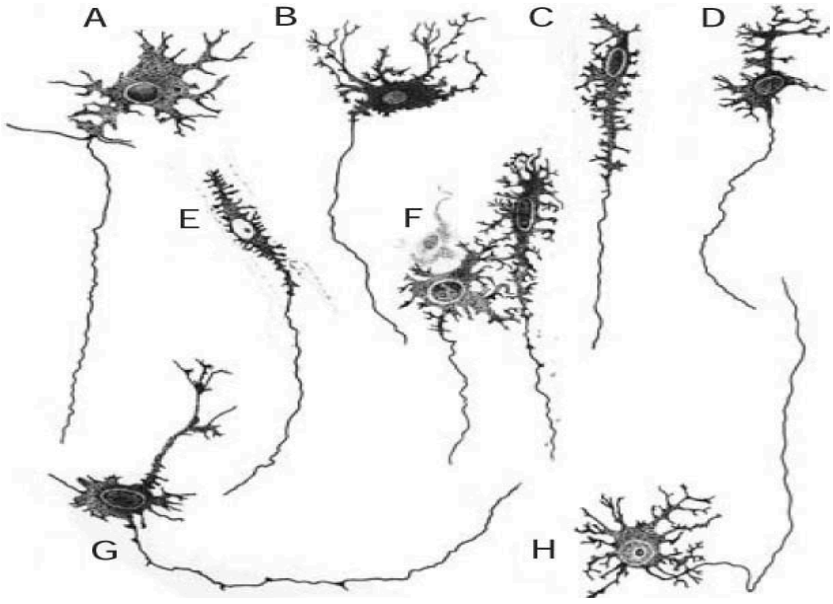

1.4.2 Dogiel type II

Dogiel type II neurons are the most prominent neurons in the myenteric and the submucosal plexus of the colon and the small intestine but are absent in the stomach (Brehmer *et al.*, 1999; Furness, 2006). They are multi-axonal and have large cell bodies that are either round or oval in shape. The major diameter and the minor diameter of type II neurons are ≥ 22-47 μm and 13-22 μm respectively (Furness, 2006). These neurons contains ~3-30 dendrites that leave ganglion of origin and have a broader field of influence (Furness, 2006; Sarna, 2010). These cells make up majority of intrinsic primary afferent neurons (IPANs) of the submucosal and the myenteric plexus and show electrophysiological after-hyperpolarization (AH) phenomenon following an action potential (Hodgkiss & Lees, 1983; Tamura, 1992; Brehmer *et al.*, 1999).

Figure 1.5 Schematic diagrams of Dogiel type II neurons example as classified by Dogiel.
Reprinted: The enteric nervous system (Book) John B. Furness, copyright (2006)

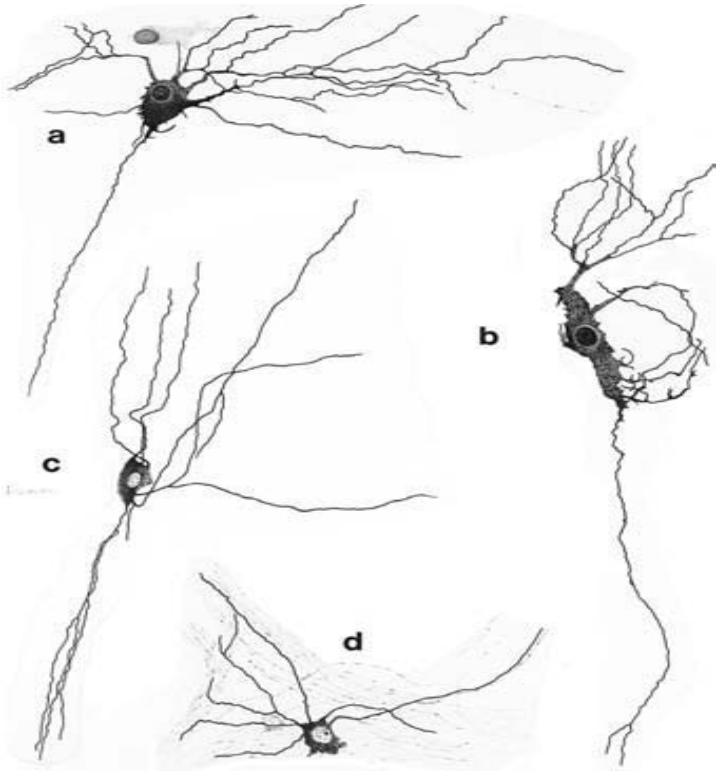

1.4.3 Dogiel type III

Dogiel type III neurons consist of ~2-10 smooth dendrites that gets thinner with branching distance (Brehmer *et al.*, 1999). Although Dogiel type III neurons end within the ganglion of origin, their dendritic length are comparatively longer than that type I (Brehmer *et al.*, 1999). The axon of a Dogiel type III neuron begins either from small conical protrusion of the cell body, or from a dendrite. Dogiel type III neurons make up a majority of descending interneurons (Furness, 2007b).

Figure 1.6 Schematic diagrams of Dogiel type III neurons example as classified by Dogiel. Reprinted: The enteric nervous system (Book) John B. Furness, copyright (2006)

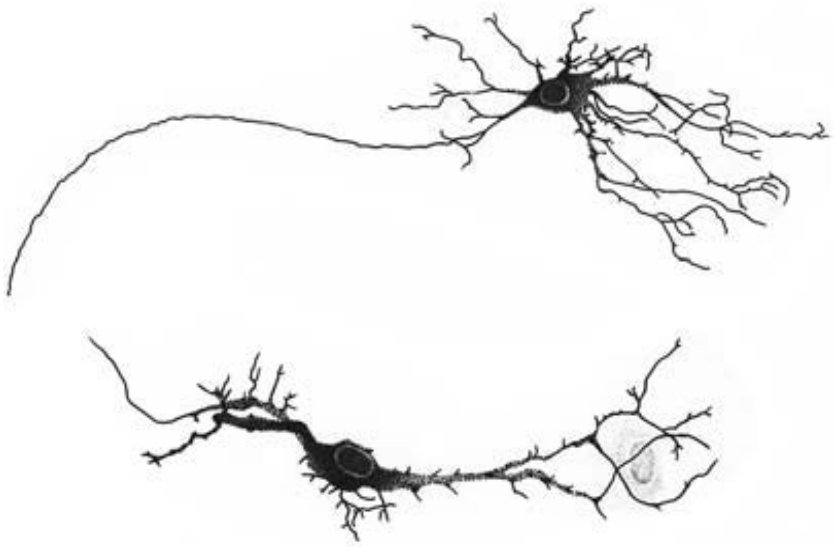

1.5 Structural and physiological characteristics of the GI Smooth muscle cells

Smooth muscles make up a majority of contractile tissues in the GI tract. In the GI tract smooth muscle cells are functionally coupled via gap junctions. This causes GI smooth muscle to produce synchronous contraction and relaxation (Anuras, 1992). The synchronicity of smooth muscles helps in propulsion and mixing of luminal content, modulation of reservoir capacity (notably in the stomach and colon), and expulsion of fecal matter, pathogens and noxious chemicals from the GI tract (Furness, 2012).

1.5.1 Structure of the GI smooth muscle

GI smooth muscles are small (<10μm in diameter) spindle shaped cells that are arranged in bundles or 'fascicae'. GI smooth muscles contain the contractile actin and myosin proteins to mediate contractions and relaxations (Anuras, 1992). In the smooth muscles these proteins are not arranged in sarcomeres, and therefore appear unstriated. In the smooth muscles, actin filament bundles are anchored to "dense bodies" (α- actinin, an actin binding protein) that are present either on the sarcolemma or on the cytoskeleton of the cell. The smooth muscle cell also contains membranous tubules called sarcoplasmic reticulum, which is a major intracellular calcium (Ca^{2+}) storage site. In the surface of the smooth muscle cell there are small flask shaped involutions called "Caveolae" that protrude ~100 nm into the cells. Caveolae helps to increase the surface area of the plasma membrane and are smooth muscle analogue of skeletal muscle T-tubule system.

1.5.2 Smooth muscle contraction

Smooth muscle contractility is primarily mediated via an increase in free intracellular Ca^{2+} concentrations. At a lower intracellular Ca^{2+} concentration (i.e < 10^{-7} M), the smooth muscle fails to contract. However after depolarization, an increase in intracellular Ca^{2+}

concentration causes smooth muscle contractile actin and myosin proteins to interact with one another resulting in contraction.

Depolarizing stimulus leads to an increase in intracellular Ca^{2+} concentration via an influx of Ca^{2+} through voltage gated Ca^{2+} channels or via agonist (neurotransmitters, hormones) induced stimulation of G-proteins (Somlyo & Somlyo, 1994). Stimulation of G proteins increases phospholipase C activity which produces two potent second messengers from the membrane lipid phosphatidylinositol 4,5-bisphosphate, namely: diacylglycerol (DG) and inositol 1,4,5-trisphosphate (IP_3) (Webb, 2003). DG in presence of Ca^{2+} activates protein kinase C (PKC), which later phosphorylates Ca^{2+} channels and other proteins, to regulate cross-bridge cycling. IP_3 on the other hand binds to IP_3 receptors on the sarcoplasmic reticulum, causing release of Ca^{2+} via Ca^{2+} induced Ca^{2+} release (CICR) mechanisms (Anuras, 1992). At higher intracellular Ca^{2+} concentration, Ca^{2+} ions bind to Ca^{2+} binding protein called 'calmodulin'. The Ca^{2+}-calmodulin (CaCM) complex activates Myosin Light Chain Kinase (MLCK). MLCK phosphorylates the myosin head specifically at Ser^{19} residue of the 20 kDa myosin protein (Somlyo & Somlyo, 1994; Borman *et al.*, 2002). Phophorylation of myosin head causes the myosin head to interact with the actin filament, which initiates cross-bridge cycle, and results in smooth muscle contraction.

Since, high intracellular Ca^{2+} concentration are toxic to the cells, the increase in intracellular Ca^{2+} concentration is transient. Under low Ca^{2+} concentration however, the contractile response is maintained by a Ca^{2+}-sensitizing mechanism bought about via activation of G protein 'Rho A'. Rho A activates Rho kinase which in turn inhibits the activity of a heterotrimeric protein called 'myosin phosphatase' (MP)(Webb, 2003). Inhibition of MP

activity causes myosin head to stay phosphorylated, causing prolonged contraction even at lower intracellular Ca^{2+} levels (Webb, 2003).

Figure 1.7 Schematic diagram illustrating smooth muscle contraction. Increase in intracellular Ca^{2+} directly via opening of voltage gated Ca^{2+} channels or indirectly via agonist induced G-protein activation leads to formation of CaCM complex. CaCM complex activates MLCK causing myosin head to bind to actin filament resulting in smooth muscle contraction. Rho A activation of Rho-Kinase prevents myosin phosphatase activity causing prolonged contraction. Reprinted from Advances in Physiology Education, volume 27, R. Clinton Webb, Smooth Muscle Contraction and Relaxation, p201-206, copyright (2003). Abbreviations: DG, diacylglycerol; PKC, protein kinase C; MLC, myosin light chain kinase.

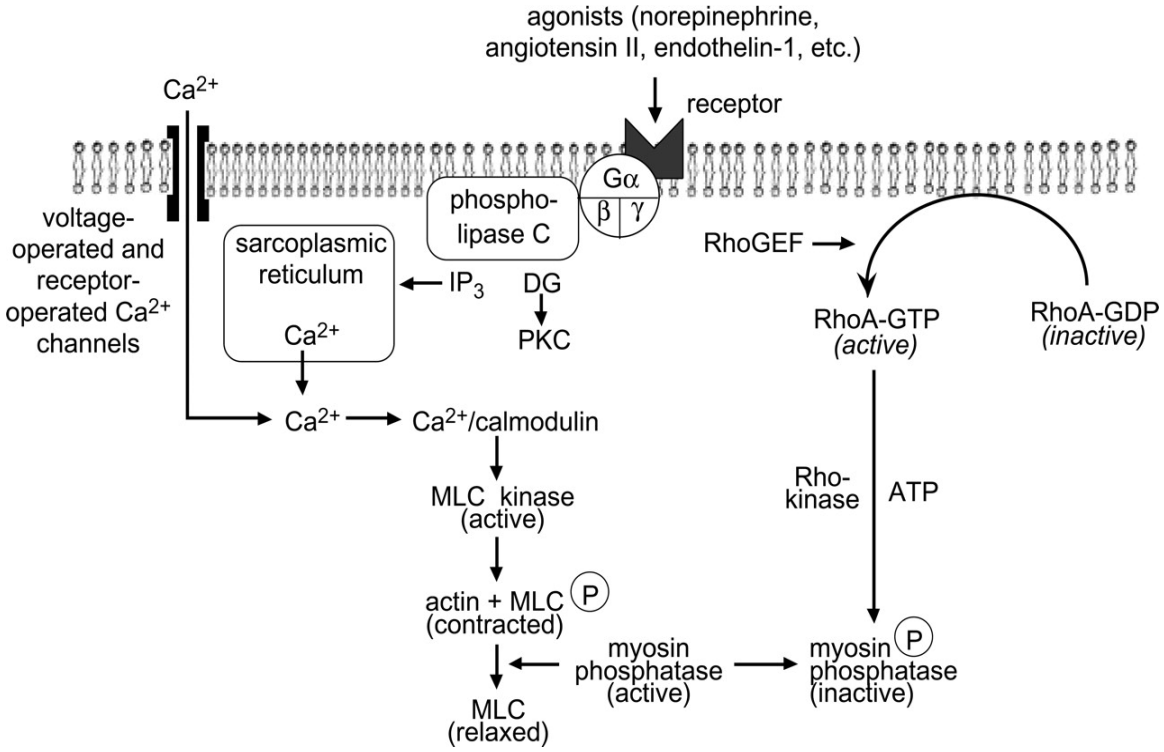

1.5.3 Smooth muscle relaxation

Removal of a contractile stimulus (agonist stimulation) causes decrease in intracellular Ca^{2+} concentration via closure of voltage-gated Ca^{2+} channels and decrease in IP_3 mediated Ca^{2+} release from the intracellular stores. At lower intracellular Ca^{2+} concentration, CaCM complex is down regulated leading to subsequent down regulation of MLCK activity. Down regulated MLCK is unable to phosphorylate the regulatory head of the myosin light chain (Webb, 2003).

Myosin phosphatase (MP) on the other hand catalyzes dephosphorylation of phosphate from the myosin light chain (LC20) and prevents the interaction between the actin and myosin filament causing cessation of contraction (Borman *et al.*, 2002). The Ca^{2+} concentration is returned back to the normal levels via Ca, Mg-ATPases and Na^{+}/Ca^{2+} exchangers that are located either on the surface of the SR or on the plasma membrane.

Figure 1.8 Schematic diagram illustrating smooth muscle relaxation. Decrease in intracellular Ca^{2+} directly via closure of voltage gated Ca^{2+} channels or indirectly via removal of agonist induced G-protein activation leads to disintegration of CaCM complex and activates MP. MP prevents interaction of actin and myosin causing smooth muscle relaxation. The resting Ca^{2+} concentration is bought back to normal levels via Ca, Mg-ATPase and Na^{+}/Ca^{2+} exchangers located on the SR and the plasma membrane. Reprinted from Advances in Physiology Education, volume 27, R. Clinton Webb, Smooth Muscle Contraction and Relaxation, p201-206, copyright (2003). Abbreviations: MLC, myosin light chain.

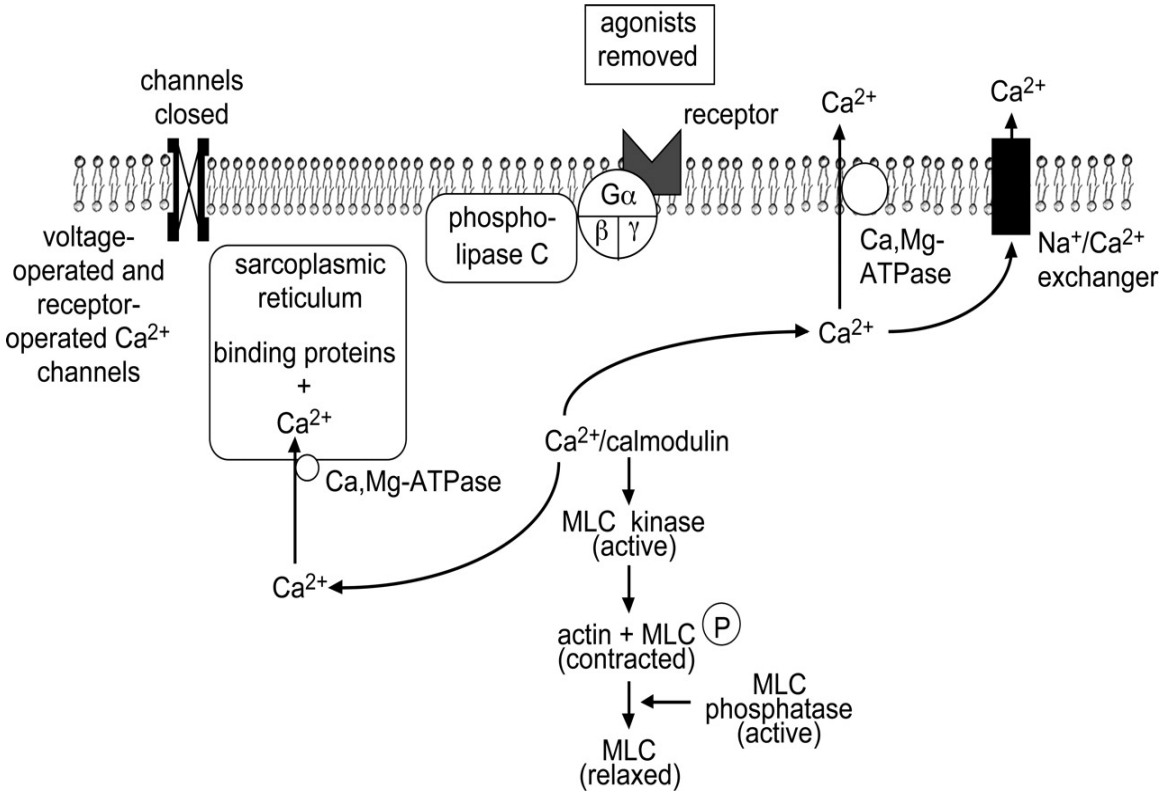

1.6 Interstitial cells of Cajal (ICCs)

ICC are the "pacemaker cells" of the GI tract, which produce rhythmic slow waves to modulate smooth muscle contraction. Although ICCs were first identified by Santiago Ramon y Cajal in 1893 as neuron like cells, ultrastructural studies later revealed that ICCs shared characteristics that resemble primitive muscle cells or fibroblast like cells (Faussone Pellegrini *et al.*, 1977; Komuro, 1989). For example, they contained numerous elongated processes, rough and the smooth endoplasmic reticulum, made close contact with enteric nerve terminals, smooth muscles, and also formed numerous gap junctions both with each other, and with the smooth muscle cells (Al-Shboul, 2013). ICCs are now known to be mesenchymal cells, which share common developmental pathway with the smooth muscle cells (Fintl & Hudson, 2010). ICCs in the GI tract express receptor tyrosine kinase (c-Kit), which is essential for the function and development of these cells (Sanders *et al.*, 2006). Blockade of c-Kit prevents binding of ligand steel factor stem cells factors (SCF) and impairs ICC development in mouse GI tract (Sanders *et al.*, 1999).

1.6.1 Function of ICCs

ICCs are electrically coupled to smooth muscle cells (Cousins *et al.*, 2003). Therefore, currents generated in the ICCs are continuously transmitted to smooth muscle cells to set up the frequency of GI contractions (Sanders *et al.*, 2006). ICC organizes smooth muscle synchronicity and contractile behavior via 'slow wave' generation (Sanders *et al.*, 2006; Fintl & Hudson, 2010; Al-Shboul, 2013). Slow waves are continuous rhythmic pacemaker currents that cause oscillation of the membrane potential and alternating periods of high and low smooth muscle excitability. A slow waves consist of a rapid upstroke, longer plateau phase and repolarization of the cell membrane potential (Al-Shboul, 2013). In periods of high excitability the plateau phase

of slow waves rises above the threshold for L-type Ca^{2+} channel activation and leads to action potential generation and smooth muscle contraction (Sanders *et al.*, 2006). Thus, the rhythmicity of slow wave activity in the GI smooth muscles modulates smooth muscle contractility and subsequent GI motility patterns (Fintl & Hudson, 2010; Drumm *et al.*, 2014).

1.6.2 Generation of pacemaker current and slow wave production

Mechanisms involved in generation of slow waves are still not entirely understood and the identity of ion channels that generates pacemaker currents in the ICC is controversial (Huizinga *et al.*, 2002; Zhu *et al.*, 2003). A most plausible hypothesis proposes that pacemaker current is initiated at least in part via non-selective cation channels (NSCCs) in the ICCs (Sanders *et al.*, 2006). According to this hypothesis, reduction in intracellular Ca^{2+} concentration activates NSCCs in the plasma membrane resulting in inward pacemaker currents and cellular depolarization. Cellular depolarization then leads to opening of voltage gated Ca^{2+} channels (VGCC) and subsequent discharge of IP_3 receptors. Ca^{2+} induced Ca^{2+} release from the IP_3 receptors also stimulates Ca^{2+} reuptake into the mitochondria. This effectively reduces cytoplasmic Ca^{2+} concentration causing activation of NSCC and the generation of pacemaker currents (Sanders *et al.*, 2006). Propagation of slow waves into the neighboring ICCs and smooth muscles are achieved via dihydropyridine resistant voltage gated Ca^{2+} channels (Sanders *et al.*, 2006; Bayguinov *et al.*, 2007). It is now known that besides VGCC and NSCC, Ca^{2+} activated Cl^- channels (CaCCs) are also activated by intracellular Ca^{2+} and play an important role to generate pacemaker slow wave currents (Zhu *et al.*, 2009). Ca^{2+} level in the cytoplasmic volume is regulated via smooth endoplasmic reticulum Ca^{2+} ATPase (SERCA) pumps and mitochondrial Na^+/Ca^{2+} exchangers (Sanders *et al.*, 2006).

1.7 Neuromuscular transmission in the GI tract

Neuromuscular transmission in the GI tract occurs in the neuromuscular junction. Unlike skeletal muscles, smooth muscle neuromuscular junction lack well defined structural specializations comparable with motor end plate (Hoyle & Burnstock, 2010). Instead, smooth muscle neuromuscular junctions are labile structures with varicosities that are able to move along the length of an axon (Hoyle & Burnstock, 2010). One aspect of this is that autonomic nerves that participate in neuromuscular transmission do not release transmitter solely from terminals, but also from varicosities that occur at intervals of 5-15 μm along axons (Hoyle & Burnstock, 2010). Because of such variations smooth muscle neuromuscular junctions are susceptible to neuromodulatory influence in both pre and post junctional sites leading to exacerbated or diminished neurotransmitter release and uptake (Hoyle & Burnstock, 2010).

Neuromuscular transmission in the GI tract plays a major role in regulating GI motility. Two major class of motor neurons that regulate GI motility are the inhibitory and the excitatory motor neurons. These motor neurons make junctional connections with GI smooth muscle cells that are electrotonically coupled by gap junctions to mediate smooth muscle contractions and relaxation. Besides smooth muscles, ICCs also play a major role in mediating neuromuscular transmission (Ward *et al.*, 2006) and smooth muscle excitability (Fintl & Hudson, 2010). Absence of ICC results in loss of excitatory (cholinergic) and inhibitory (nitrergic) neural responses (Ward *et al.*, 2000; Ward *et al.*, 2006).

1.7.1 Inhibitory neuromuscular transmission in the GI tract

The current model of inhibitory neuromuscular transmission contains inhibitory motor neurons that release purines (ATP/ β-NAD), (Xue *et al.*, 1999; Mutafova-Yambolieva *et al.*, 2007), nitric oxide (NO) (El-Mahmoudy *et al.*, 2006), vasoactive intestinal peptide (VIP) (El-

Mahmoudy *et al.*, 2006) and pituitary activating cyclic AMP (Katsoulis *et al.*, 1996) peptide. These inhibitory neurotransmitter cause transient hyperpolarization of the post junctional smooth muscle cells and takes the membrane potential away from threshold for action potential generation resulting in smooth muscle relaxation. This is referred to as inhibitory junction potential (IJP). The neurotransmitter, receptors and ion channels involved in mediating inhibitory junction potentials are described in greater detail in chapter 2.

1.7.2 Excitatory neuromuscular transmission in the GI tract

Excitatory neuromuscular transmission occurs via the actions of excitatory motor neurons. These neurons release excitatory neurotransmitters such as ACh and tachykinins (such as substance P) that either act directly on smooth muscles or indirectly through ICCs (M Costa, 2000) to cause smooth muscle depolarization. This depolarization is referred to as the excitatory junction potentials (EJPs). If the depolarization caused by the EJP is sufficient to overcome the threshold for action potential generation, action potentials will be generated and propagated across individual smooth muscle cells via gap junction causing smooth muscle contraction (Furness, 2007a).

Figure 1.9 Excitatory and inhibitory neuromuscular transmission in the GI tract. Balance between excitatory and inhibitory neuromuscular communication is crucial to maintain proper GI motility. Abbreviations: ENS, enteric nervous system; ATP, adenosine triphosphate; β-NAD, β nicotinamide adenine dinucleotide; ACh, acetyl choline; SP, substance p.

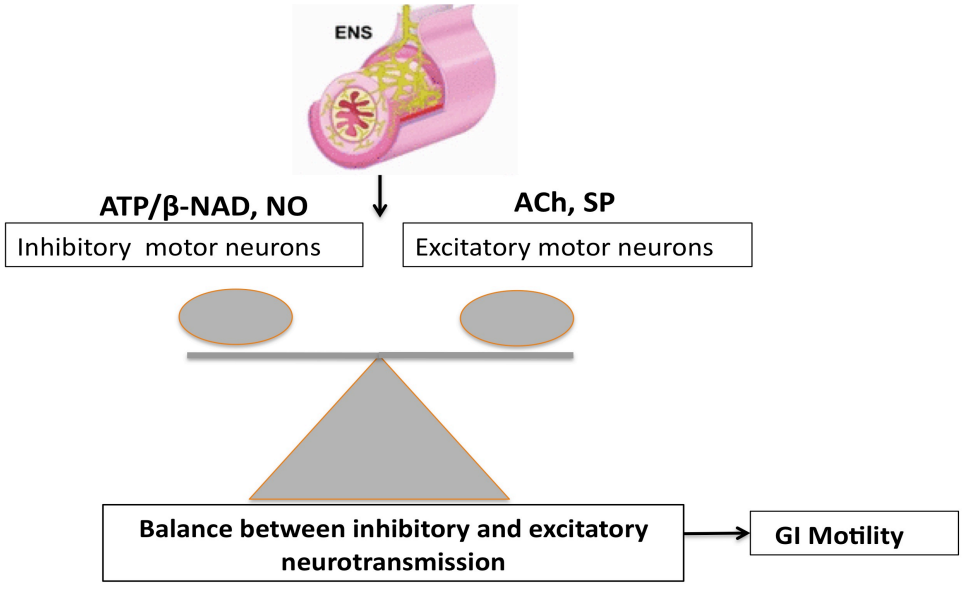

1

1.8 GI motility

GI motility refers to the process by which the luminal contents are moved across the length of the GI tract. It was earlier shown that segments of the intestine that are either removed from the animal and placed in artificial nutrient solution (Mall, 1896), or have connections to the CNS severed still displayed propulsive motility (Bayliss & Starling, 1899). This indicated that the nerve circuit necessary to produce propulsive motility is present with in the gut wall (Bayliss & Starling, 1899; Langley & Magnus, 1905). Since then, intrinsic peristaltic circuits have been studied in detail in different animals and different regions of the GI tract (Langley & Magnus, 1905; Bülbring *et al.*, 1958; Crema *et al.*, 1970; Thomas & Baldwin, 1971). These studies conclude that the requirement for GI motility is different in a region specific manner and requires varying effort of the enteric neurons, smooth muscles and the interstitial cells of Cajal (ICCs) (Tsuji *et al.*, 1992; Sanders *et al.*, 2006; Shiina *et al.*, 2010; Gudsoorkar & Quigley, 2014; Mañé *et al.*, 2014). For example, in the small intestine extensive stirring and sluggish movement of luminal contents is required for nutrients absorption, while in the colon extensive stirring is not required. Colonic contents instead needs to be moved relatively rapidly than the small intestine so that proper amount of water is absorbed, and the stool is not either over-solidified, or too loose for defecation.

To achieve such diverse motility requirements, the enteric neurons, smooth muscles and the ICCs participate differentially to generate three kinds of contractions namely rhythmic phasic contractions, giant Migrating contractions and tonic contractions whose function, spatio-temporal patterns, and regulatory mechanisms vary depending upon the location in the GI tract (Sarna, 2010).

1.8.1 Rhythmic phasic contractions (RPCs)

RPCs are randomly occurring contraction that do not activate descending relaxation circuitry and therefore propagate only over a short distance. These contractions are regulated via ICC dependent generation of smaller amplitude slow wave, and concurrent activation of excitatory cholinergic motor neurons (Sarna, 2010). The slow waves in the stomach and the small intestine are locked in a phase, which facilitates slow propagation of contractions in these regions. However, the slow waves do not show phase locking in the colon, and therefore exhibit little or no propagation (Sarna, 2010). RPCs are therefore involved in mixing and stirring of GI content for absorption of water and nutrients, but they do not to play a role in propulsive colonic motility (Sarna, 2010).

1.8.2 Giant migrating contractions (GMCs)

GMCs have larger amplitude and travel over longer distances to produce propulsion of content. In humans these contractions occur ~2-5 times a day, and helps expel feces by rapidly propagating from the colon to the rectum. GMCs are achieved by activating descending relaxation circuitry, which results in relaxation of the smooth muscles distal to the site of stimulation (Sarna, 2010). Increased GMC frequency results in rapid propagation of colonic content and lower absorption of water and electrolytes by the colonic mucosa, while the lower GMC frequency leads to prolonged contact of feces with colonic mucosa, and higher absorption of water (Bueno *et al.*, 1980). Therefore, disruptions in GMCs have been associated with colonic motor dysfunctions such as diarrhea and constipation. Unlike humans, in rodents, GMCs can easily be recorded from *ex-vivo* colonic circular smooth muscle strips and rings in organ bath experiments. Rodents therefore serve as an excellent model to study cellular pathways involved in generating GMCs (Fida *et al.*, 1997; Sarna, 2010).

1.8.3 Tonic contractions

Tonic contractions increase the tone of the smooth muscle cell. The duration of tone depends upon the volume of food ingested. Tonic contractions mostly occur in the small intestine and work with RPCs to narrow lumen size and help in effective propulsion and mixing behaviors (Ford *et al.*, 1995; Sarna, 2010).

1.9 Peristalsis

The term "Persitalsis" describes the process by which intestinal contents are moved along the length of the GI tract. Bayliss and Starling in 1899 postulated that intraluminal bolus at any point on the GI tract activates a series of reflex circuitry that causes smooth muscle contractions and relaxations rostral (oral) and caudal (aboral) to the bolus (Bayliss & Starling, 1899). Although descending relaxation circuitry is also activated during GMCs, GMCs occur infrequently and travel over longer distances unlike peristalsis, which occurs frequently and occur over shorter distances (Sarna, 2010).

1.9.1 Peristaltic circuit

Peristaltic circuit, also known the "myenteric reflex circuit ", is activated when mechanical and chemical stimuli stimulate the mucosal surface (Hukuhara & Miyake, 1959; Smith & Furness, 1988). Stimulation of the mucosal surface triggers release of serotonin (5-HT) from enterochromaffin (EC) cells (Nozawa *et al.*, 2009). 5-HT release in turn activates the mucosal endings of the IPANs (Bulbring & Crema, 1958; Foxx-Orenstein *et al.*, 1996; Nozawa *et al.*, 2009). IPANS have a distinct Dogiel type II shape and exhibit a long after hyperpolarization after an action potential, which confers directionality to the peristaltic circuit (Furness *et al.*, 1998; Furness, 2007c). IPANs form synaptic connections with interneurons in the myenteric plexus. IPANs release acetylcholine (ACh) onto the interneurons (Furness *et al.*, 1998), which in turn activates myenteric excitatory and inhibitory motoneurons of the LMMP (Costa & Furness, 1976). Finally, excitatory and inhibitory motor neurons release excitatory and inhibitory neurotransmitter in the neuromuscular junction to causes smooth muscle contraction in the oral direction, and relaxation in the aboral direction. Since myenteric plexus wraps around the entire length of the GI tract, the myenteric reflux causes propulsive contraction/relaxation

pattern to move along the entire length of the GI tract propelling food from upper esophagus to the internal anal sphincter but only over short segments at a time (M Costa, 2000).

1.10 Ca^{2+}-activated potassium (K^+) channels

Ca^{2+}-activated K^+ channels are fundamental regulators of cellular excitability (Petkov *et al.*, 2001; Sah & Faber, 2002; France *et al.*, 2012). Ca^{2+}-activated K^+ channels are activated via an increase in free intracellular Ca^{2+} concentrations, which is bought about via influx of Ca^{2+} through L-type Ca^{2+} channels, and CICR mechanisms. Activation of Ca^{2+}-activated K^+ channels leads to efflux of K^+ ions down the electrochemical gradient causing cellular hyperpolarization (Gardos, 1958). Based on molecular, pharmacological and electrophysiological properties, three distinct classes of Ca^{2+}-activated K^+ channels have been identified to date (Vergara *et al.*, 1998). These are:

Large conductance Ca^{2+}-activated K^+ channels

Intermediate conductance Ca^{2+}-activated K^+ channels

Small conductance Ca^{2+}-activated K^+ channels

1.10.1 Large conductance Ca^{2+}-activated K^+ channels (BK channel)

BK channels also known as SLO1or Maxi-K channels are derived from a single channel gene containing 27 exons, which is found in the 10^{th} and 14^{th} chromosome in humans and mice respectively (Ge *et al.*, 2014). The single channel conductance of BK channels is significantly higher than other Ca^{2+} activated K^+ channels and ranges from 200 to 400 pS (Marty, 1981). BK channels are the only class of Ca^{2+}-activated K^+ channels that are voltage sensitive. This is evident by non-linear I-V relationship, which suggests that that the amount of current passing through these channels depends on both the driving force and the probability of channel being open at a particular potential. During an action potential spike, BK channels are activated by depolarization induced opening of voltage gated Ca^{2+} channels and subsequent activation of CICR mechanisms (Faber & Sah, 2003). At intracellular Ca^{2+} concentrations $\geq$ 1µM, BK

channels are activated, leading to efflux of K^+ from the cell. Since BK channels are activated with a delay from peak of action potential spike, they contribute to spike repolarization (the falling phase of action potential), and generation of fast after-hyperpolarization (fAHP) (Storm, 1987a, b). Thus, BK channels not only control the duration of action potential but also the action potential firing frequency.

Structurally, BK channels are composed of four alpha (α) and four 4 beta (β) subunits. The α-subunit of a BK channel is encoded by a single 'slo' gene. The α subunit contains eleven hydrophobic domains (S0-S10) (Ledoux *et al.*, 2006). Out of eleven hydrophobic domains, S0-S6 domains are transmembrane domains (TMD) that make up the core of the channel. The S4 domain contains several positively charged arginine residues that confer voltage sensitivity and channel gating. The TMD S5-S6 forms the pore of the channel. Site directed mutagenesis studies have revealed that intracellular domain of the α subunit (S7-S10) contains a negatively charged aspartate amino acids residues. These residues form a Ca^{2+} bowl and regulator of conductance for K^+ (RCK) regions to act as a Ca^{2+} binding site (Vergara *et al.*, 1998; Ledoux *et al.*, 2006).

The β-subunit in the BK channel on the other hand contains two TMD with intracellular amino and carboxy-terminus. Although α subunits determine Ca^{2+} sensitivity, β subunits is responsible for translation of physiologic Ca^{2+} signals (Ledoux *et al.*, 2006). Thus, the β-subunit serves to modulate the Ca^{2+} sensitivity of the α-subunits. Genetic knockout of β subunits reduces Ca^{2+} sensitivity of the channel and disrupts BK channel function in smooth muscle and kidneys (Brenner *et al.*, 2000; Grimm & Sansom, 2010).

Until now four different β-subunit genes have been identified (β1- β4). BK β1-subunit is found in the smooth muscle cell (SMC) and in the distal nephron of murine kidney (Grimm *et*

al., 2007), BK β2- and β3-subunits are expressed in endocrine cells (Xia *et al.*, 1999; Braun *et al.*, 2008), while BK β4-subunits are expressed in neurons (Meera *et al.*, 2000) and in the distal nephron of the kidney (Grimm *et al.*, 2007). The pharmacologic antagonists for BK channels include iberiotoxin, charbydotoxin and paxilline (Galvez *et al.*, 1990; Knaus *et al.*, 1994)

1.10.1.1 β1 BK channels

The β1BK channels are mostly smooth muscle cell specific (Brenner *et al.*, 2000). β1-subunit expression in the BK channel is essential to regulate the Ca^{2+} sensitivity of the α-subunit. β1 subunit therefore plays a crucial role in regulating resting membrane potential and the excitability of smooth muscle cells (Vergara *et al.*, 1998; Ledoux *et al.*, 2006). Loss or down-regulation of BK β1-subunit expression causes membrane depolarization and increased muscle contractility which leads to various disorders including hypertension (Yang *et al.*, 2013), heart failure (Wan *et al.*, 2013), asthma (Semenov *et al.*, 2011), urinary bladder overactivity (Petkov *et al.*, 2001) and gastrointestinal motility disorders (France *et al.*, 2012).

Figure 1.10 Large conductance Ca^{2+}-activated K^+ (β1BK) channel structure. (A) β1BK channel consists of the α and the β1 subunit. (B) The α subunit contains eleven hydrophobic domain among which seven (S0-S6) are transmembrane domain. The β1 subunit consists of two transmembrane domain with intracellular amino and carboxy terminus. Reprinted from Physiology, volume 21, Ledoux et. al., Ca^{2+}-Activated Potassium Channels and the Regulation of Vascular Tone, p69-78, copyright (2006). Abbreviation: RCK, regulator of conductance for K^+.

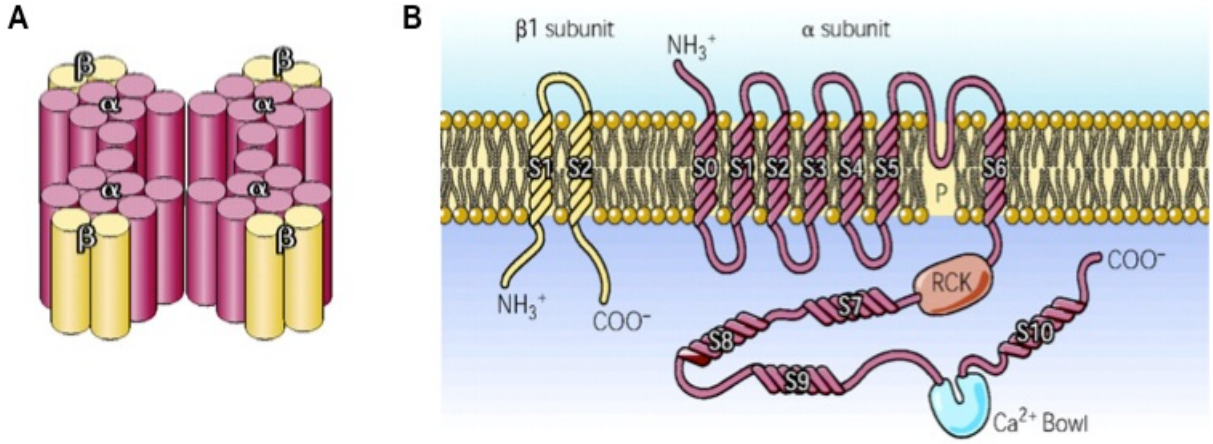

1.10.2 Small conductance Ca^{2+}-activated K^+ channels

Unlike the BK channels, the SK channels are purely Ca^{2+}-gated channels (voltage-independent). Structurally, SK channels comprises of four α-subunit (Vergara *et al.*, 1998; Ledoux *et al.*, 2006). Each α-subunit contains six (S1-S6) TMD among which TMD S5-S6 forms the pore of the channel. SK channels do not have a Ca^{2+} bowl region, instead they contain 'calmodulin', a Ca^{2+}-sensitive protein, which confers higher intracellular Ca^{2+}-sensitivity than BK channels (Ledoux *et al.*, 2006). Although positively charged S4 TMD is present in SK channels, the I-V relationship for SK channel is linear, which suggests that gating properties of SK channel is exclusively controlled by Ca^{2+}-bound calmodulin proteins (Sah & Faber, 2002). SK channels have a smaller single channel conductance than BK channels (4-20pS). SK channels contribute to slow after hyperpolarization (sAHP), and limits action potential firing (Ishii *et al.*, 1997). SK channels are expressed almost ubiquitously in CNS, nonvascular smooth muscle cell, and the endothelium. Suppression of SK channels inhibits vasodilation and increase blood pressure (Ledoux *et al.*, 2006).

Figure 1.11 Small conductance Ca^{2+}-activated K^+ (SK) channel structure. (A) SK channel contains six transmembrane domains. TMD S5-S6 acts as a pore of a channel. A Ca^{2+} sensitive protein, calmodulin, interacts with the channel's intracellular COOH terminus. (B) Binding of Ca^{2+} to calmodulin opens the gate of the SK channel. Reprinted from Physiology, volume 21, Ledoux et. al., Ca^{2+}-Activated Potassium Channels and the Regulation of Vascular Tone, p69-78, copyright (2006).

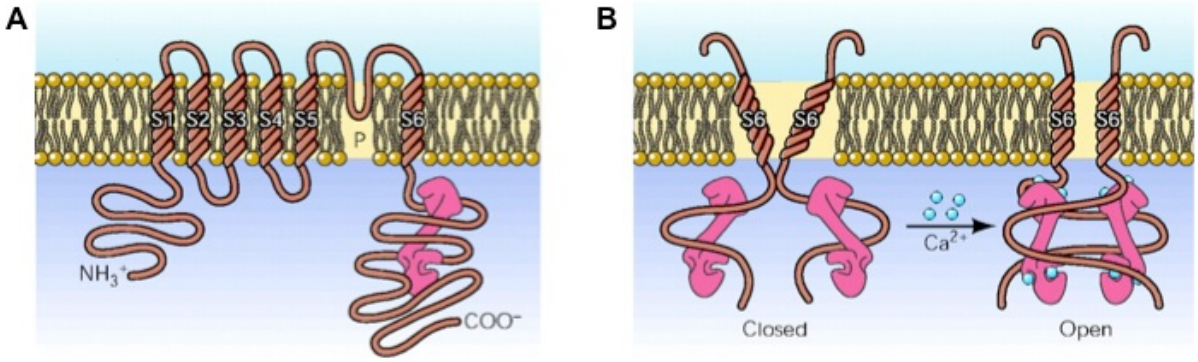

1.10.3 Intermediate conductance Ca^{2+}-activated K^+ channels

The IK channel was first identified in the red blood cells as the Gardos channel (Gardos, 1958). Since then the IK channels is found to be expressed in multiple cell types including the immune cells, endothelial cells, and neuron of the CNS and PNS (Ishii *et al.*, 1997; Turner *et al.*, 2014). The IK channels are hetero-tetrameric channels. The IK and the SK channels arise from the same gene family but only share ~50% amino acid sequence homology (Ishii *et al.*, 1997). Like the SK channels, the IK channels contain calmodulin, and is activated only by increase in intracellular Ca^{2+} concentration (Turner *et al.*, 2014). The single channel conductance of IK channels are, however, higher than SK channels (20-85 pS) (Ishii *et al.*, 1997). Pharmacologically, IK channels differ completely from SK and BK channels as they are reversibly blocked by charybdotoxin and clotrimazole but not by apamin and iberiotoxin (Ishii *et al.*, 1997).

The major characteristics feature of these channels is summarized in table below.

Table 1.1 Electrophysiological and pharmacological characteristics of Ca^{2+}-activated K^+ channels

Channel Property	Ca^{2+} activated K^+ Channel subtypes		
	BK	**IK**	**SK**
$[Ca^{2+}]i$ Range	1 – 10 μM	50 – 900 nM	50 – 900 nM
Voltage-dependence	Yes	None	None
Single-channel conductance	100 – 250 pS	20 – 80 pS	4 – 20 pS
Blockers	Charybdotoxin (nM), Paxilline (Nm), Iberiotoxin (nM), TEA (< 1mM)	α-KTx (nM) Clotrimazole (nM)	Apamin (nM) Scyllatoxin (nM) Curare (μM)

1.11 Obesity and its associated disorders

Accumulation of body fat leads to obesity. In humans, obesity is defined as a body mass index (BMI) of 30 kg/m^2 (body weight in kilograms divided by height in meters squared). High fat (HF) diet consumption is a major cause of obesity in humans (Y Lee, 2013). Diet-induced obesity (DIO) in turn is a risk factor for Type 2 diabetes (T2D) (Colditz *et al.*, 1995), cardiovascular diseases (Huang *et al.*, 1998), gall bladder diseases (Stampfer *et al.*, 1992), degenerative arthritis (Heliövaara *et al.*, 1993), cancer (Garfinkel, 1985; De Nunzio *et al.*, 2011) and GI motility disorders (Pecora *et al.*, 1981; vd Baan-Slootweg *et al.*, 2011). In 2011, ≥ 284 million people worldwide were obese with T2D (Farag & Gaballa, 2011). By 2030, ~440 million people (8% of the world population) are expected to be affected driving health care expenditures to exceed $490 billion (Shamseddeen *et al.*, 2011). DIO therefore presents a significant challenge as it is a major health care concern worldwide.

1.11.1 High fat (HF) diet-induced obesity (DIO) and disruption in colonic motility

HF DIO and T2D patients exhibit elevated free fatty acids level and increased susceptibility to GI motility complications (Mushref & Srinivasan, 2013; Voss *et al.*, 2013). Approximately, 75% of patients suffering from obesity and obesity-associated disorders such as T2D experience nausea, bloating, diarrhea, constipation, gastroparesis, abdominal pain, and heartburn (Delgado-Aros *et al.*, 2004; Xing & Chen, 2004). DIO mice that were fed 12 weeks of HF diet showed accelerated colonic transit time and enhanced cholinergic and serotonergic signaling in the ENS (Reichardt *et al.*, 2013), while 4-6 months of HF feeding caused substantial loss of myenteric neurons and increased intramuscular lipid accumulation in the ileum and the colon (Voss *et al.*, 2013; Beraldi *et al.*, 2014). Among myenteric neurons, inhibitory motor neurons are significantly impaired in mouse model of HF DIO and T2D (Chandrasekharan &

Srinivasan, 2007; Rivera *et al.*, 2011; Mushref & Srinivasan, 2013). Colon specimens from patients with T2D exhibit oxidative stress concurrent with loss of myenteric neurons (Chandrasekharan *et al.*, 2011a). However, how HF diet translates to colonic dysmotility in obesity is not yet entirely understood. In chapter 3, I studied the pathogenesis of HF diet associated colonic dysmotility in great details.

1.12 Oxidative stress

Oxidative stress is an imbalance between production of free radicals and antioxidants such that the production of free radicals overwhelms the production of antioxidants. Important sources of oxidative stress include the mitochondria respiratory cycles, nicotinamide adenine dinucleotide phosphate oxidase (NADPH oxidase) formed in immune cells, and enzymes such as fatty acyl CoA oxidase, monoamine oxidase and xanthine oxidase (Baggiolini & Wymann, 1990; Simonson *et al.*, 1993; Fridovich, 1995; Murphy *et al.*, 1998; Marikovsky *et al.*, 2003; Thayer *et al.*, 2011).

In the mitochondria ~4% of the electrons that are released from energy molecules such as NADH and $FADH_2$ lead to the formation of superoxides (O_2^-) and do not participate in ATP production (Fridovich, 1995). Under normal circumstance, reactive oxygen species (ROS) such as O_2^- levels are tightly regulated via antioxidants such as superoxide dismutase (SOD), catalase and reduced glutathione (GSH). In the cell, SOD catalyzes dismutation of O_2^-, converting O_2^- into hydrogen peroxide (H_2O_2) while GSH further reduces H_2O_2 to H_2O. However, when the electron transport chain is chronically or acutely overloaded in order to break down glucose and fats, ROS production is increased either through mitochondrial uncoupling or via β oxidation. This causes oxidation of inner mitochondrial membrane and disruption of ATP synthesis leading to even further increase in ROS generation (Vincent *et al.*, 2004). In addition to increased ROS in obesity and T2D, antioxidants such as catalase and GSH are reduced under hyperglycemic conditions causing increased H_2O_2 levels in cells (Lu *et al.*, 2006). ROS including H_2O_2 not only affects the host cell, but also diffuses across the plasma membrane to affect the neighboring cells (Vincent *et al.*, 2004).

1.12.1 Effects of oxidative stress on biomolecules

1.12.1.1 Nucleic acids

ROS induced oxidation of DNA nucleotides gives rise to 8-hydroxydeoxyguanosine, whereas oxidation of RNA nucleotides forms 8-hydroxyguanosine. In the DNA, 8-hydroxydeoxyguanosine is mutagenic and therefore carcinogenic while in the RNA, 8-hydroxyguanosine causes reduced protein translation capacity (Bar-Or *et al.*, 2015).

1.12.1.2 Lipids

ROS oxidizes long-chain fatty acids in the cell membrane to form peroxidation products such as malondialdehyde (MDA). MDA react with amines (that are present in the proteins) to generate another toxic compound called aldehyde, 4-hydroxynonenal (HNE) (Bar-Or *et al.*, 2015). These products are not only toxic to neuronal membrane and impair neurotransmitter release and uptake but they also impair mitochondrial function at the synapse (Keller *et al.*, 1997).

1.12.1.3 Proteins

Proteins are readily oxidized by free radicals at the amino terminus, carboxy terminus or at side chains to produce peroxides, keto-acids, and other oxidation derivatives (Bar-Or *et al.*, 2015). This causes protein degradation and misfolding which is commonly observed in Alzheimer's disease and Amyotrophic lateral sclerosis (ALS). Protein oxidation is also a major signal for facilitation of ubiquitin attachment. Ubiquitin, a 8.5 kDa regulatory protein, is a major signal for protein degradation by proteosomes (Iwai *et al.*, 1998).

Figure 1.12 Model describing mechanisms of oxidation of biomolecules.

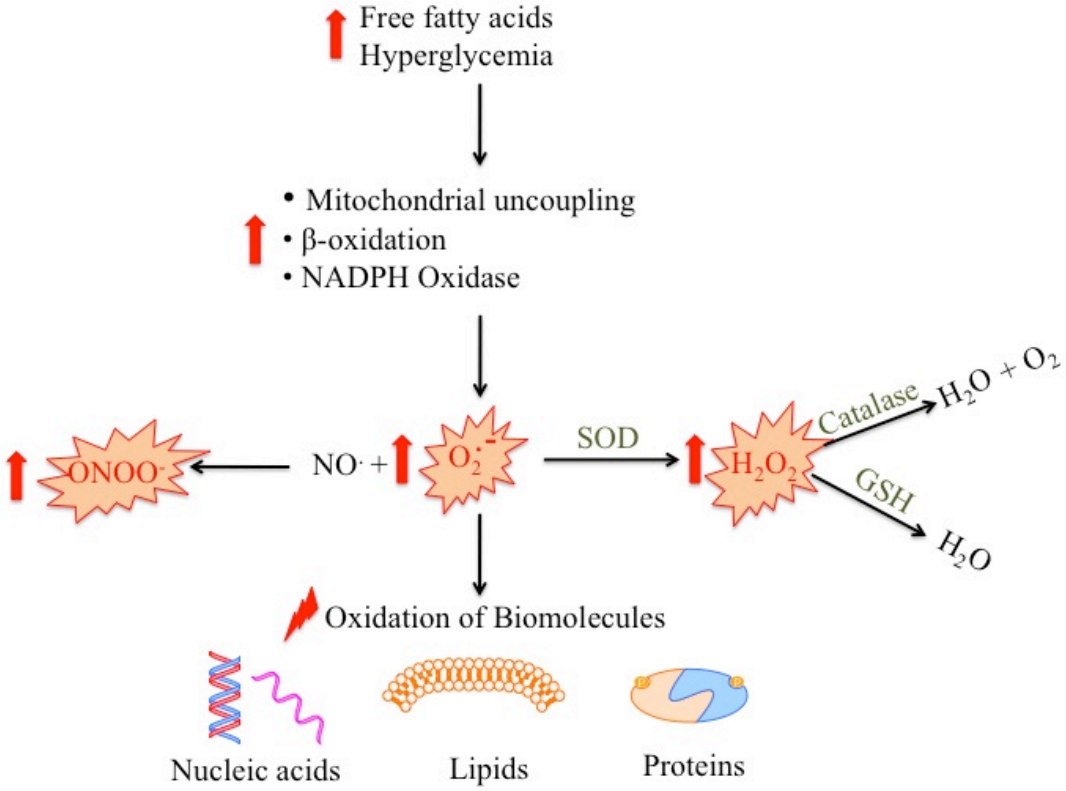

1.12.2 Obesity and oxidative stress

Obesity is identified as a major risk factor for development of various metabolic disorders including T2D, hyperglycemia, dyslipidemia, and hypertension. Although the mechanistic relationship between obesity and its associated disorders is not completely understood, oxidative stress induced free radical formation is regarded as key player in pathogenesis of obesity-associated disorders.

Emerging studies indicate that increased oxidative stress in accumulated fat is at least in part the underlying cause of development of GI dysmotility in obesity (Furukawa *et al.*, 2004). In obese mice, H_2O_2 generation is selectively increased in adipose tissue accompanied by increased NADPH oxidase mRNA expression, and decreased expression of SOD, catalases and GSH (Furukawa *et al.*, 2004). Treatment with NADPH oxidase inhibitor in obese mice reduces

ROS production in adipose tissue and improved diabetes and hyperlipidemia suggesting that increased ROS generation in accumulated fat is an early instigator of metabolic syndrome in obesity (Furukawa *et al.*, 2004).

Figure 1.13 Model indicating how accumulated fat in obesity leads to obesity associated disorders.

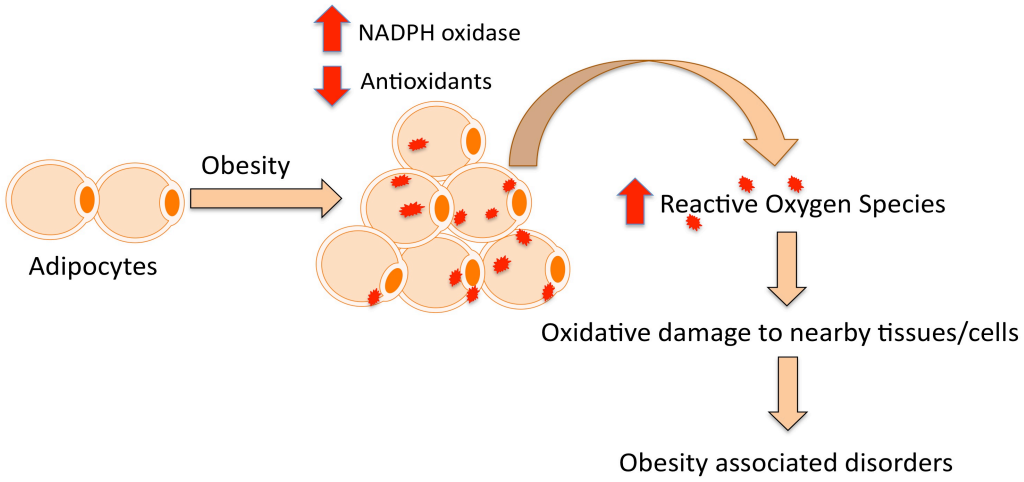

1.12.3 Impact of oxidative stress on inhibitory nitrergic signaling in the GI tract

ROS such as $O_2^{\bullet-}$ and H_2O_2 are formed continually through biological reactions, however, they are not reactive enough to cause large scale tissue damage (Halliwell & Gutteridge, 1989). Early on, most oxidative damage was ascribed to the highly reactive hydroxyl radical ($^{\bullet}OH$), which is formed as a result of Fenton reaction from H_2O_2 (Halliwell & Gutteridge, 1989). However this hypothesis is controversial for two reasons. First, $^{\bullet}OH$ radical is extremely reactive and therefore can only diffuse few angstrom before reacting with a target tissues, and second, a much higher concentration of free metal (iron) and H_2O_2 than that is available in an *in-vivo* condition is required to cause large scale oxidative damage and subsequent biological disorders (Beckman, 1994; Crow & Beckman, 1996).

In GI tissues another highly reactive free radical called peroxynitrite anion ($ONOO^-$) is involved in causing oxidative stress (Murphy *et al.*, 1998; Rivera *et al.*, 2011). $ONOO^-$ is more potent oxidant than H_2O_2 or O_2^- and can together oxidize proteins, lipids and DNA (Chandrasekharan *et al.*, 2011b). $ONOO^-$ anions are produced by reaction between NO and $O_2^{\bullet-}$ anion (Murphy *et al.*, 1998). In the human GI tract, NO is synthesized in inhibitory NO neurons via action of Ca^{2+} sensitive enzyme called neuronal nitric oxide synthase (nNOS). nNOS catalyzes conversion of arginine into NO, a diffusible inhibitory neurotransmitter. NO once released into the neuromuscular junction can diffuse into the post junctional smooth muscle cells to control inhibitory neuromuscular transmission and cause smooth muscle relaxation (Matsuda & Miller, 2010). Since NO passively diffuses from nNOS neurons to smooth muscle cells both nNOS neurons and smooth muscle cells are vulnerable to oxidative stress. NO and $ONOO^-$ anions oxidizes proteins, and cause post-translation modification, either by binding specifically to cysteine residue (to form nitrosothiols) or by reacting with tyrosine residues in the protein to produce 3-nitroso derivatives (tyr3 nitrosylation) (Rivera *et al.*, 2011).

Figure 1.14 Mechanism of peroxynitrite ($ONOO^-$) production in the inhibitory nitric oxide (NO) neurons. NO scavenges superoxide anions in the inhibitory nNOS neurons to produce peroxynitrite ($ONOO^-$). $ONOO^-$ is extremely potent than NO or O_2^- and causes oxidation of biological molecules including (1) nucleic acids (2) lipids and (3) proteins.

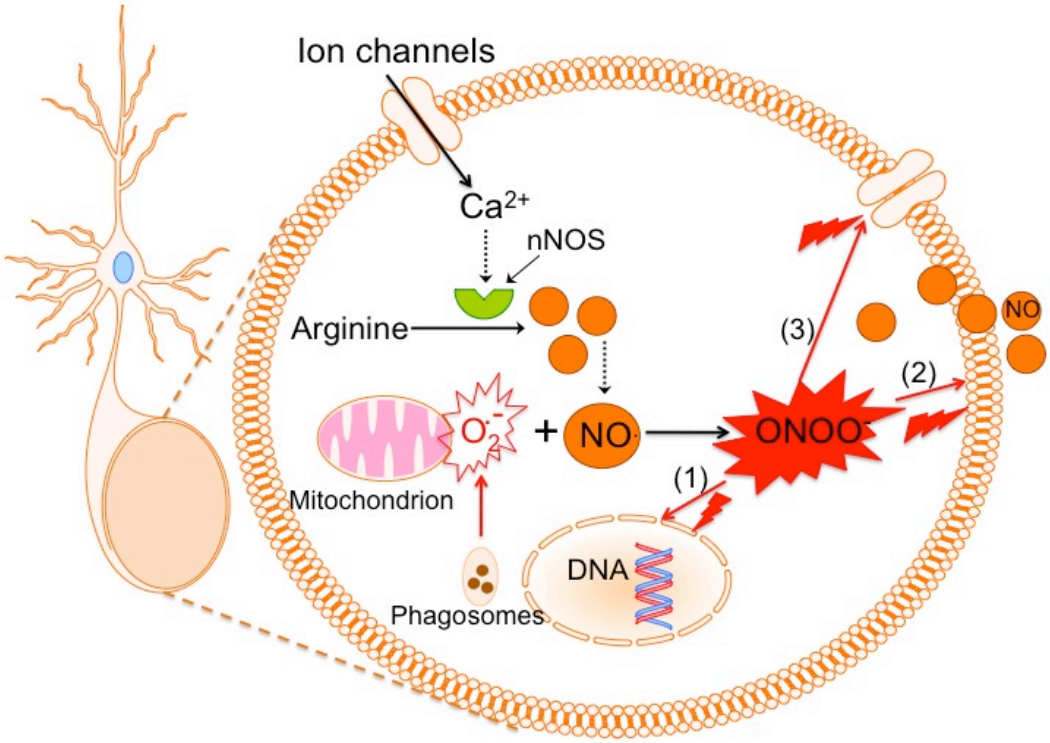

1.12.4 Impact of oxidative stress on β1BK channel function

The β1BK channel is present throughout the smooth muscle and plays a crucial role in regulating the excitability of the vascular, GI and urinary bladder smooth muscle cells (Vergara *et al.*, 1998; Petkov *et al.*, 2001; France *et al.*, 2012). The β1 subunit achieves this function and modulates BK channel activity by enhancing apparent Ca^{2+} sensitivity of the pore forming α subunit and also by slowing activation / deactivation kinetics (Cox & Aldrich, 2000; Qian & Magleby, 2003). In vascular smooth muscle cell, ROS preferentially attacks Ca^{2+} sensing cysteine residue leading to disruption of Ca^{2+} sensing mechanisms and causing the channel to behave as a β1 subunit KO (Tang *et al.*, 2004). Furthermore, β1 subunit is also amplifies oxidative regulation of the β1BK channel (Santarelli *et al.*, 2004). In rat cerebral arteries $ONOO^-$

decreases BK channel open probability in a dose dependent fashion, and this effect is reversed by addition of GSH (Brzezinska *et al.*, 2000). Cerebral arteries of diabetic mice also exhibit decreased BK channel β1/α subunit ratio, and altered Ca^{2+} spark generation (Rueda *et al.*, 2013). This results is similar to the results from cerebral artery of β1KO mice which exhibits altered Ca^{2+} spark/spontaneous transient outward current coupling (Plüger *et al.*, 2000) suggesting that β1BK channels from diabetic mice behaves similar to β1KO mice. Besides this, low antioxidants production as seen in HF mouse model (Furukawa *et al.*, 2004), also exacerbates oxidation of BK channels (Tang *et al.*, 2004; Li *et al.*, 2011). These studies suggest that oxidative stress is a key modulator of β1BK channel expression and function.

Figure 1.15 Mechanism of disruption of β1BK channel function via oxidative stress. Neuronal and non-neuronal NO (produced via action of enzymes like xanthanine oxidoreductase and reaction of H_2O_2 with arginine) production results in increased $ONOO^-$ formation in the smooth muscles. $ONOO^-$, H_2O_2 and O_2^- oxidizes amino acids within the β1BK channel and affects its function and expression.

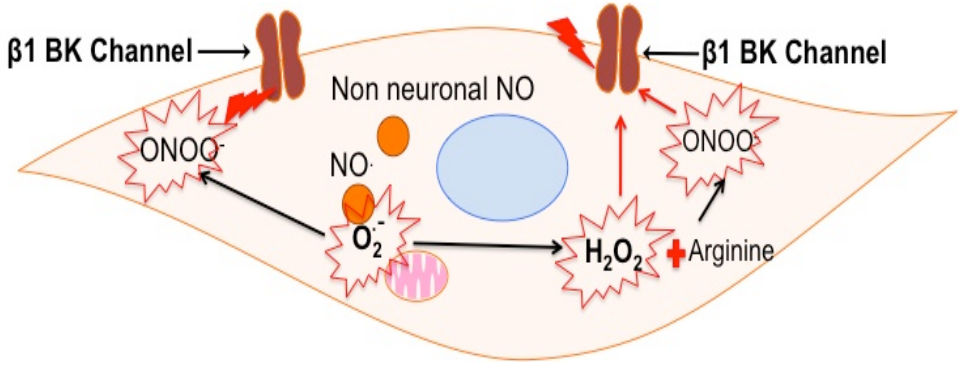

1.13 BK channel and Inhibitory nitric oxide signaling

Exogenous NO activates BK channels in the smooth muscle cells (Mistry & Garland, 1998; L'Heureux *et al.*, 2010). Activation of BK channel by NO occurs via cyclic GMP-dependent protein kinase G (PKG) activation, and via S-nitrosylation of cysteine sulfhydryl residue of the BK channel (George & Shibata, 1995; Mistry & Garland, 1998; Jaffrey *et al.*, 2001; Hess *et al.*, 2005).

In the rat hippocampus NO donor, SNP, restored BK channel activity in nNOS deficient neurons caused by intermittent hypoxia induced oxidative stress (Tjong *et al.*, 2008). Besides this, NO is also involved in rapid anterograde trafficking of β1 subunit from the endosomes to the cell membrane in order to helps associate itself with BKα subunit. NO thus causes elevated Ca^{2+} sensitivity and activity in myocytes (Leo *et al.*, 2014). My studies (discussed in chapter 3) also show that lower NO availability in DIO translate to altered smooth muscle excitability in DIO. Taken together these results suggest that NO and BK channel function are intricately linked.

Figure 1.16 Mechanism of NO production and BK channel activation in the neuromuscular junction. Activation of arginine via nNOS leads to production of NO. NO passively diffuses in the cell and causes activation of soluble guanylyl cyclase (GC), leading to increased cyclic GMP production and activation of protein kinase G (PKG). (1) PKG phosphorylates BK channel and affect channel function. (2) In addition, NO also oxidizes protein thiol to affect BK channel function.

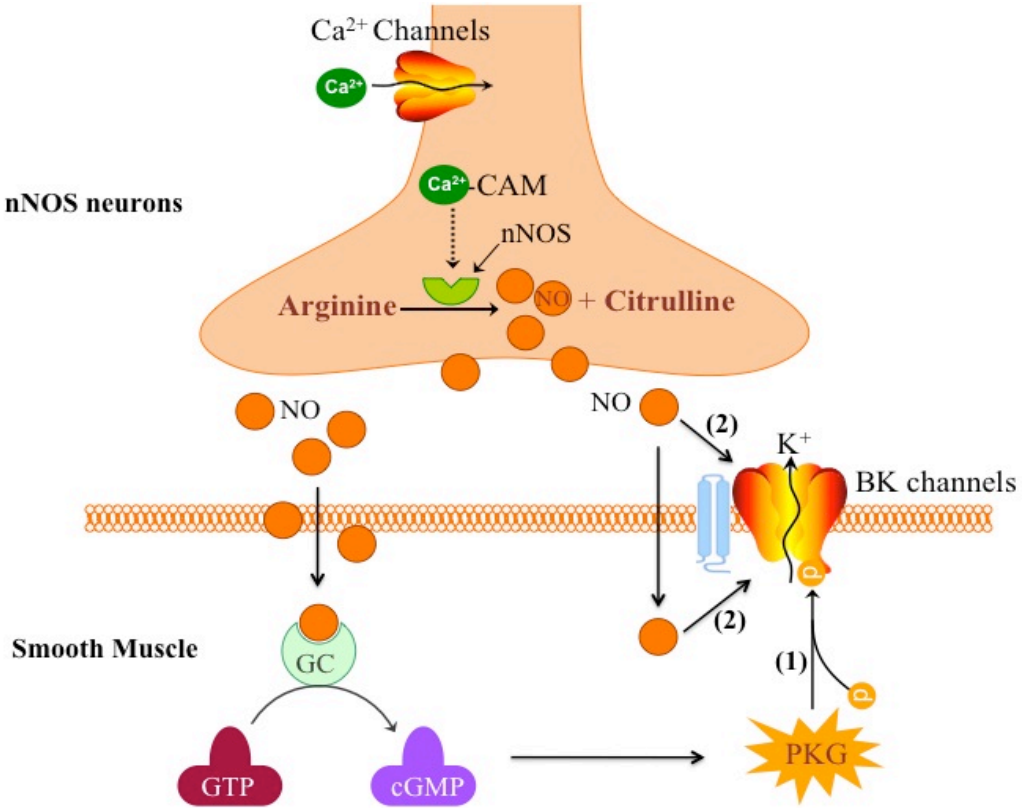

1.14 Hypothesis and specific aims

The overall aim of this research was to identify the pathogenesis of colonic dysmotility in obesity. My overall hypothesis is that HF diet leads to oxidative stress induced loss of inhibitory nNOs neurons, and impaired β1BK channel function/expression. This causes impaired neuromuscular transmission and smooth muscle excitability and ultimately leads to colonic dysmotility. Our overall hypothesis was studied using 3 specific aims

Specific aim 1: To identify the neurotransmitters, the receptors and ion channels that mediate neuromuscular transmission in the mouse distal colon

Specific aim 2: To identify the role of β1BK channel function/expression in regulating neuromuscular communication and smooth muscle excitability in the mouse distal colon

Specific aim 3: To identify the pathogenesis of HF diet induced colonic dysmotility in the mouse distal colon

BIBLIOGRAPHY

BIBLIOGRAPHY

Al-Shboul OA. (2013). The importance of interstitial cells of cajal in the gastrointestinal tract. *Saudi J Gastroenterol* **19,** 3-15.

Anuras S. (1992). *Motility disorders of the Gastrointestinal Tract*. Raven Press.

Baggiolini M & Wymann MP. (1990). Turning on the respiratory burst. *Trends Biochem Sci* **15,** 69-72.

Bar-Or D, Bar-Or R, Rael LT & Brody EN. (2015). Oxidative stress in severe acute illness. *Redox Biol* **4C,** 340-345.

Bayguinov O, Ward SM, Kenyon JL & Sanders KM. (2007). Voltage-gated Ca2+ currents are necessary for slow-wave propagation in the canine gastric antrum. *Am J Physiol Cell Physiol* **293,** C1645-1659.

Bayliss WM & Starling EH. (1899). The movements and innervation of the small intestine. *J Physiol* **24,** 99-143.

Beckman JS. (1994). Peroxynitrite versus hydroxyl radical: the role of nitric oxide in superoxide-dependent cerebral injury. *Ann N Y Acad Sci* **738,** 69-75.

Beraldi EJ, Soares A, Borges SC, de Souza AC, Natali MR, Bazotte RB & Buttow NC. (2014). High-Fat Diet Promotes Neuronal Loss in the Myenteric Plexus of the Large Intestine in Mice. *Dig Dis Sci*.

Borman MA, MacDonald JA, Murányi A, Hartshorne DJ & Haystead TA. (2002). Smooth muscle myosin phosphatase-associated kinase induces Ca2+ sensitization via myosin phosphatase inhibition. *J Biol Chem* **277,** 23441-23446.

Braun M, Ramracheya R, Bengtsson M, Zhang Q, Karanauskaite J, Partridge C, Johnson PR & Rorsman P. (2008). Voltage-gated ion channels in human pancreatic beta-cells: electrophysiological characterization and role in insulin secretion. *Diabetes* **57,** 1618-1628.

Brehmer A, Schrodl F & Neuhuber W. (1999). Morphological classifications of enteric neurons--100 years after Dogiel. *Anat Embryol (Berl)* **200,** 125-135.

Brenner R, Peréz GJ, Bonev AD, Eckman DM, Kosek JC, Wiler SW, Patterson AJ, Nelson MT & Aldrich RW. (2000). Vasoregulation by the beta1 subunit of the calcium-activated potassium channel. *Nature* **407,** 870-876.

Brzezinska AK, Gebremedhin D, Chilian WM, Kalyanaraman B & Elliott SJ. (2000). Peroxynitrite reversibly inhibits Ca(2+)-activated K(+) channels in rat cerebral artery smooth muscle cells. *Am J Physiol Heart Circ Physiol* **278,** H1883-1890.

Bueno L, Fioramonti J, Ruckebusch Y, Frexinos J & Coulom P. (1980). Evaluation of colonic myoelectrical activity in health and functional disorders. *Gut* **21,** 480-485.

Bulbring E & Crema A. (1958). Observations concerning the action of 5-hydroxytryptamine on the peristaltic reflex. *Br J Pharmacol Chemother* **13,** 444-457.

Bülbring E, Crema A & Saxby OB. (1958). A method for recording peristalsis in isolated intestine. *Br J Pharmacol Chemother* **13,** 440-443.

Chandrasekharan B, Anitha M, Blatt R, Shahnavaz N, Kooby D, Staley C, Mwangi S, Jones DP, Sitaraman SV & Srinivasan S. (2011a). Colonic motor dysfunction in human diabetes is associated with enteric neuronal loss and increased oxidative stress. *Neurogastroenterology and Motility* **23**.

Chandrasekharan B, Anitha M, Blatt R, Shahnavaz N, Kooby D, Staley C, Mwangi S, Jones DP, Sitaraman SV & Srinivasan S. (2011b). Colonic motor dysfunction in human diabetes is associated with enteric neuronal loss and increased oxidative stress. *Neurogastroenterol Motil* **23,** 131-138, e126.

Chandrasekharan B & Srinivasan S. (2007). Diabetes and the enteric nervous system. *Neurogastroenterol Motil* **19,** 951-960.

Colditz GA, Willett WC, Rotnitzky A & Manson JE. (1995). Weight gain as a risk factor for clinical diabetes mellitus in women. *Ann Intern Med* **122,** 481-486.

Costa M & Furness JB. (1976). The peristaltic reflex: an analysis of the nerve pathways and their pharmacology. *Naunyn Schmiedebergs Arch Pharmacol* **294,** 47-60.

Cousins HM, Edwards FR, Hickey H, Hill CE & Hirst GD. (2003). Electrical coupling between the myenteric interstitial cells of Cajal and adjacent muscle layers in the guinea-pig gastric antrum. *J Physiol* **550,** 829-844.

Cox DH & Aldrich RW. (2000). Role of the beta1 subunit in large-conductance Ca(2+)-activated K(+) channel gating energetics. Mechanisms of enhanced Ca(2+) sensitivity. *J Gen Physiol* **116,** 411-432.

Crema A, Frigo GM & Lecchini S. (1970). A pharmacological analysis of the peristaltic reflex in the isolated colon of the guinea-pig or cat. *Br J Pharmacol* **39,** 334-345.

Crow JP & Beckman JS. (1996). The importance of superoxide in nitric oxide-dependent toxicity: evidence for peroxynitrite-mediated injury. *Adv Exp Med Biol* **387,** 147-161.

De Nunzio C, Freedland SJ, Miano L, Finazzi Agrò E, Bañez L & Tubaro A. (2011). The uncertain relationship between obesity and prostate cancer: An Italian biopsy cohort analysis. *Eur J Surg Oncol*.

Delgado-Aros S, Locke GR, Camilleri M, Talley NJ, Fett S, Zinsmeister AR & Melton LJ. (2004). Obesity is associated with increased risk of gastrointestinal symptoms: a population-based study. *Am J Gastroenterol* **99,** 1801-1806.

Drumm BT, Koh SD, Andersson KE & Ward SM. (2014). Calcium signalling in Cajal-like interstitial cells of the lower urinary tract. *Nat Rev Urol* **11,** 555-564.

El-Mahmoudy A, Khalifa M, Draid M, Shiina T, Shimizu Y, El-Sayed M & Takewaki T. (2006). NANC inhibitory neuromuscular transmission in the hamster distal colon. *Pharmacol Res* **54,** 452-460.

Faber ES & Sah P. (2003). Calcium-activated potassium channels: multiple contributions to neuronal function. *Neuroscientist* **9,** 181-194.

Farag YMK & Gaballa MR. (2011). Diabesity: an overview of a rising epidemic. *Nephrology Dialysis Transplantation* **26,** 28-35.

Faussone Pellegrini MS, Cortesini C & Romagnoli P. (1977). [Ultrastructure of the tunica muscularis of the cardial portion of the human esophagus and stomach, with special reference to the so-called Cajal's interstitial cells]. *Arch Ital Anat Embriol* **82,** 157-177.

Fida R, Lyster DJ, Bywater RA & Taylor GS. (1997). Colonic migrating motor complexes (CMMCs) in the isolated mouse colon. *Neurogastroenterol Motil* **9,** 99-107.

Fintl C & Hudson NP. (2010). The interstitial cells of Cajal of the equine gastrointestinal tract: what we know so far. *Equine Vet J* **42,** 372-377.

Ford MJ, Camilleri M, Wiste JA & Hanson RB. (1995). Differences in colonic tone and phasic response to a meal in the transverse and sigmoid human colon. *Gut* **37,** 264-269.

Foxx-Orenstein AE, Kuemmerle JF & Grider JR. (1996). Distinct 5-HT receptors mediate the peristaltic reflex induced by mucosal stimuli in human and guinea pig intestine. *Gastroenterology* **111,** 1281-1290.

France M, Bhattarai Y, Galligan JJ & Xu H. (2012). Impaired propulsive motility in the distal but not proximal colon of BK channel β1-subunit knockout mice. *Neurogastroenterol Motil* **24,** e450-459.

Fridovich I. (1995). Superoxide radical and superoxide dismutases. *Annu Rev Biochem* **64,** 97-112.

Furness JB. (2006). *The Enteric Nervous System*.

Furness JB. (2007a). Constituent neurons of the Enteric Nervous system. In *The Enteric Nervous System*, pp. 54-55. Blackwell Publishing, Malden, MA, USA.

Furness JB. (2007b). *Constituent neurons of the enteric nervous system, in The Enteric Nervous System*. Blackwell publishing, Malden, MA, USA.

Furness JB. (2007c). Reflex circuitry of the enteric nervous system. In *The Enteric Nervous System*, pp. 80-102. Blackwell Publishing, Malden, MA, USA.

Furness JB. (2012). The enteric nervous system and neurogastroenterology. *Nat Rev Gastroenterol Hepatol* **9,** 286-294.

Furness JB, Kunze WA, Bertrand PP, Clerc N & Bornstein JC. (1998). Intrinsic primary afferent neurons of the intestine. *Prog Neurobiol* **54,** 1-18.

Furukawa S, Fujita T, Shimabukuro M, Iwaki M, Yamada Y, Nakajima Y, Nakayama O, Makishima M, Matsuda M & Shimomura I. (2004). Increased oxidative stress in obesity and its impact on metabolic syndrome. *J Clin Invest* **114,** 1752-1761.

Galvez A, Gimenez-Gallego G, Reuben JP, Roy-Contancin L, Feigenbaum P, Kaczorowski GJ & Garcia ML. (1990). Purification and characterization of a unique, potent, peptidyl probe for the high conductance calcium-activated potassium channel from venom of the scorpion Buthus tamulus. *J Biol Chem* **265,** 11083-11090.

Gardos G. (1958). The function of calcium in the potassium permeability of human erythrocytes. *Biochim Biophys Acta* **30,** 653-654.

Garfinkel L. (1985). Overweight and cancer. *Ann Intern Med* **103,** 1034-1036.

Ge L, Hoa NT, Wilson Z, Arismendi-Morillo G, Kong XT, Tajhya RB, Beeton C & Jadus MR. (2014). Big Potassium (BK) ion channels in biology, disease and possible targets for cancer immunotherapy. *Int Immunopharmacol* **22,** 427-443.

George MJ & Shibata EF. (1995). Regulation of calcium-activated potassium channels by S-nitrosothiol compounds and cyclic guanosine monophosphate in rabbit coronary artery myocytes. *J Investig Med* **43,** 451-458.

Gribovskaja-Rupp I, Babygirija R, Takahashi T & Ludwig K. (2014). Autonomic nerve regulation of colonic peristalsis in Guinea pigs. *J Neurogastroenterol Motil* **20,** 185-196.

Grimm PR, Foutz RM, Brenner R & Sansom SC. (2007). Identification and localization of BK-beta subunits in the distal nephron of the mouse kidney. *Am J Physiol Renal Physiol* **293,** F350-359.

Grimm PR & Sansom SC. (2010). BK channels and a new form of hypertension. *Kidney Int* **78,** 956-962.

Gudsoorkar VS & Quigley EM. (2014). Colorectal sensation and motility. *Curr Opin Gastroenterol* **30,** 75-83.

Halliwell BH & Gutteridge JMC. (1989). *Free Radicals in Biology and Medicine.* Oxford University Press, Oxford.

Heliövaara M, Mäkelä M, Impivaara O, Knekt P, Aromaa A & Sievers K. (1993). Association of overweight, trauma and workload with coxarthrosis. A health survey of 7,217 persons. *Acta Orthop Scand* **64,** 513-518.

Hess DT, Matsumoto A, Kim SO, Marshall HE & Stamler JS. (2005). Protein S-nitrosylation: purview and parameters. *Nat Rev Mol Cell Biol* **6,** 150-166.

Hodgkiss JP & Lees GM. (1983). Morphological studies of electrophysiologically-identified myenteric plexus neurons of the guinea-pig ileum. *Neuroscience* **8,** 593-608.

Hoyle CHV & Burnstock G. (2010). Neuromuscular transmission in the gastrointestinal tract. In *Comprehensive Physiology*. John Wiley & Sons, Inc.

Huang Z, Willett WC, Manson JE, Rosner B, Stampfer MJ, Speizer FE & Colditz GA. (1998). Body weight, weight change, and risk for hypertension in women. *Ann Intern Med* **128,** 81-88.

Huizinga JD, Zhu Y, Ye J & Molleman A. (2002). High-conductance chloride channels generate pacemaker currents in interstitial cells of Cajal. *Gastroenterology* **123,** 1627-1636.

Hukuhara T & Miyake T. (1959). The intrinsic reflexes in the colon. *Jpn J Physiol* **9**

Ishii TM, Silvia C, Hirschberg B, Bond CT, Adelman JP & Maylie J. (1997). A human intermediate conductance calcium-activated potassium channel. *Proc Natl Acad Sci U S A* **94,** 11651-11656.

Iwai K, Drake SK, Wehr NB, Weissman AM, LaVaute T, Minato N, Klausner RD, Levine RL & Rouault TA. (1998). Iron-dependent oxidation, ubiquitination, and degradation of iron regulatory protein 2: implications for degradation of oxidized proteins. *Proc Natl Acad Sci U S A* **95,** 4924-4928.

Jaffrey SR, Erdjument-Bromage H, Ferris CD, Tempst P & Snyder SH. (2001). Protein S-nitrosylation: a physiological signal for neuronal nitric oxide. *Nat Cell Biol* **3,** 193-197.

Kandel E, Schwartz J & Thomas J. (2000). *Principles of Neural Science*. McGraw-Hill Medical.

Katsoulis S, Schmidt WE, Schwarzhoff R, Folsch UR, Jin JG, Grider JR & Makhlouf GM. (1996). Inhibitory transmission in guinea pig stomach mediated by distinct receptors for pituitary adenylate cyclase-activating peptide. *J Pharmacol Exp Ther* **278,** 199-204.

Keller JN, Mark RJ, Bruce AJ, Blanc E, Rothstein JD, Uchida K, Waeg G & Mattson MP. (1997). 4-Hydroxynonenal, an aldehydic product of membrane lipid peroxidation, impairs glutamate transport and mitochondrial function in synaptosomes. *Neuroscience* **80,** 685-696.

Knaus HG, Eberhart A, Glossmann H, Munujos P, Kaczorowski GJ & Garcia ML. (1994). Pharmacology and structure of high conductance calcium-activated potassium channels. *Cell Signal* **6,** 861-870.

Komuro T. (1989). Three-dimensional observation of the fibroblast-like cells associated with the rat myenteric plexus, with special reference to the interstitial cells of Cajal. *Cell Tissue Res* **255,** 343-351.

Kunisawa Y & Komuro T. (2008). Interstitial cells of Cajal associated with the submucosal plexus of the Guinea-pig stomach. *Neurosci Lett* **434,** 273-276.

L'Heureux MC, Muinuddin A, Gaisano HY & Diamant NE. (2010). Nitric oxide activation of a potassium channel (BK(Ca)) in feline lower esophageal sphincter. *World J Gastroenterol* **16,** 5852-5860.

Langley JN & Magnus R. (1905). Some observations of the movements of the intestine before and after degenerative section of the mesenteric nerves. *J Physiol* **33,** 34-51.

Ledoux J, Werner ME, Brayden JE & Nelson MT. (2006). Calcium-activated potassium channels and the regulation of vascular tone. *Physiology (Bethesda)* **21,** 69-78.

Leo MD, Bannister JP, Narayanan D, Nair A, Grubbs JE, Gabrick KS, Boop FA & Jaggar JH. (2014). Dynamic regulation of β1 subunit trafficking controls vascular contractility. *Proc Natl Acad Sci U S A* **111,** 2361-2366.

Li S, Deng Z, Wei L, Liang L, Ai W, Shou X & Chen X. (2011). Reduction of large-conductance Ca^{2}(+) -activated K(+) channel with compensatory increase of nitric oxide in insulin resistant rats. *Diabetes Metab Res Rev* **27,** 461-469.

Lu T, He T, Katusic ZS & Lee HC. (2006). Molecular mechanisms mediating inhibition of human large conductance Ca2+-activated K+ channels by high glucose. *Circ Res* **99,** 607-616.

M Costa SJHB, G W Hennig. (2000). Chapter 2-summary. *Gut* **47,** iv26.

Mall F. (1896). A study of intestinal contraction, ed. Hospital JH, pp. 37-75.

Marikovsky M, Ziv V, Nevo N, Harris-Cerruti C & Mahler O. (2003). Cu/Zn superoxide dismutase plays important role in immune response. *J Immunol* **170,** 2993-3001.

Marty A. (1981). Ca-dependent K channels with large unitary conductance in chromaffin cell membranes. *Nature* **291,** 497-500.

Matsuda NM & Miller SM. (2010). Non-adrenergic non-cholinergic inhibition of gastrointestinal smooth muscle and its intracellular mechanism(s). *Fundam Clin Pharmacol* **24,** 261-268.

Mañé N, Gil V, Martínez-Cutillas M, Clavé P, Gallego D & Jiménez M. (2014). Differential functional role of purinergic and nitrergic inhibitory cotransmitters in human colonic relaxation. *Acta Physiol (Oxf)* **212,** 293-305.

Meera P, Wallner M & Toro L. (2000). A neuronal beta subunit (KCNMB4) makes the large conductance, voltage- and Ca2+-activated K+ channel resistant to charybdotoxin and iberiotoxin. *Proc Natl Acad Sci U S A* **97,** 5562-5567.

Mistry DK & Garland CJ. (1998). Nitric oxide (NO)-induced activation of large conductance Ca2+-dependent K+ channels (BK(Ca)) in smooth muscle cells isolated from the rat mesenteric artery. *Br J Pharmacol* **124,** 1131-1140.

Murphy MP, Packer MA, Scarlett JL & Martin SW. (1998). Peroxynitrite: a biologically significant oxidant. *Gen Pharmacol* **31,** 179-186.

Mushref MA & Srinivasan S. (2013). Effect of high fat-diet and obesity on gastrointestinal motility. *Ann Transl Med* **1,** 14.

Mutafova-Yambolieva VN, Hwang SJ, Hao X, Chen H, Zhu MX, Wood JD, Ward SM & Sanders KM. (2007). Beta-nicotinamide adenine dinucleotide is an inhibitory neurotransmitter in visceral smooth muscle. *Proc Natl Acad Sci U S A* **104,** 16359-16364.

Neunlist M, Aubert P, Bonnaud S, Van Landeghem L, Coron E, Wedel T, Naveilhan P, Ruhl A, Lardeux B, Savidge T, Paris F & Galmiche JP. (2007). Enteric glia inhibit intestinal epithelial cell proliferation partly through a TGF-beta1-dependent pathway. *Am J Physiol Gastrointest Liver Physiol* **292,** G231-241.

Nozawa K, Kawabata-Shoda E, Doihara H, Kojima R, Okada H, Mochizuki S, Sano Y, Inamura K, Matsushime H, Koizumi T, Yokoyama T & Ito H. (2009). TRPA1 regulates gastrointestinal motility through serotonin release from enterochromaffin cells. *Proc Natl Acad Sci U S A* **106,** 3408-3413.

Ordög T, Ward SM & Sanders KM. (1999). Interstitial cells of cajal generate electrical slow waves in the murine stomach. *J Physiol* **518 (Pt 1),** 257-269.

Pecora P, Suraci C, Antonelli M, De Maria S & Marrocco W. (1981). Constipation and obesity: a statistical analysis. *Boll Soc Ital Biol Sper* **57,** 2384-2388.

Petkov GV, Bonev AD, Heppner TJ, Brenner R, Aldrich RW & Nelson MT. (2001). Beta1-subunit of the Ca2+-activated K+ channel regulates contractile activity of mouse urinary bladder smooth muscle. *J Physiol* **537,** 443-452.

Plüger S, Faulhaber J, Fürstenau M, Löhn M, Waldschütz R, Gollasch M, Haller H, Luft FC, Ehmke H & Pongs O. (2000). Mice with disrupted BK channel beta1 subunit gene feature abnormal Ca(2+) spark/STOC coupling and elevated blood pressure. *Circ Res* **87,** E53-60.

Qian X & Magleby KL. (2003). Beta1 subunits facilitate gating of BK channels by acting through the Ca2+, but not the Mg2+, activating mechanisms. *Proc Natl Acad Sci U S A* **100,** 10061-10066.

Reichardt F, Baudry C, Gruber L, Mazzuoli G, Moriez R, Scherling C, Kollmann P, Daniel H, Kisling S, Haller D, Neunlist M & Schemann M. (2013). Properties of myenteric neurones and mucosal functions in the distal colon of diet-induced obese mice. *J Physiol* **591,** 5125-5139.

Rivera LR, Poole DP, Thacker M & Furness JB. (2011). The involvement of nitric oxide synthase neurons in enteric neuropathies. *Neurogastroenterol Motil* **23,** 980-988.

Rueda A, Fernández-Velasco M, Benitah JP & Gómez AM. (2013). Abnormal Ca2+ spark/STOC coupling in cerebral artery smooth muscle cells of obese type 2 diabetic mice. *PLoS One* **8,** e53321.

Sah P & Faber ESL. (2002). Channels underlying neuronal calcium-activated potassium currents. *Progress in Neurobiology* **66,** 345-353.

Sanders KM, Koh SD & Ward SM. (2006). Interstitial cells of cajal as pacemakers in the gastrointestinal tract. *Annu Rev Physiol* **68,** 307-343.

Sanders KM, Ordög T, Koh SD, Torihashi S & Ward SM. (1999). Development and plasticity of interstitial cells of Cajal. *Neurogastroenterol Motil* **11,** 311-338.

Santarelli LC, Chen J, Heinemann SH & Hoshi T. (2004). The beta1 subunit enhances oxidative regulation of large-conductance calcium-activated K+ channels. *J Gen Physiol* **124,** 357-370.

Sarna SK. (2010). *Colonic Motility: From Bench side to bedside*. Morgan and Claypool, San Rafael.

Semenov I, Wang B, Herlihy JT & Brenner R. (2011). BK channel β1 subunits regulate airway contraction secondary to M2 muscarinic acetylcholine receptor mediated depolarization. *J Physiol* **589,** 1803-1817.

Shamseddeen H, Getty JZ, Hamdallah IN & Ali MR. (2011). Epidemiology and economic impact of obesity and type 2 diabetes. *Surg Clin North Am* **91,** 1163-1172, vii.

Shiina T, Shima T, Wörl J, Neuhuber WL & Shimizu Y. (2010). The neural regulation of the mammalian esophageal motility and its implication for esophageal diseases. *Pathophysiology* **17,** 129-133.

Simonson SG, Zhang J, Canada AT, Su YF, Benveniste H & Piantadosi CA. (1993). Hydrogen peroxide production by monoamine oxidase during ischemia-reperfusion in the rat brain. *J Cereb Blood Flow Metab* **13,** 125-134.

Smith TK & Furness JB. (1988). Reflex changes in circular muscle activity elicited by stroking the mucosa: an electrophysiological analysis in the isolated guinea-pig ileum. *J Auton Nerv Syst* **25,** 205-218.

Somlyo AP & Somlyo AV. (1994). Signal transduction and regulation in smooth muscle. *Nature* **372,** 231-236.

Stampfer MJ, Maclure KM, Colditz GA, Manson JE & Willett WC. (1992). Risk of symptomatic gallstones in women with severe obesity. *Am J Clin Nutr* **55,** 652-658.

Storm JF. (1987a). Action potential repolarization and a fast after-hyperpolarization in rat hippocampal pyramidal cells. *J Physiol* **385,** 733-759.

Storm JF. (1987b). Intracellular injection of a Ca2+ chelator inhibits spike repolarization in hippocampal neurons. *Brain Res* **435,** 387-392.

Tamura K. (1992). Morphology of electrophysiologically identified myenteric neurons in the guinea pig rectum. *Am J Physiol* **262,** G545-552.

Tang XD, Garcia ML, Heinemann SH & Hoshi T. (2004). Reactive oxygen species impair Slo1 BK channel function by altering cysteine-mediated calcium sensing. *Nat Struct Mol Biol* **11,** 171-178.

Thayer TC, Delano M, Liu C, Chen J, Padgett LE, Tse HM, Annamali M, Piganelli JD, Moldawer LL & Mathews CE. (2011). Superoxide production by macrophages and T cells is critical for the induction of autoreactivity and type 1 diabetes. *Diabetes* **60,** 2144-2151.

Thomas JE & Baldwin MV. (1971). The intestinal mucosal reflex in the unanesthetized dog. *Am J Dig Dis* **16,** 642-647.

Tjong YW, Li M, Hung MW, Wang K & Fung ML. (2008). Nitric oxide deficit in chronic intermittent hypoxia impairs large conductance calcium-activated potassium channel activity in rat hippocampal neurons. *Free Radic Biol Med* **44,** 547-557.

Tsuji S, Anglade P, Ozaki T, Sazi T & Yokoyama S. (1992). Peristaltic movement evoked in intestinal tube devoid of mucosa and submucosa. *Jpn J Physiol* **42,** 363-375.

Turner RW, Kruskic M, Teves M, Scheidl-Yee T, Hameed S & Zamponi GW. (2014). Neuronal expression of the intermediate conductance calcium-activated potassium channel KCa3.1 in the mammalian central nervous system. *Pflugers Arch*.

Uchida K & Kamikawa Y. (2007). Muscularis mucosae - the forgotten sibling. *J Smooth Muscle Res* **43,** 157-177.

vd Baan-Slootweg OH, Liem O, Bekkali N, van Aalderen WM, Rijcken TH, Di Lorenzo C & Benninga MA. (2011). Constipation and colonic transit times in children with morbid obesity. *J Pediatr Gastroenterol Nutr* **52,** 442-445.

Vergara C, Latorre R, Marrion NV & Adelman JP. (1998). Calcium-activated potassium channels. *Curr Opin Neurobiol* **8,** 321-329.

Vincent AM, Russell JW, Low P & Feldman EL. (2004). Oxidative stress in the pathogenesis of diabetic neuropathy. *Endocr Rev* **25,** 612-628.

Voss U, Sand E, Olde B & Ekblad E. (2013). Enteric neuropathy can be induced by high fat diet in vivo and palmitic acid exposure in vitro. *PLoS One* **8,** e81413.

Wan E, Kushner JS, Zakharov S, Nui XW, Chudasama N, Kelly C, Waase M, Doshi D, Liu G, Iwata S, Shiomi T, Katchman A, D'Armiento J, Homma S & Marx SO. (2013). Reduced vascular smooth muscle BK channel current underlies heart failure-induced vasoconstriction in mice. *FASEB J* **27,** 1859-1867.

Ward SM, Beckett EA, Wang X, Baker F, Khoyi M & Sanders KM. (2000). Interstitial cells of Cajal mediate cholinergic neurotransmission from enteric motor neurons. *J Neurosci* **20,** 1393-1403.

Ward SM, McLaren GJ & Sanders KM. (2006). Interstitial cells of Cajal in the deep muscular plexus mediate enteric motor neurotransmission in the mouse small intestine. *J Physiol* **573,** 147-159.

Webb RC. (2003). Smooth muscle contraction and relaxation. *Adv Physiol Educ* **27,** 201-206.

Xia XM, Ding JP & Lingle CJ. (1999). Molecular basis for the inactivation of Ca2+- and voltage-dependent BK channels in adrenal chromaffin cells and rat insulinoma tumor cells. *J Neurosci* **19,** 5255-5264.

Xing J & Chen JD. (2004). Alterations of gastrointestinal motility in obesity. *Obes Res* **12,** 1723-1732.

Xue L, Farrugia G, Sarr MG & Szurszewski JH. (1999). ATP is a mediator of the fast inhibitory junction potential in human jejunal circular smooth muscle. *Am J Physiol* **276,** G1373-1379.

Y Lee C. (2013). The Effect of High-Fat Diet-Induced Pathophysiological Changes in the Gut on Obesity: What Should be the Ideal Treatment? *Clin Transl Gastroenterol* **4,** e39.

Yang Y, Li PY, Cheng J, Mao L, Wen J, Tan XQ, Liu ZF & Zeng XR. (2013). Function of BKCa channels is reduced in human vascular smooth muscle cells from Han Chinese patients with hypertension. *Hypertension* **61,** 519-525.

Yntema CL & Hammond WS. (1954). The origin of intrinsic ganglia of trunk viscera from vagal neural crest in the chick embryo. *J Comp Neurol* **101,** 515-541.

Young HM & Newgreen D. (2001). Enteric neural crest-derived cells: origin, identification, migration, and differentiation. *Anat Rec* **262,** 1-15.

Yu YB & Li YQ. (2014). Enteric glial cells and their role in the intestinal epithelial barrier. *World J Gastroenterol* **20,** 11273-11280.

Zhu MH, Kim TW, Ro S, Yan W, Ward SM, Koh SD & Sanders KM. (2009). A Ca(2+)-activated Cl(-) conductance in interstitial cells of Cajal linked to slow wave currents and pacemaker activity. *J Physiol* **587,** 4905-4918.

Zhu Y, Golden CM, Ye J, Wang XY, Akbarali HI & Huizinga JD. (2003). ERG K+ currents regulate pacemaker activity in ICC. *Am J Physiol Gastrointest Liver Physiol* **285,** G1249-1258.

CHAPTER 2

MECHANISM OF INHIBITORY NEUROMUSCULAR TRANSMISSION IN THE MOUSE DISTAL COLON

2.1 Abstract

Inhibitory neuromuscular transmission is responsible for relaxation of gastrointestinal (GI) smooth muscle. Disruption in GI smooth muscle relaxation especially in the colon can lead to various GI motility complications. The aim of this study was to identify the neurotransmitters and smooth muscle mechanisms responsible for GI smooth muscle relaxation. I studied inhibitory junction potentials (IJPs) in the mouse colon caused by electric field stimulation (EFS; 0.2 s train, 10 Hz, 90-100 V). IJPs were biphasic consisting of fast initial hyperpolarization (fIJP) followed by sustained slow hyperpolarization (sIJP). MRS 2179 (10 μM), a purinergic P2Y1 receptor antagonist, blocked fIJPs but not sIJPs. L-NNA (100 μM), a nitric oxide synthase inhibitor, blocked sIJPs but not fIJPs. MRS 2179 plus L-NNA blocked fIJPs and sIJPs. Fast and sIJPs were inhibited by apamin and niflumic acid (NFA), a SK channel and Ca^{2+} activated Cl^- (CaCCs) channel blockers respectively. ATP, β–nicotinamide adenine dinucleotide (β–NAD) and adenosine 5′-[β-thio]diphosphate (ADP-β-S) caused smooth muscle hyperpolarization. ATP produced larger hyperpolarizations than β–NAD. Polyoxotungstate 1 (POM-1), an ecto-nucleotidases inhibitor, blocked fIJPs and ATP response but not ADP-β-S responses. ADP-β-S responses were blocked by MRS 2179. These data suggests that IJPs are mediated via ATP acting on P2Y1 receptors and NO, both of which activates SK channels and CaCCs channels to cause relaxation of colonic smooth muscle.

2.2 Introduction

Disturbances in colonic smooth muscle relaxation leads to constipation, bowel incontinence and other gastrointestinal (GI) motility disturbances (Engel, 2004). Colonic smooth muscle relaxation occurs via the release of inhibitory neurotransmitters from the non-adrenergic, non-cholinergic (NANC) inhibitory motor neurons. Action of inhibitory neurotransmitters on smooth muscle produces a hyperpolarizing response, known as the inhibitory junction potential (IJP). IJPs are electrophysiological correlate of smooth muscle relaxation.

IJPs are mediated by purinergic, and nitrergic (nitric oxide mediated) pathways (Serio *et al.*, 2003; Mañé *et al.*, 2014). Purinergic signaling involves activation of post-junctional P2 receptors on the smooth muscles to mediate fast IJPs (fIJPs) (Zhang *et al.*, 2010) whereas the nitrergic pathway requires nitric oxide (NO) action on smooth muscle cells to mediate slow IJPs (sIJPs) (Xue *et al.*, 1999; Lies *et al.*, 2014). Purinergic and nitrergic pathways activate different ion channels on smooth muscles to mediate fIJPs and sIJPs. Although small conductance Ca^{2+}-activated K^+ channels (SK channel) contribute to IJP production, the contribution of other channels to IJPs is unclear (Zhang *et al.*, 2010; Martínez-Cutillas *et al.*, 2014). The Cl^- channel blocker 4,4' – diisothiocyanostilbene- 2,2' disulfonic acid (DIDS), blocks IJPs in guinea pig ileal circular smooth muscle cells, indicating that IJPs were partly due to closure of Cl^- channels (Crist *et al.*, 1991). In a more recent study, a more selective Ca^{2+}- activated Cl^- channel (CaCCs) blocker, niflumic acid (NFA; 200 μM) blocked the sIJPs but not the fIJP in opossum esophageal smooth muscle (Zhang & Paterson, 2002). The contribution of CaCC to IJPs in other tissues is unclear.

P2Y1 receptors mediate fIJPs, but the exact identity of the purinergic neurotransmitter is controversial. Functional studies suggests that ATP is the inhibitory purine neurotransmitter in

the gut (Xue *et al.*, 1999). α,β-meATP, a stable analogue of ATP, closely mimics IJPs or muscle relaxation in the human and the rat colon (Martínez-Cutillas *et al.*, 2014). However, other studies suggest that ATP does not mimic the effect of a neurotransmitter (Hwang *et al.*, 2011). Due to these controversial reports, investigators continue to refer to the actual neurotransmitter as a purine substance. β–nicotinamide adenine dinucleotide (β–NAD), a purine molecule, may be the purine neurotransmitter as it is released in response to nerve stimulation in the murine vascular and visceral smooth muscle cells and exogenous application of β–NAD mimics IJPs (Smyth *et al.*, 2004; Mutafova-Yambolieva *et al.*, 2007; Goyal, 2011). In addition, electrical stimulation of human and non-human primate colon evoked co-release of ATP and β–NAD (Hwang *et al.*, 2011). The release of β–NAD was neuronally mediated as opposed to ATP release (Hwang *et al.*, 2011). I attempted to address this controversy and evaluate whether ATP or β–NAD mediate IJPs. One way to resolve this issue is by evaluating the effects of ecto-nucleotidase (NTPDase) inhibitors on GI smooth muscle responses caused by local and brief application of ATP and ADP to mimic IJPs. NTPDase specifically metabolizes ATP into ADP, which is a primary agonist for post-junctional P2Y-receptors (Müller *et al.*, 2006; Wall *et al.*, 2008). Inhibition of NTPDase can help to identify the neurotransmitter involved in inhibitory purinergic neuromuscular signaling.

2.3 Materials and methods

2.3.1 Ethics statement

All studies were conducted in accordance with the National Institutes of Health Guide for the Care and Use of Laboratory Animals (NIH Publication No. 85-23, revised 1996) and approved by Institutional Animal Care and Use Committee of Michigan State University.

2.3.2 Animals

Male C57BL/6J mice, 10-12 weeks old were obtained from Jackson laboratories (Bar Harbor, ME, USA). Animals were kept in 12/12 hr light/dark cycle and had access to food and water *ad libitum*. Mice were euthanized by isoflurane anesthesia followed by cervical dislocation.

2.3.3 Electrophysiological recordings

The distal colon segment was quickly removed and placed in carboxygenated Kreb's solution and transferred to a petri dish. The mesenteric fat was removed and the segment was opened along the mesenteric border. The tissue segment was stretched and pinned flat on the Sylgard® base with fine pins (0.1 mm) (Fine Science Tools, Foster City, CA). The chamber was placed on the stage of an inverted microscope and was immobilized using modeling clay. Carboxygenated Krebs solution heated to 37°C was continuously flowed through the chamber at the rate of 3-4 ml/min. Drugs were added at a known concentration to the flowing Krebs solution using a system of 3-way stopcocks. The circular smooth muscle cells were impaled with glass microelectrode filled with 2 M KCl (40 - 80 MΩ tip resistance). Membrane potential was recorded using an Axoclamp 2A amplifier, a digidata 1332A analog-digital converter, and axoscope 9.2 software (all from Molecular Devices, Sunnyvale, CA). Electrical field stimulation was applied using two parallel silver wires placed 3.5 cm apart (Ø=0.03", A-M systems,

Carlsborg, WA). The wires were placed perpendicular to the longitudinal axis of the preparation. The electrical field stimulation (EFS) had following parameters: total train duration, 200 ms; Frequency, 10 Hz; pulse duration 0.8 ms; stimulation voltage 90-100 V. The amplitude and the area of EFS induced inhibitory junction potential (IJP) were measured before and after the infusion of each drug. The Ca^{2+} channel blocker nifedipine (1μM) was added to abolish spontaneous muscle contraction and obtain stable impalements for neurogenic recordings.

2.3.4 Local drug applications

ATP, Adenosine 5′-[β-thio]diphosphate (ADP-β-S) and β–nicotinamide adenine dinucleotide (β-NAD), were loaded into the micropipette (~10 μm tip diameter) positioned close to the recording site where agonists were applied by pressure ejection (5-10 psi, 20 ms puff duration) (Pico-spritzer; General Valve, East Hanover, NJ). The amplitude and the area under the curve of drug-induced responses were measured.

2.3.5 Solution and Drugs

Krebs solution composition was as follows (mM): Glucose, 11; NaCl, 117; $NaHCO_3$, 25; KCl, 4.7; $NaH_2PO_4.H_2O$, 1.2; $CaCl_2$. $2H_2O$, 2.5 and $MgCl_2$. $6H_2O$, 1.2 (pH 7.3–7.4). The Krebs solution was bubbled with 95% O_2 and 5% CO_2 mixture. All reagents were obtained from J.T. Baker (Phillipsburg, NJ). The following drugs were used: nifedipine (1 μM), Nω-nitro-L-arginine (L-NNA, 100 μM), 2′-deoxy-N6-methyladenosine 3′,5′-bisphosphate tetrasodium salt (MRS 2179, 10 μM), apamin (0.1 μM), paxilline (0.5 μM), niflumic acid (50 μM), adenosine 5'-triphosphate disodium salt solution (ATP, 5 mM), sodium polyoxotungstate 1 POM-1 (10 μM), adenosine 5′-[β-thio]diphosphate trilithium salt (ADP-β-S; 5 μM) and β-nicotinamide adenine dinucleotide hydrate (β-NAD, 5 mM). Stock solutions of nifedipine and niflumic acid were prepared by dissolving in dimethyl sulfoxide (DMSO). Stock solution of L-NNA was prepared

by dissolving in 1N HCl. Stock solutions for all of the other drugs were prepared by dissolving the drug in distilled water. POM-1 was obtained from Tocris Bioscience (Bristol, UK) while the rest of the drugs were obtained from Sigma-Aldrich (St. Louis, MO, USA).

2.3.6 Statistics

Data were analyzed only from individual recordings that lasted ≥2 min. Normalized responses to the drug were measured by evaluating both the amplitude and the area of EFS-induced IJP responses. Effects of drug on the amplitude and area of IJP were compared using paired *t*-test. Two-group comparison was made using two-way ANOVA with Bonferroni post-hoc test. Data are mean ± SEM. Differences were considered significant when $p<0.05$. Analysis was done in GraphPad Prism 4.0 software (San Diego, CA).

2.4 Results

2.4.1 Nifedipine application does not affect Resting membrane potential (RMP) in the mouse colon

Nifedipine (1 μM) did not change the RMP of the colonic smooth muscle cells. This indicates that L-type Ca^{2+} channels do not play a vital role in mediating resting membrane in mouse colonic smooth muscles. Nifedipine can therefore be used to obtain stable impalements to record IJP in the mouse distal colon.

Figure 2.1 Effect of nifedipine on colonic smooth muscle resting membrane potential. Nifedipine (1 μM) did not change the resting membrane potential (RMP) of colonic circular smooth muscle cells (n=6, p>0.05).

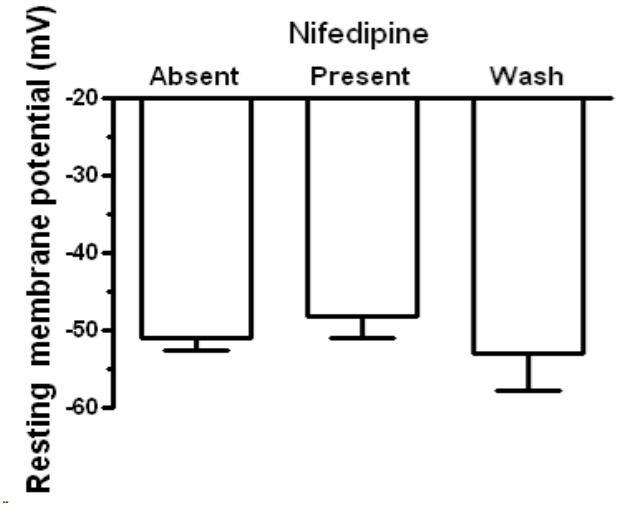

2.4.2 IJPs display both uniphasic and biphasic patterns

When electrical field stimulation (10 Hz, 0.2 s) was used to elicit an IJP, two types of IJPs were identified. An initial fIJP characterized by larger amplitude and shorter time duration followed by a smaller amplitude and longer duration slow IJP (sIJP). In some instances fIJP and the sIJP merged to form a uniphasic IJP. The amplitude and the area of the IJP were used as a measure of fIJP and sIJP respectively.

Figure 2.2 IJPs have both a uniphasic and biphasic patterns. IJPs were obtained in (A) absence and in presence (B and C) of nifedipine (1μM). The shapes of IJP are either uniphasic (A and C) or biphasic. (B) Biphasic IJP consists of shorter duration fast IJP followed by a longer lasting slow IJP. NS: nerve stimulation.

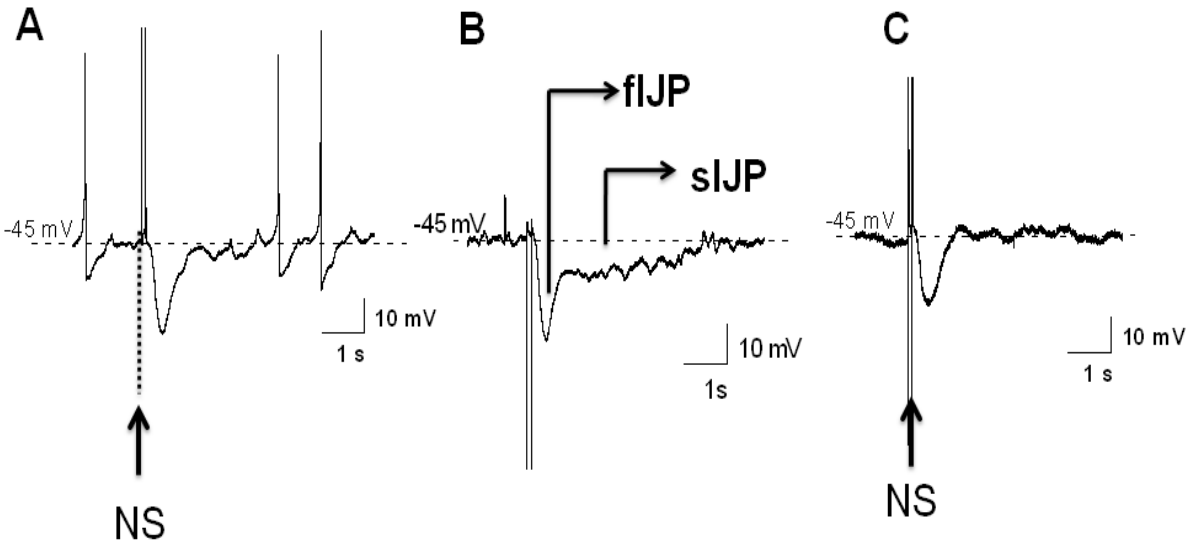

2.4.3 IJPs are neurogenic

In order to verify the neuronal origin of the IJP, tetrodotoxin (TTX), a voltage gated sodium (Na^+) channel blocker was used. TTX blocks axonal action potential (Bane *et al.*, 2014). This impairs neurotransmitter release in the neuromuscular junction. TTX completely blocked IJPs confirming a neuronal response.

Figure 2.3 Schematic diagram illustrating neuromuscular transmission in the mouse colon. (A) Electrical stimulation opens voltage gated Na^+ and K^+ channels causing action potential generation in the inhibitory motor neurons. Action potential upon reaching the synaptic terminal activates Ca^{2+} entry via voltage gated Ca^{2+} channel causing neurotransmitter release in the neuromuscular junction. Post-junctional hyperpolarizing response is then measured from the smooth muscles via sharp microelectrode connected to a differential amplifier. (B) Tetrodotoxin (TTX; 0.3µM) blocks voltage gated Na^+ channels and completely abolishes IJP in mouse distal colon.

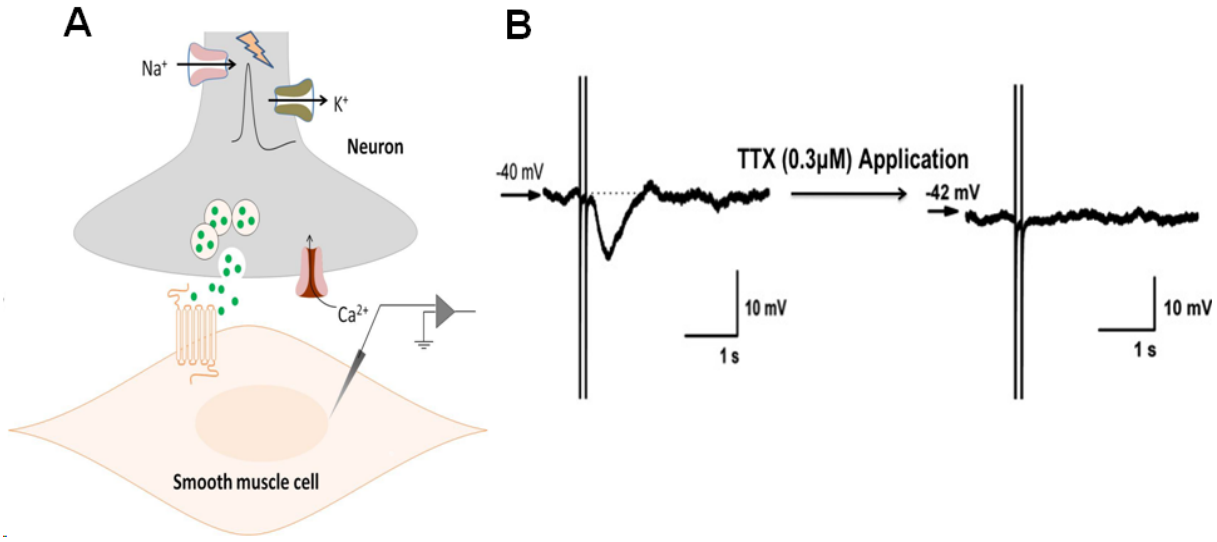

2.4.4 Identification of receptors and neurotransmitters that mediate IJPs in the mouse colon

In order to identify the receptors that mediate IJP in the mouse colon I applied MRS 2179, a P2Y1 receptor antagonist, on colonic smooth muscles (Figure 2.4). The RMP of the smooth muscle cells was unaffected by MRS 2179. MRS 2179 reduced IJP amplitude by 66 ± 4% but did not reduce the IJP area. This suggests that the P2Y1 receptor mediates the fIJP but not the sIJP. Next I studied the effect of L-NNA on evoked IJP (Figure 2.5). Nω-nitro-L-arginine (L-NNA), a NOS inhibitor, did not affect the smooth muscle RMP. L-NNA did not reduce the amplitude of IJP but reduced the IJP area by 33 ± 8% (*p<0.05). This suggests that NO mediates the sIJP but not the fIJP. Finally, I co-applied MRS 2179 and LNNA together (Figure 2.6). When MRS 2179 and L-NNA were co-applied both the amplitude and the area of evoked IJP was inhibited by 89 ± 6% and 88 ± 8% respectively. This suggests that IJPs in the mouse distal colon are mediated via P2Y1 receptors and NO mediated pathways.

Figure 2.4 The effect of P2Y1 receptor blocker on evoked IJPs. (A) MRS 2179 (10 μM) did not change the RMP. (B) Time course of inhibition of normalized IJP amplitude and area after MRS 2179 application. MRS 2179 shows maximum inhibition effect after 4 min of application. (C) Five minutes of MRS 2179 application significantly reduces the IJP amplitude but not the area (n=6, *p<0.05).

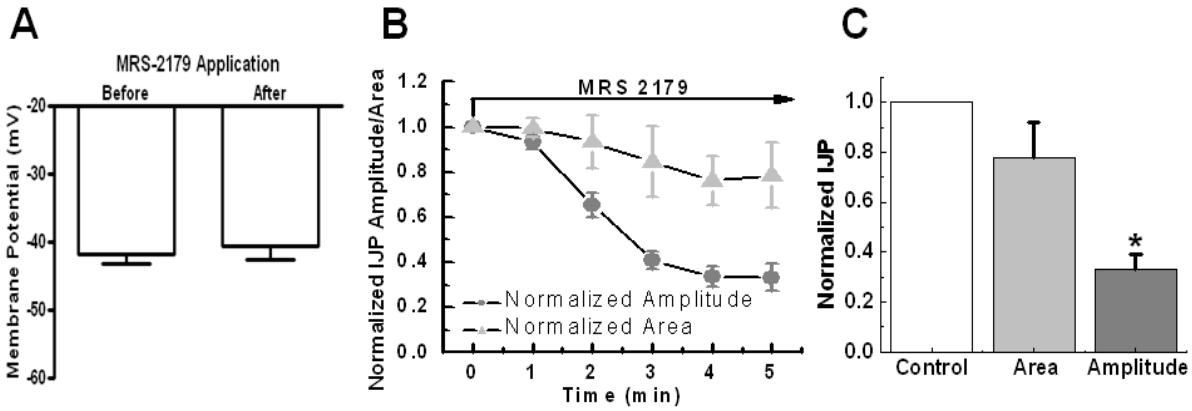

Figure 2.5 The effect of NOS inhibition on evoked IJPs. (A) L-NNA (100 μM), a NOS inhibitor, did not change the resting membrane potential. (B) Time course of L-NNA effect on normalized IJP amplitude and area after L-NNA application. (C) Five min of L-NNA application significantly reduced IJP area but not the amplitude (n=6, *p<0.05).

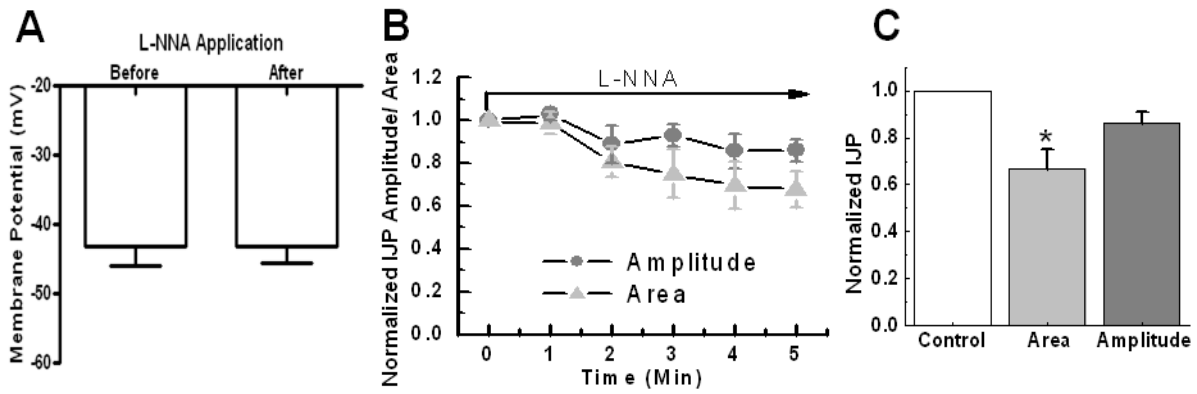

Figure 2.6 Effects of MRS 2179 and L-NNA co-application. (A) MRS 2179 and L-NNA co-application did not change the RMP. (B) Time course of MRS 2179 and L-NNA co-application on normalized IJP amplitude and area. MRS 2179 was applied for four min followed by co-application of MRS 2179 and L-NNA. (C) MRS 2179 and L-NNA co-application blocked both the amplitude and the area of the IJP (n=8, *p<0.05).

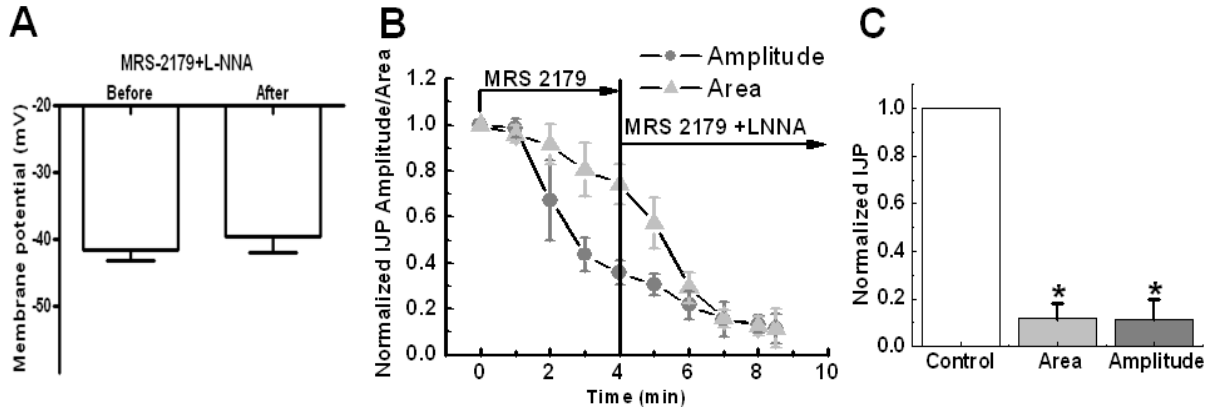

2.4.5 Identification of smooth muscle ion channels involved in mediating IJPs.

The SK channel blocker, apamin, was used to determine if SK channels are involved in mediating IJPs (Figure 2.7). Apamin application depolarizes the membrane potential by 4 ± 1.7 mV, and inhibits both the amplitude and the area of IJP by 40 ± 8% and by 35 ± 6% respectively. I used niflumic acid (NFA), to examine the role of CaCCs in inhibitory neuromuscular transmission (Figure 2.8). NFA hyperpolarized the membrane potential by 5 ± 2 mV and reduces both the area and the amplitude of the IJP by 44 ± 6% and 52 ± 6% respectively. I also co-applied apamin and NFA on the tissue (Figure 2.9). Co-application of NFA with apamin abolished IJPs mimicking the action of MRS 2179 and L-NNA co-application. These data suggests that IJPs are mediated via SK and CaCCs in the mouse distal colon.

Figure 2.7 Effects of SK channel blocker on evoked IJPs. (A) Apamin (0.1 μM) application significantly depolarizes the colonic smooth muscle. (B) Time course of apamin effect on normalized IJP amplitude and area. Apamin shows maximum effect after 3 min of application. (C) Five minutes of apamin application significantly reduced both the area and the amplitude of the IJP (n=6, *p<0.05).

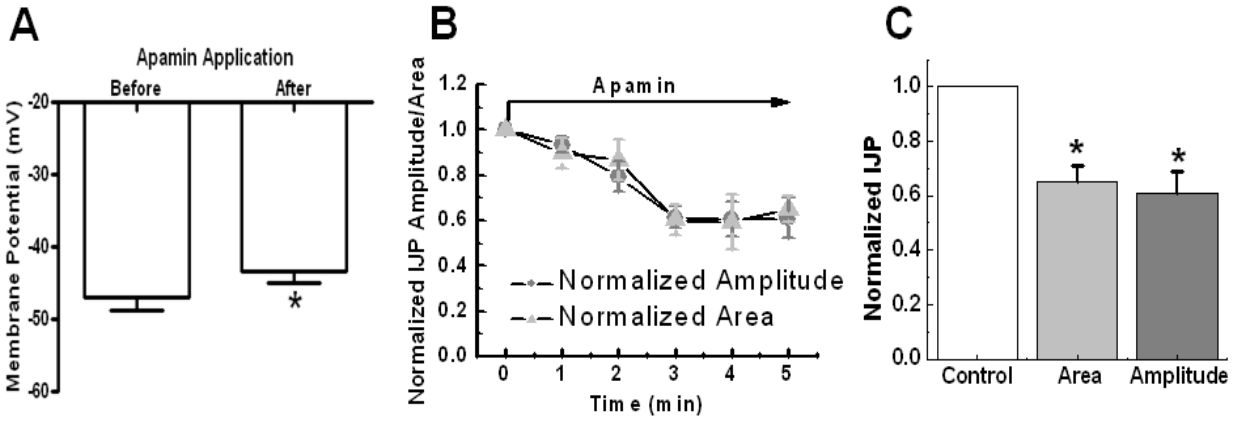

Figure 2.8 Effects of CaCC blocker on evoked IJP. (A) NFA (50 μM), a CaCC blocker, hyperpolarized the membrane potential by 5 ± 2 mV. (B) Time course of NFA effect on normalized IJP amplitude and area. The inhibitory effects of NFA on IJPs peaks after six minutes of application. (C) NFA application for six minutes significantly reduces both the area and the amplitude of the IJP (n=6, *p<0.05)

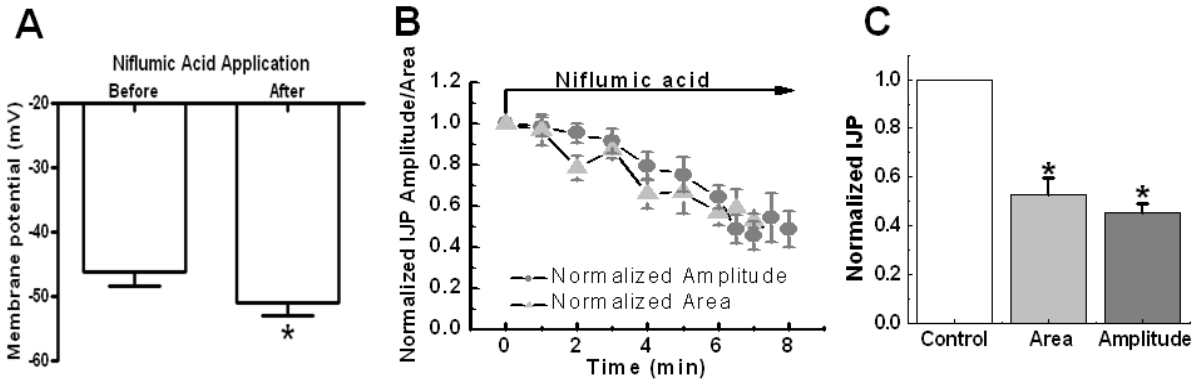

Figure 2.9 Effects of apamin and niflumic acid (NFA) co-application. (A) Apamin and niflumic acid co-application did not affect the resting membrane potential. (B) Time course of NFA and apamin co-application on normalized IJP. NFA (50 μM) applied for four min followed by co-application of NFA and Apamin blocks IJPs. (C) Both the amplitude and the area of the IJP is disrupted (n=6, *p<0.05).

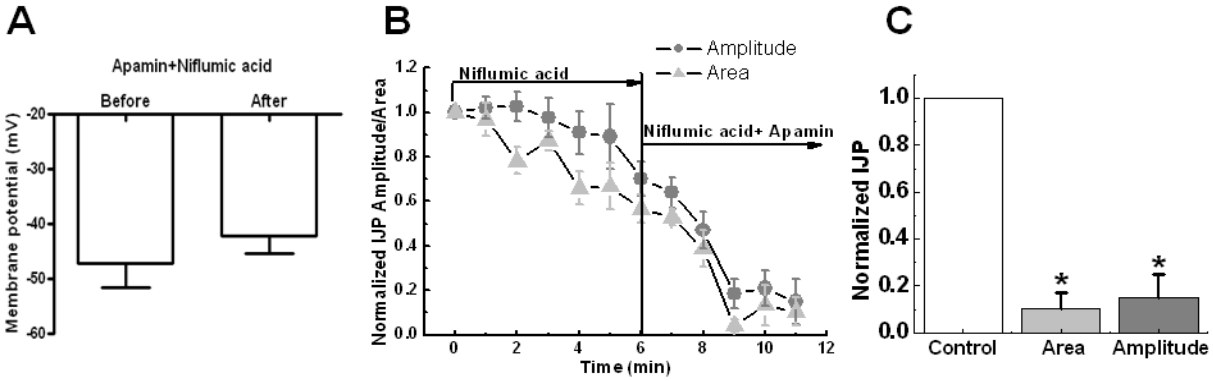

2.4.6 Identification of specific purinergic neurotransmitter involved in mediating the IJP.

It is controversial whether the ATP or β-NAD mediates IJPs in the GI tract. Therefore, in order to identify the neurotransmitter mediating the IJP, ATP and β-NAD were applied from a micropipette near the recording site and electrophysiological responses were measured. ATP produced larger significantly larger hyperpolarizations compared to β-NAD (Figure 2.10). ADP, a metabolite of ATP, is more effective in causing smooth muscle hyperpolarization. Therefore, POM-1, an ectonucleotidase inhibitor (Wall *et al.*, 2008) was used to study the role of ecto-nucleotidases in mediating inhibitory neuromuscular transmission (Figure 2.11). POM-1 decreased the amplitude and the area of IJP. POM-1 was then used to test if also inhibits local ATP response (Figure 2.12). I found that ATP responses were completely blocked by POM-1 verifying that an ATP metabolite mediates hyperpolarizing responses (n=3). Next I studied the effects of POM-1 on exogenous Adenosine 5′-[β-thio]diphosphate (ADP-β-S) application (Figure 2.13). ADP-β-S produced hyperpolarizing responses that were not blocked by POM-1. Finally, MRS 2179 was exogenously applied to verify that these effects were mediated via P2Y1 receptor activation (Figure 2.14). MRS 2179 completely abolished ADP-β-S induced hyperpolarizing responses in a reversible manner.

Figure 2.10 ATP and β-NAD induced hyperpolarizing response in the mouse distal colon. Representative hyperpolarizing response to 5 mM, 20 ms (A) ATP and (B) β-NAD puff. (C) ATP/ β-NAD response amplitude – puff duration calibration curve. Response amplitude/area reaches plateau at 20ms puff duration. ATP produced larger hyperpolarization amplitude (20 ± 2 mV) compared to β-NAD (10 ± 3 mV). (D) ATP/β-NAD response area – puff duration calibration curve. ATP produced larger hyperpolarization (67 ± 11 mV) compared to β-NAD (29 ± 10 mV) (n=8 ATP, n=5 β-NAD, *p<0.05)

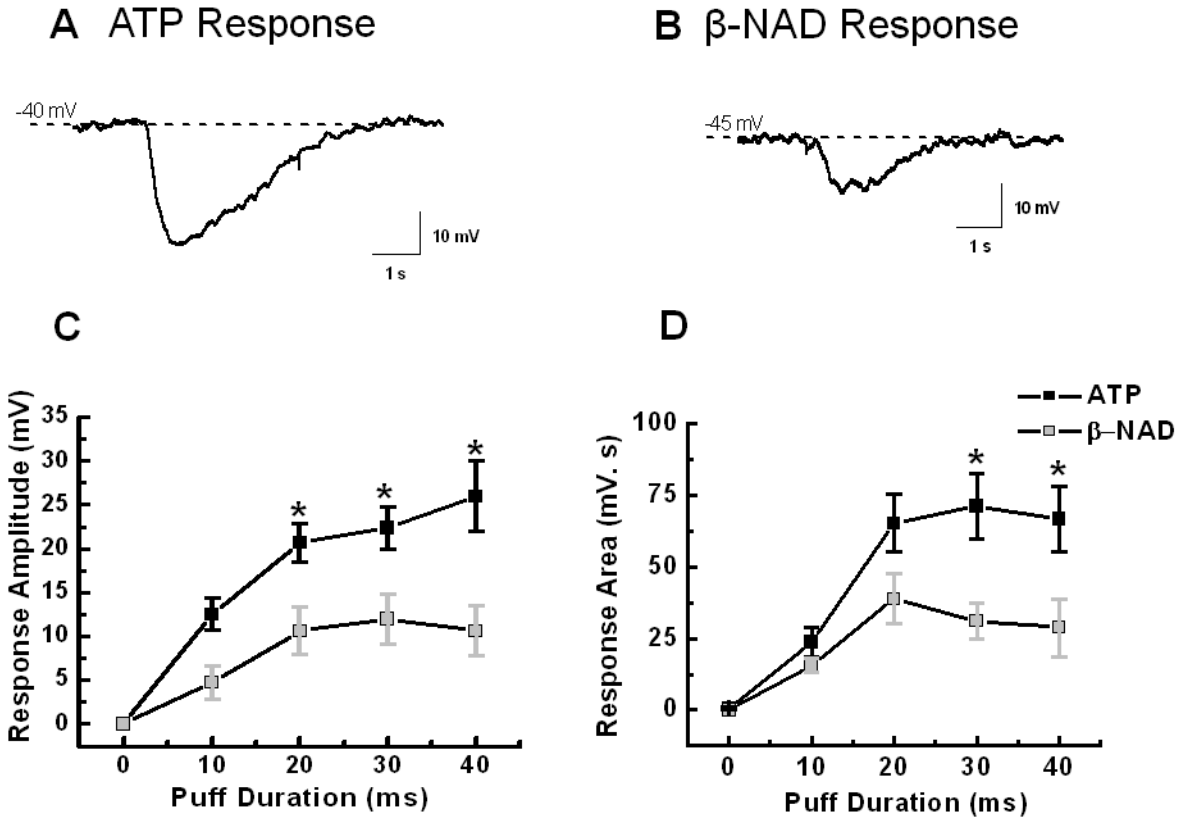

Figure 2.11 Effects of POM-1 on the amplitude and area of IJP in the mouse distal colon. (A) POM-1 application depolarized the membrane potential by 3 ± 3 mV. (B) Time course of POM-1 application on normalized IJP. (C) POM-1 inhibits both the amplitude and the area of the IJP by 76 ± 7% and 66 ± 14% respectively. (D) Representative trace of effect of POM-1 on IJP. Data are mean ± S.E.M (n=6, *p<0.05)

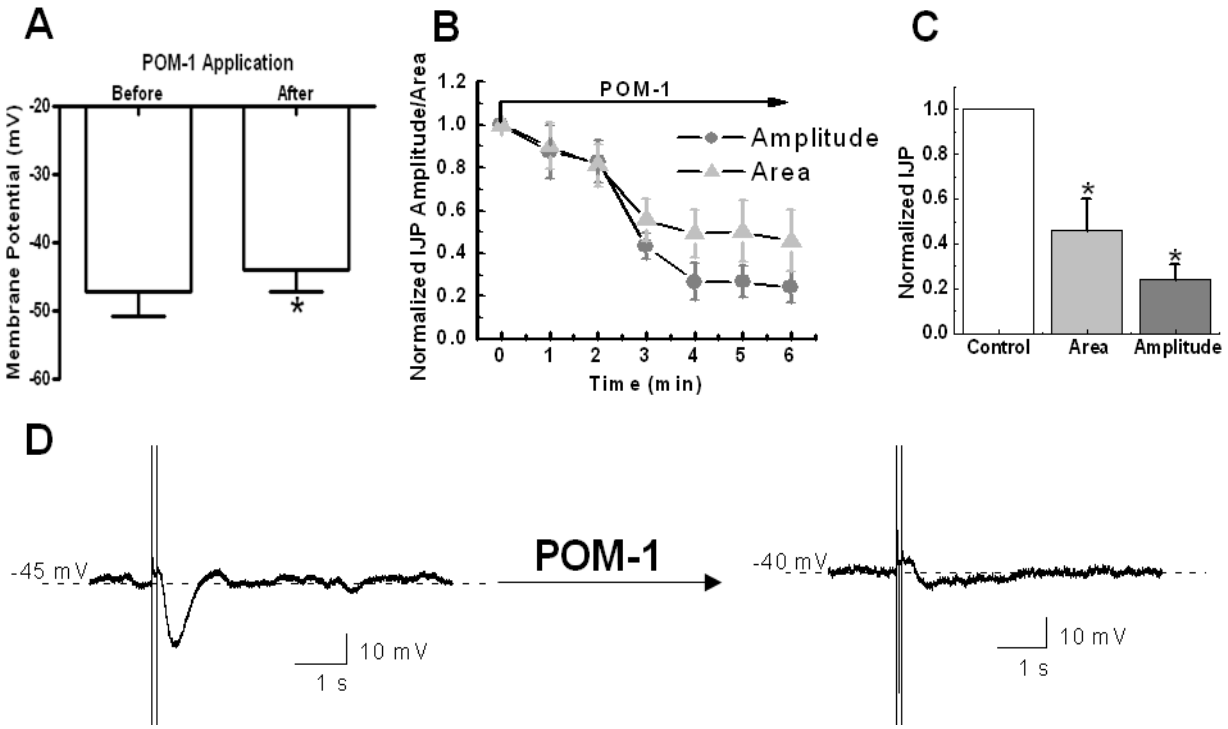

Figure 2.12 Effect of POM-1 on ATP response.

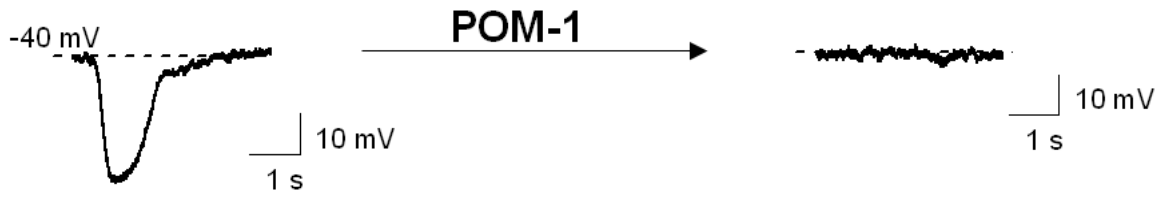

Figure 2.13 Effect of POM-1 on exogenous Adenosine 5′-[β-thio]diphosphate (ADP-β-S). ADP-β-S (5 mM), a stable ADP analogue produced prominent hyperpolarizing responses. Application of POM-1 did not inhibit ADP-β-S induced hyperpolarizing responses.

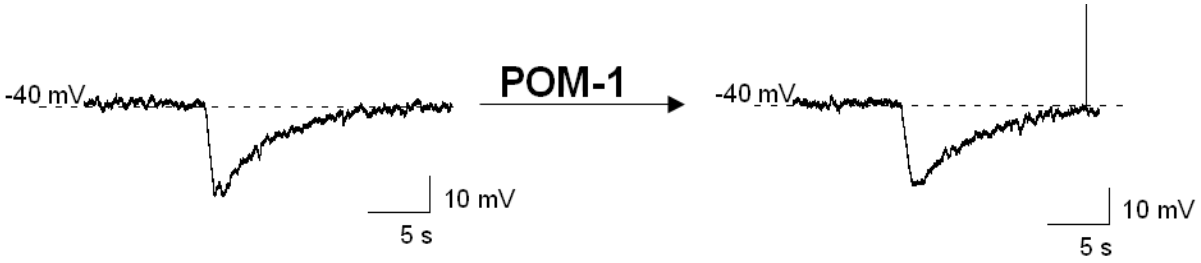

Figure 2.14 Effect of MRS 2179 on exogenous ADP-β-S. ADP-β-S (5 mM) produced a prominent hyperpolarization, which was reversibly blocked by MRS 2179 (100 μM), a P2Y1 receptor antagonist.

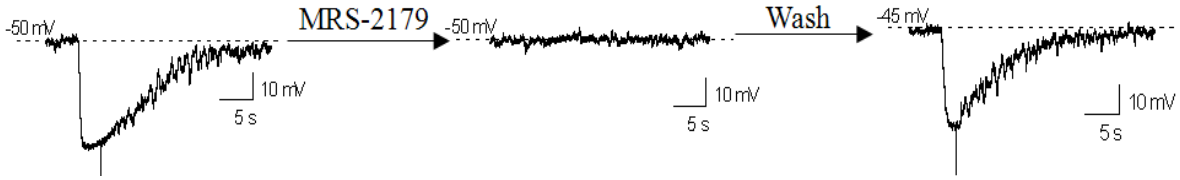

2.5 Discussion

These results provide evidence that IJPs are mediated by a purine and NO and involve P2Y1 receptors, SK and the $I_{Cl(Ca)}$ channels based on following data: 1) blockade of the IJP by MRS-2179 and L-NNA, 2) blockade of the IJP by apamin and NFA, 3) blockade of the IJP and ATP responses by POM 1, and 4) blockade of ADP-β-S responses by MRS 2179.

The fIJP is mediated via purinergic signaling mechanisms (Xue *et al.*, 1999). Purinergic signaling is complex because there are several nucleotide candidate mediators including ATP, ADP, UTP, UDP and β-NAD, which activate multiple P2 receptors (Burnstock, 2006a). In this study MRS-2179, a P2Y1 receptor specific antagonist reduced peak IJP amplitude but not duration. This suggests that IJP is at least in part mediated by P2Y1 receptors.

NO signaling produces a smaller amplitude but longer lasting slow hyperpolarization (sIJP) (Serio *et al.*, 2003; El-Mahmoudy *et al.*, 2006; Grasa *et al.*, 2009; Mañé *et al.*, 2014). NO is produced in the myenteric neurons via activation of Ca^{2+} sensitive nNOS. We found that L-NNA, a nNOS inhibitor, significantly decreased IJP area but not amplitude. This suggests that NO acts on post junctional smooth muscle target to mediate MRS 2179 insensitive sIJP. Neither MRS 2179 nor L-NNA changed resting membrane potential. Co-application of MRS 2179 and L-NNA completely blocked the IJP without changing resting membrane potential.

P2Y1 receptor activation leads to increase in intracellular Ca^{2+} concentration via inositol triphosphate (IP_3) dependent Ca^{2+} release from the intracellular stores (Hu *et al.*, 2003; Matsuda & Miller, 2010). NO production on the other hand, leads to activation of guanylate cyclase (GC) in the smooth muscle (El-Mahmoudy *et al.*, 2006). GC catalyzes the conversion of GTP to cyclic GMP which activates protein kinase G (PKG) (Carvajal *et al.*, 2000; El-Mahmoudy *et al.*, 2006). The increase in intracellular Ca^{2+} concentration and PKG production activate different

ion channels to mediate IJP either directly via activation of Ca^{2+} dependent K^+ channels or indirectly via PKG dependent phosphorylation of K^+ channels (Matsuda & Miller, 2010). PKG also phosphorylates phospholamban (PLB) which causes disinhibition of smooth endoplasmic reticulum Ca^{2+} ATPase (SERCA) and reduces $[Ca^{2+}_i]$. Subsequent reduction in $[Ca^{2+}_i]$ leads to closure of Ca^{2+}-activated Cl^- channels (Hartzell *et al.*, 2005).

Therefore in order to delineate the ion channels mediating IJPs, apamin was used to block smooth muscle SK channels. Apamin depolarized the membrane potential and reduced IJP area and amplitude. However, there was a significant proportion of IJP that were apamin and paxilline (data not shown) insensitive (Zhang *et al.*, 2000; Zhang *et al.*, 2010).

Previous studies showed that closure of CaCCs causes IJPs in opossum esophageal smooth muscle and in guinea pig ileum (Zhang & Paterson, 2002). In the guinea pig ileum, apamin insensitive IJPs had a reversal potential of -25 mV, which was close to Cl^- reversal potential (-20-30 mV) suggesting that Cl^- ion mediates junction potential in these tissues (Crist *et al.*, 1991). It is hypothesized that subplasmalemmal Cl^- efflux from Cl^- channels is essential for Ca^{2+} efflux from the sarcoplamsic reticulum (SR) (Janssen, 2002). NFA dependent inhibition of CaCCs can therefore hyperpolarize the membrane and disrupt SR Ca^{2+} release into the subplasmalemmal space, which is essential for IJP production (Cruickshank *et al.*, 2003). To test if CaCC contributes to IJPs in the mouse colon CaCCs blocker, NFA was used. I used lower concentration of NFA than used previously in the literature because NFA in concentrations $\geq$ 100 μM blocks cation channels in the smooth muscle (Zhang & Paterson, 2002). NFA hyperpolarizes the membrane potential and blocks both the amplitude and the area of IJPs. The NFA sensitive IJP was apamin insensitive and co-application of apamin and NFA blocked IJPs similar to MRS 2179 and L-NNA co-application. Taken together these data suggests that IJP is

mediated via ATP and NO mediated activation of SK and $I_{Cl(Ca)}$ channels. The opposing activity of SK and $I_{Cl(Ca)}$ sets the resting membrane potential of smooth muscle in the mouse distal colon.

Next, I set to identify the purine molecule involved in mediating fIJP. The literature suggests either ATP or β-NAD as the likely purine candidate involved in mediating fIJP (Xue *et al.*, 1999; Burnstock, 2006b; Hwang *et al.*, 2011). ATP and β-NAD both activate P2Y1 purinoceptors in smooth muscle. ATP and β-NAD were locally applied and their hyperpolarizing responses were measured. ATP had significantly greater response amplitude and area than β-NAD across varying puff durations suggesting greater ATP sensitivity than β-NAD.

ATP is metabolized in the extracellular space by ecto-nucleotidases (NTPDases 1,2 and 3) where it is broken down to ADP. ADP then act on post junctional P2 receptors (Müller *et al.*, 2006). ARL 67156 and polyoxotungstate 1 (POM-1) are the two major NTPDase effective drugs available (Wall *et al.*, 2008). Among these POM-1 is a more potent inhibitor of NTPDases than ARL67156 because unlike ARL67156, which only inhibits NTPDases1 and 3, POM-1 inhibits NTPDase1, 2 and 3 (Müller *et al.*, 2006). POM-1 is also more efficacious and stable in aqueous solution and biological pH than ARL67156 (Wall *et al.*, 2008). POM-1 was therefore chosen as an inhibitor of NTPDase to test if ATP plays role in regulating inhibitory neuromuscular transmission in the distal colon. POM-1 almost completely inhibits both the IJP and ATP response, suggesting that ATP puff mimics IJP production in the mouse distal colon. Small portion of POM-1 insensitive IJP are possibly NO dependent because they have much smaller amplitude but larger duration. ADP-β-S response on the other hand is insensitive to POM-1 but is blocked completely by MRS-2179 in a reversible manner. Taken together these results suggest that ATP release from the inhibitory motor neurons is the neurotransmitter involved in

mediating IJP signaling. In conclusion, these data suggests that ATP acting on P2Y1 receptors and NO affects SK and CaCCs to mediate IJP in the mouse distal colon.

BIBLIOGRAPHY

BIBLIOGRAPHY

Bane V, Lehane M, Dikshit M, O'Riordan A & Furey A. (2014). Tetrodotoxin: chemistry, toxicity, source, distribution and detection. *Toxins (Basel)* **6,** 693-755.

Burnstock G. (2006a). Purinergic signalling--an overview. *Novartis Found Symp* **276,** 26-48; discussion 48-57, 275-281.

Burnstock G. (2006b). Purinergic signalling. *Br J Pharmacol* **147 Suppl 1,** S172-181.

Carvajal JA, Germain AM, Huidobro-Toro JP & Weiner CP. (2000). Molecular mechanism of cGMP-mediated smooth muscle relaxation. *J Cell Physiol* **184,** 409-420.

Crist JR, He XD & Goyal RK. (1991). Chloride-mediated junction potentials in circular muscle of the guinea pig ileum. *Am J Physiol* **261,** G742-751.

Cruickshank SF, Baxter LM & Drummond RM. (2003). The Cl(-) channel blocker niflumic acid releases Ca(2+) from an intracellular store in rat pulmonary artery smooth muscle cells. *Br J Pharmacol* **140,** 1442-1450.

El-Mahmoudy A, Khalifa M, Draid M, Shiina T, Shimizu Y, El-Sayed M & Takewaki T. (2006). NANC inhibitory neuromuscular transmission in the hamster distal colon. *Pharmacol Res* **54,** 452-460.

Engel J. (2004). Neurologic Bladder, Bowel and Sexual Dysfunction. In *Constipation and Fecal incontinence*.

Goyal RK. (2011). Evidence for β-nicotinamide adenine dinucleotide as a purinergic, inhibitory neurotransmitter in doubt. *Gastroenterology* **141,** e27; author reply e27-28.

Grasa L, Gil V, Gallego D, Martín MT & Jiménez M. (2009). P2Y(1) receptors mediate inhibitory neuromuscular transmission in the rat colon. *Br J Pharmacol* **158,** 1641-1652.

Hartzell C, Putzier I & Arreola J. (2005). Calcium-activated chloride channels. *Annu Rev Physiol* **67,** 719-758.

Hu HZ, Gao N, Zhu MX, Liu S, Ren J, Gao C, Xia Y & Wood JD. (2003). Slow excitatory synaptic transmission mediated by P2Y1 receptors in the guinea-pig enteric nervous system. *J Physiol* **550,** 493-504.

Hwang SJ, Durnin L, Dwyer L, Rhee PL, Ward SM, Koh SD, Sanders KM & Mutafova-Yambolieva VN. (2011). β-nicotinamide adenine dinucleotide is an enteric inhibitory neurotransmitter in human and nonhuman primate colons. *Gastroenterology* **140,** 608-617.e606.

Janssen LJ. (2002). Ionic mechanisms and Ca(2+) regulation in airway smooth muscle contraction: do the data contradict dogma? *Am J Physiol Lung Cell Mol Physiol* **282,** L1161-1178.

Lies B, Gil V, Groneberg D, Seidler B, Saur D, Wischmeyer E, Jiménez M & Friebe A. (2014). Interstitial cells of Cajal mediate nitrergic inhibitory neurotransmission in the murine gastrointestinal tract. *Am J Physiol Gastrointest Liver Physiol* **307,** G98-106.

Martínez-Cutillas M, Gil V, Gallego D, Mañé N, Clavé P, Martín MT & Jiménez M. (2014). α,β-meATP mimics the effects of the purinergic neurotransmitter in the human and rat colon. *Eur J Pharmacol* **740,** 442-454.

Matsuda NM & Miller SM. (2010). Non-adrenergic non-cholinergic inhibition of gastrointestinal smooth muscle and its intracellular mechanism(s). *Fundam Clin Pharmacol* **24,** 261-268.

Mañé N, Gil V, Martínez-Cutillas M, Clavé P, Gallego D & Jiménez M. (2014). Differential functional role of purinergic and nitrergic inhibitory cotransmitters in human colonic relaxation. *Acta Physiol (Oxf)* **212,** 293-305.

Mutafova-Yambolieva VN, Hwang SJ, Hao X, Chen H, Zhu MX, Wood JD, Ward SM & Sanders KM. (2007). Beta-nicotinamide adenine dinucleotide is an inhibitory neurotransmitter in visceral smooth muscle. *Proc Natl Acad Sci U S A* **104,** 16359-16364.

Müller CE, Iqbal J, Baqi Y, Zimmermann H, Röllich A & Stephan H. (2006). Polyoxometalates--a new class of potent ecto-nucleoside triphosphate diphosphohydrolase (NTPDase) inhibitors. *Bioorg Med Chem Lett* **16,** 5943-5947.

Serio R, Alessandro M, Zizzo MG, Tamburello MP & Mulè F. (2003). Neurotransmitters involved in the fast inhibitory junction potentials in mouse distal colon. *Eur J Pharmacol* **460,** 183-190.

Smyth LM, Bobalova J, Mendoza MG, Lew C & Mutafova-Yambolieva VN. (2004). Release of beta-nicotinamide adenine dinucleotide upon stimulation of postganglionic nerve terminals in blood vessels and urinary bladder. *J Biol Chem* **279,** 48893-48903.

Wall MJ, Wigmore G, Lopatár J, Frenguelli BG & Dale N. (2008). The novel NTPDase inhibitor sodium polyoxotungstate (POM-1) inhibits ATP breakdown but also blocks central synaptic transmission, an action independent of NTPDase inhibition. *Neuropharmacology* **55,** 1251-1258.

Xue L, Farrugia G, Sarr MG & Szurszewski JH. (1999). ATP is a mediator of the fast inhibitory junction potential in human jejunal circular smooth muscle. *Am J Physiol* **276,** G1373-1379.

Zhang Y, Lomax AE & Paterson WG. (2010). P2Y1 receptors mediate apamin-sensitive and -insensitive inhibitory junction potentials in murine colonic circular smooth muscle. *J Pharmacol Exp Ther* **333,** 602-611.

Zhang Y, Miller DV & Paterson WG. (2000). Opposing roles of K(+) and Cl(-) channels in maintenance of opossum lower esophageal sphincter tone. *Am J Physiol Gastrointest Liver Physiol* **279,** G1226-1234.

Zhang Y & Paterson WG. (2002). Role of Ca2+-activated Cl- channels and MLCK in slow IJP in opossum esophageal smooth muscle. *Am J Physiol Gastrointest Liver Physiol* **283,** G104-114.

CHAPTER 3

β1BK CHANNEL REGULATES SMOOTH MUSCLE EXCITABILITY IN THE MOUSE DISTAL COLON.

3.1 Abstract

Smooth muscle specific large conductance Ca^{2+} activating K^+ (β1BK) channels consist of an α and β1 subunit. The α subunit is a pore forming subunit while the β1 subunit modulates channel gating and activation properties. β1BK channel plays an important role in regulating cellular excitability and neurotransmitter release in the neuromuscular junction. Altered β1 subunit expression disrupts coupling between Ca^{2+} spark and β1BK channel mediated outward K^+ currents resulting in increased muscle tone and excitability in urinary bladder, vascular and tracheal smooth muscles. However, its effect on GI smooth muscle is yet unknown. I therefore studied the effects of β1BK channel function on neuromuscular transmission and colonic smooth muscle excitability *in-vitro* using WT and BK β1-subunit KO mice. I found that while β1-subunit KO mice do not show any impairment in inhibitory junction potential (IJPs), the smooth muscles in β1-subunit KO have a depolarized membrane potential and higher action potential firing frequency. This suggests that although β1BK channels are not involved in mediating neuromuscular transmission, they are crucial in regulating smooth muscle excitability in the mouse distal colon.

3.2 Introduction

Large conductance Ca^{2+} activating K^+ (BK) channels are voltage gated and Ca^{2+} sensitive channels that lead to net K^+ efflux causing membrane hyperpolarization. BK channels are expressed in various cells types including skeletal muscle cell (Tricarico *et al.*, 2005), smooth muscle cell (Brenner *et al.*, 2000b; Chang *et al.*, 2006; Rueda *et al.*, 2013; Shi *et al.*, 2013a; Zheng *et al.*, 2013), neurons (Meera *et al.*, 2000) and endocrine cells (Braun *et al.*, 2008). BK channel consists of an α and β subunit. The α subunit is a pore forming subunit while the β-subunit is an accessory subunit that enhances Ca^{2+} sensitivity of the pore forming α subunit (Nelson *et al.*, 1995; Brenner *et al.*, 2000b; Cox & Aldrich, 2000; Ohi *et al.*, 2001; Qian & Magleby, 2003; Sweet & Cox, 2009). Based on molecular and electrophysiological studies, 4 different β-subunits (β1-β4) of BK channel have been identified (Brenner *et al.*, 2000a). Among these subunits, the β1 subunit in particular is smooth muscle specific and plays a vital role to mediate smooth muscle tone in vascular (Leo *et al.*, 2014; Pabbidi *et al.*, 2014) and urinary bladder (Petkov *et al.*, 2001) smooth muscle cells. In smooth muscle β1BK channels are located very close to intracellular calcium release sites. When Ca^{2+} enters through L-type calcium channels, it activates further Ca^{2+} release through ryanodine receptors (via Ca^{2+} induced Ca^{2+} release mechanisms) of the smooth endoplasmic reticulum resulting in high intracellular Ca^{2+} (>10 μmol L^{-1}) concentration. Increase in intracellular Ca^{2+} above the threshold activates β1BK channel and initiates spontaneous transient outward current to cause closure of L type Ca^{2+} channels and smooth muscle relaxation (Nelson *et al.*, 1995; Bolton & Imaizumi, 1996). Although altered expression of β1subunit of the BK channel impairs vascular smooth muscle and urinary bladder smooth muscle relaxation to cause hypertension (Plüger *et al.*, 2000; Yang *et al.*,

2013), heart failure (Wan *et al.*, 2013), and urinary bladder over-activity (Petkov *et al.*, 2001) the functional effect of altered β1BK channel expression in GI smooth muscles is yet unknown.

The β1-subunit KO mouse model has been studied in myocytes from urinary bladder (Petkov *et al.*, 2001), trachea (Semenov *et al.*, 2006; Evseev *et al.*, 2013) and colon (Hagen *et al.*, 2003) where they exhibit lower β1BK channel open probabilities and reduced coupling of Ca^{2+} sparks and outward K^+ currents. In addition, the BK channel also controls quantal release of neurotransmitter in the neuromuscular junction (Wang *et al.*, 2001). I therefore hypothesized that reduced coupling of Ca^{2+} sparks and β1BK channel mediated spontaneous outward K^+ currents in β1-subunit KO mice leads to impaired neuromuscular communication and/or altered smooth muscle excitability in the mouse distal colon. In order to test this hypothesis I used intracellular recordings and measured inhibitory junction potentials (IJPs) and action potential firing activity in the GI smooth muscle cells.

3.3 Materials and Methods

3.3.1 Ethics Statement

All studies were conducted in accordance with the National Institutes of Health Guide for the Care and Use of Laboratory Animals (NIH Publication No. 85-23, revised 1996) and approved by Institutional Animal Care and Use Committee of Michigan State University.

3.3.2 Animals

All animal use protocols were approved by the Institutional Animal Care and Use Committee at Michigan State University. Homozygous β1-subunit KO mice were obtained from Dr. Robert Brenner, University of Texas Health Science Center at San Antonio and bred in-house at Michigan State University. C57BL/6 (WT) mice were either fed standard chow diet, control diet (10 kcal% fat; D12450B) or HF diet (60 kcal% fat; D12492), all from Jackson Laboratories (Bar Harbor, ME, USA). β1-subunit KO mice were weaned at 3 weeks of age. Mice consuming normal diet were studied at 10–12 weeks of age (male, 25–30 g) and mice on control or HF diets were studied at 18-22 weeks (male, 30-52 g). Mice were euthanized using isoflurane anesthesia followed by cervical dislocation.

3.3.3 Electrophysiological recordings

Conventional intracellular electrophysiological techniques were used to record IJPs and smooth muscle electrical activity in the distal colon of WT and β1-subunit KO mice. Small segments of distal colon were placed in a petri dish containing Krebs buffer solution. The segment was cut open along the mesenteric border and pinned flat. The mucosa and submucosa were removed using fine forceps. A ~5 mm^2 section was cut out and transferred to a silastic elastomer-lined recording chamber. The section was stretched lightly and pinned to the chamber floor using small stainless steel pins. The chamber was placed on the stage of an inverted

microscope and the chamber was then perfused with oxygenated (95% O_2, 5% CO_2) Krebs buffer solution (37 °C) at a flow rate of 3 mL min^{-1}. Drugs were added in known concentrations to the flowing Krebs solution using a system of three-way stopcocks. Drug concentrations reached steady state in the recording chamber within 4 min.

Smooth muscle cells were impaled with glass microelectrodes (filled with 2 M KCl, tip resistance = 60–90 MΩ). IJPs were recorder in presence and in absence of nifedipine (1μM). Although the tissue was anchored to the floor of the recording chamber, there was still substantial muscle movement throughout the recording periods when nifedipine was not applied. Despite this complication, it was possible to maintain impalements for periods of 2–60 min. Membrane potential was recorded using an Axoclamp 2A amplifier, a Digidata 1322A analog-digital converter, and Axoscope 9.2 software (all from Molecular Devices, Sunnyvale, CA, USA). Data were only collected and analyzed from individual recordings that lasted ≥ 2 min.

3.3.4 Drugs

Drugs and reagents were obtained from Sigma Aldrich Chemical Company (St. Louis, MO, USA).

3.3.5 Statistics

Two group comparisons were made using two-way ANOVA with Bonferroni post-hoc test, paired or unpaired Student's t-test, and Fisher's exact test. $p < 0.05$ was considered statistically significant. Data are reported as mean ± SEM.

3.4 Results

3.4.1 β1Bk channel does not mediate inhibitory neuromuscular transmission in the mouse distal colon

To assess if β1BK channels play a role in mediating neuromuscular transmission in mouse distal colon, I stimulated colonic tissues at varying voltage (20 -140 V) and measured the corresponding amplitude and the area of the IJPs in presence and in absence of nifedipine. I found that both the amplitude and the area of IJPs were similar between WT and β1-subunit KO either in presence or in absence of nifedipine ($p>0.05$, two-way Anova with Bonferroni post-hoc).

Figure 3.1 IJP measurements from WT and β1-subunit KO. Voltage – Amplitude/Area calibration curve in presence (A and B) and in absence (C and D) of nifedipine. Amplitude (A and C) and the area (B and D) of the inhibitory junction potentials (IJPs) are similar between WT and KO.

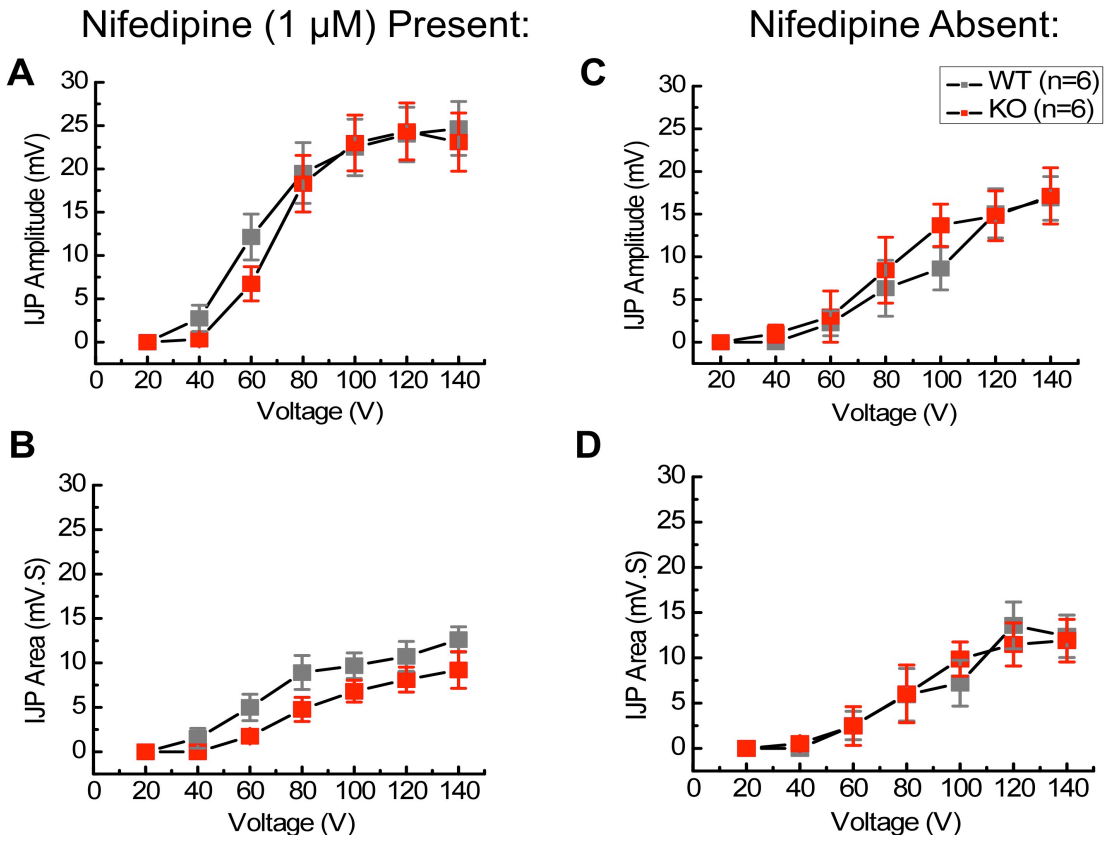

Since IJPs were not disrupted in β1-subunit KO mice, we tested if paxilline, a α subunit blocker of the BK channel plays a role in mediating IJPs. I applied paxilline (0.5 μmol L^{-1}) on colonic smooth muscles preparation and found that paxilline had no effect on either the amplitude or the area of the IJP. However, apamin (0.1μmol L^{-1}), a SK channel blocker significantly decrease both the amplitude and the area of the IJP in both wild type and β1-subunit KO.

Figure 3.2 Effects of paxilline on IJPs. Paxilline did not impair the either the (A) Amplitude or the (B) Area of IJP in β1-subunit KO mice. Data are represented as normalized values.

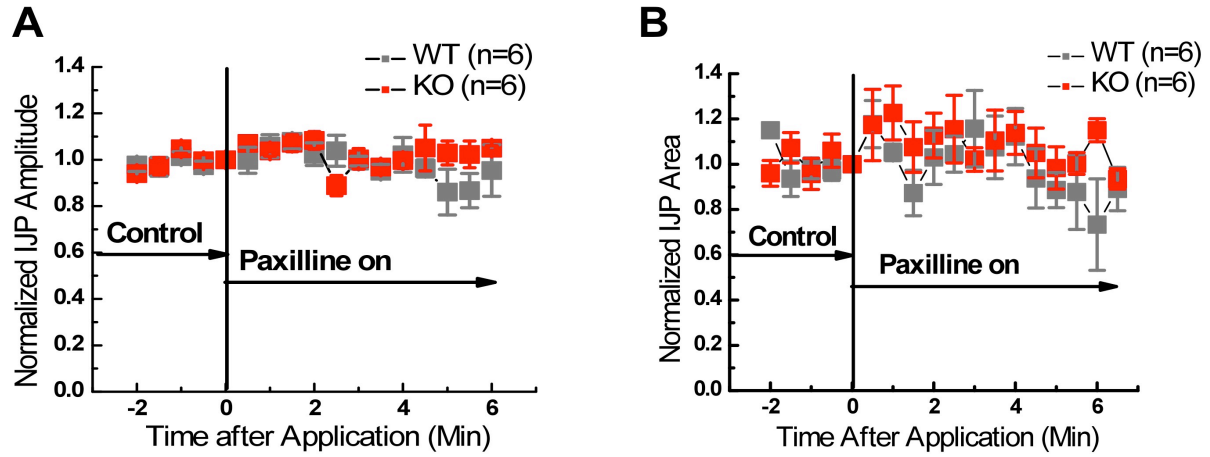

Figure 3.3 Effect of co-application of apamin and paxilline on IJPs. Apamin and paxilline co-application significantly decreased both the IJP amplitude and area by 50 ± 5%, and 62 ± 6% respectively in both wild type and β1-subunit KO. Data are represented as normalized values.

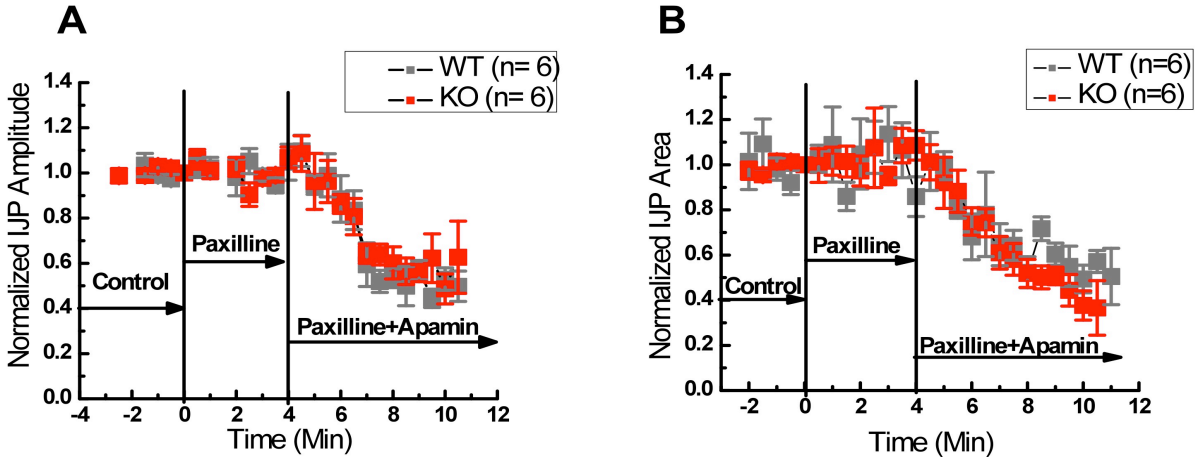

3.4.2 Tetrodotoxin (TTX) application does not block smooth muscle action potential in colonic smooth muscles

Since IJPs were not impaired in either in β1-subunit KO mice or in paxilline applied tissues, we conclude that β1BK channel do not play a role in mediating IJPs. I tested if β1BK channels mediate smooth muscle excitability and action potential firing. In order to study how β1BK channel affect smooth muscle excitability and action potential firing, intracellular recordings were obtained from circular smooth muscle cells *in-vitro* in the distal colon of WT and β1-subunit KO mice in absence of nifedipine. I verified that the action potentials were non neurogenic by applying TTX (0. 3 μmol L^{-1}), a Na^{+} channel blocker. TTX did not block action potential generation in muscles from either WT or β1-subunit KO mice.

Figure 3.4 Effect of tetrodotoxin (TTX) on smooth muscle action potential. TTX does not block action potential generation from colonic smooth muscles verifying non-neuronal action potential firing.

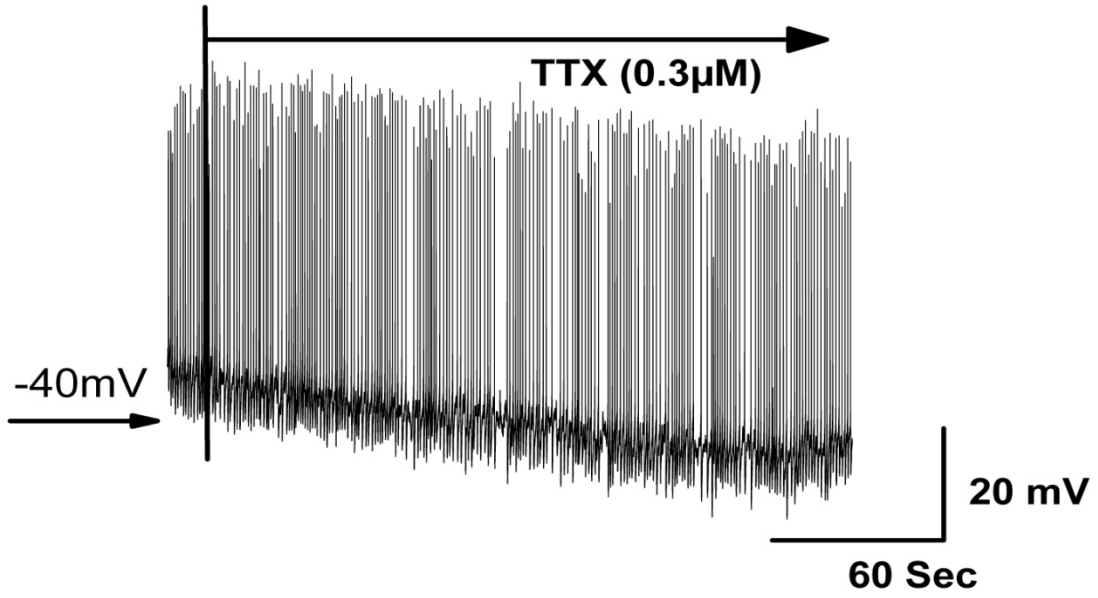

3.4.3 Increased action potential activity in distal colonic smooth muscle from β1-subunit KO mice

I used intracellular recording to measure smooth muscle action potentials in WT and β1-subunit KO mice. Recordings were obtained from 42 cells in distal colonic tissues from 11 WT mice. I found that action potential firing occurred in short bursts with a 10.4 ± 0.6 s interburst interval in 30 cells whereas action potentials occurred continuously in the remaining 12 cells in WT (Figure 3.5A). Recordings were obtained from 29 cells in distal colonic tissues from seven β1-subunit KO mice. In KOs, action potential firing occurred continuously in 23 cells whereas bursting occurred in the remaining six cells (Figure 3.5B). The proportion of bursting cells was significantly higher in WT compared to β1-subunit KO mice ($p<0.05$, Fisher's exact test). The average action potential firing frequency was also greater in tissues from β1-subunit KO compared to WT mice (Figure 3.5C). The resting membrane potential in circular smooth muscle cells from the distal colon of β1-subunit KO mice was significantly more depolarized compared to that in WT preparations (Figure 3.5D).

Figure 3.5 Action potential firing pattern in WT and β1-subunit KO. (A) Representative recording of action potential firing pattern in the distal colon of a WT mice. Action potentials occur in short bursts with a ~10 s inter-burst interval. (B) Recording of continuous action potential firing in the distal colon of a β1-subunit KO mouse. (C) Mean action potential firing rate is greater in distal colon of β1-subunit KO (*n*=31 cells from 7 mice) compared to WT (*n*=42 cells from 11 mice) mice (*p<0.05). (D) Resting membrane potential in distal colon circular smooth muscle cells were more depolarized from β1-subunit KO compared to WT mice in absence of nifedipine (*p<0.05). Reprinted from Neurogastroenterology & Motility, volume 24, France et al., Impaired propulsive motility in the distal but not proximal colon of BK channel β1-subunit knockout mice, p e450-9, copyright (2012).

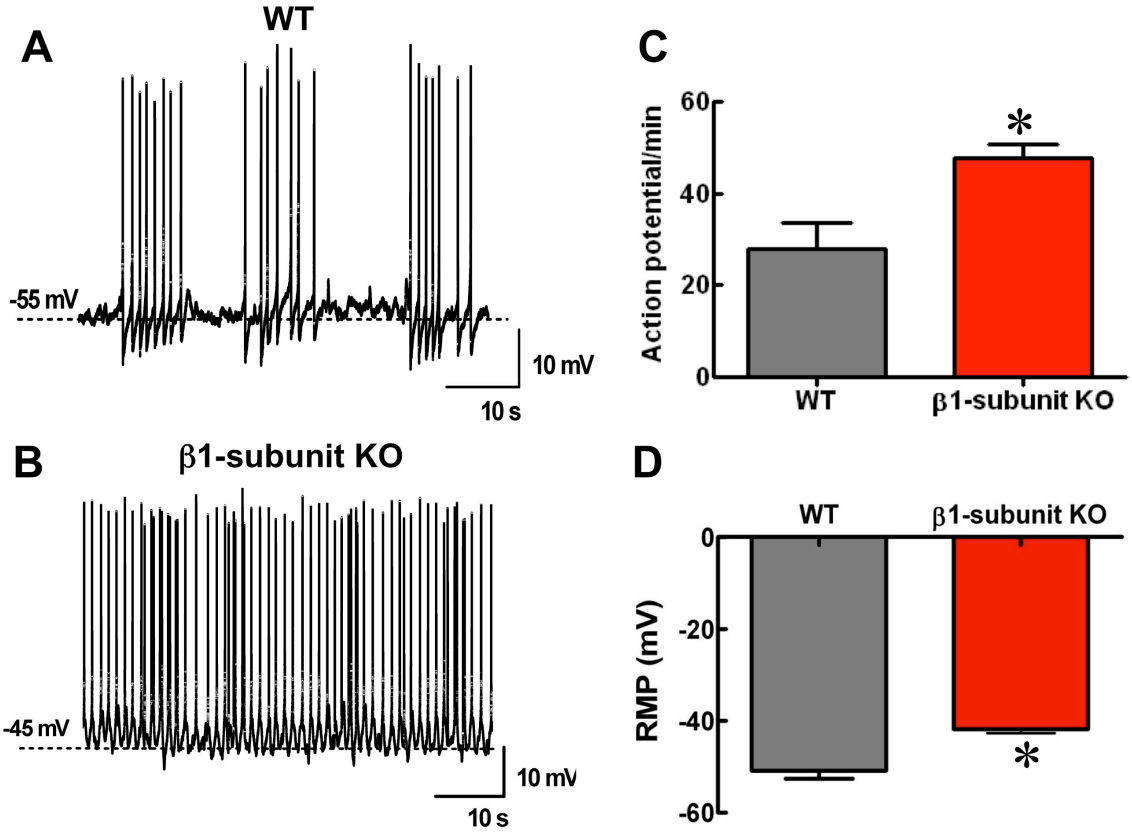

3.4.4 Effects of nifedipine application in action potential generation and smooth muscle membrane potential in WT and β1-subunit KO

The L-type Ca^{2+} channel antagonist nifedipine (1 μmol L^{-1}) completely blocked action potential firing in distal colon circular smooth muscle cells from WT and β1-subunit KO mice (Figure 3.6). Nifedipine depolarized the membrane potential in distal colon circular smooth muscle cells from WT mice (Figure 3.6A, mean depolarization after 5 min nifedipine application =4.4 ± 2.2 mV). Conversely, nifedipine did not change the membrane potential of distal colon smooth muscle cells from β1-subunit KO mice (Figure 3.6B, mean depolarization after 5 min nifedipine application = 2.6 ± 2.3 mV). No difference in resting membrane potential was seen after nifedipine application.

Figure 3.6 Nifedipine blocks action potential firing in WT and BK β1-subunit KOs. Nifedipine caused a small depolarization in tissues from WT but not BK β1-subunit KO mice. (C) RMP was similar in both WT and β1-subunit KO in presence of nifedipine (1 μM). Reprinted from Neurogastroenterology & Motility, volume 24, France et al., Impaired propulsive motility in the distal but not proximal colon of BK channel β1-subunit knockout mice, p e450-9, copyright (2012).

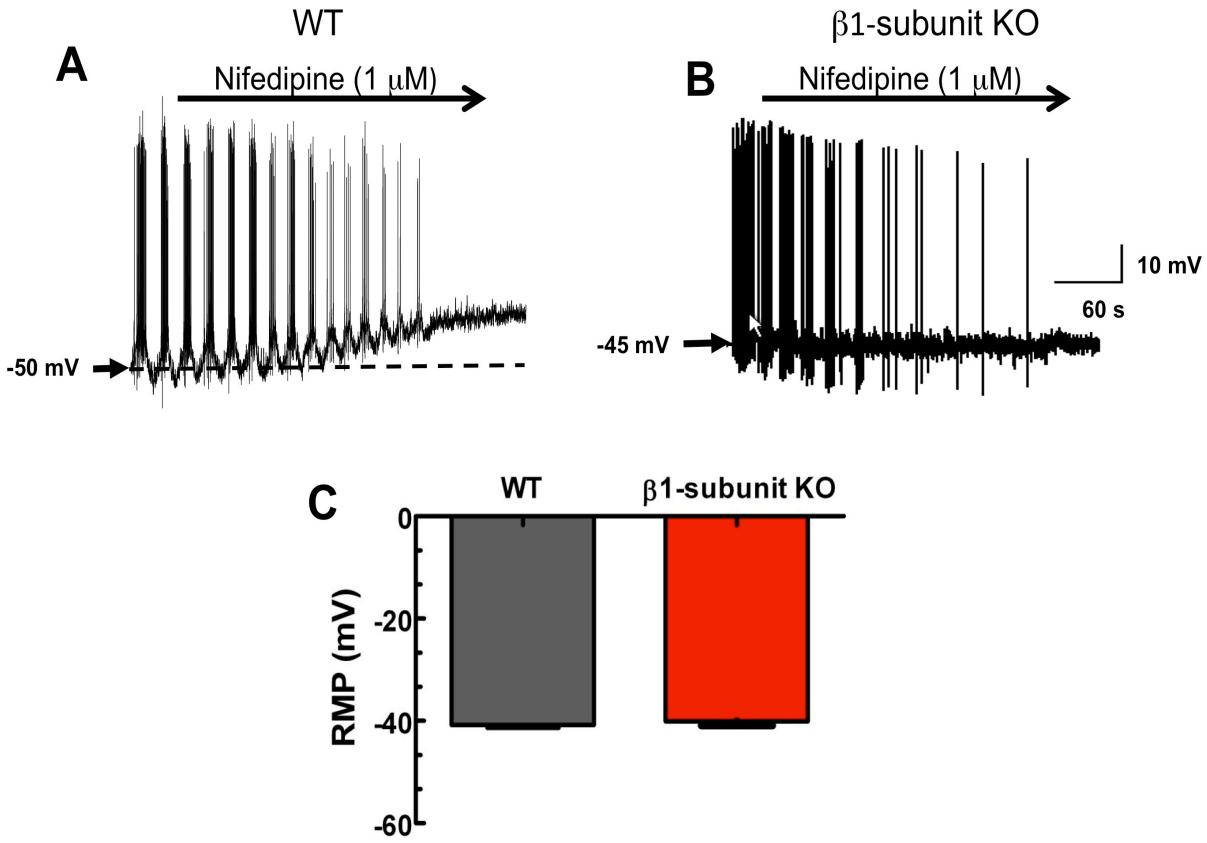

3.4.5 Effects of Paxilline on membrane potential and action potential firing in distal colonic smooth muscle of WT mice

Since paxilline is a BK channel blocker, it would be expected that paxilline treatment should mimic the effects of β1-subunit KO. Paxilline treatment for a minimum of 4 min caused a membrane potential depolarization Figure 3.7, top trace). Paxilline did not change the bursting action potential firing pattern, but it did cause an increase in the number of action potentials during each burst (Figure 3.7, bottom traces) suggesting that blocking the BK channel has different effects on smooth muscle activity compared with deletion of a molecular component of the channel.

Figure 3.7 Effect of paxilline on smooth muscle action potential firing. Upper trace shows a slow time base recording of action potential bursting in WT distal colonic smooth muscles. Paxilline causes a membrane depolarization but action potential bursting persists. Lower traces show expanded views of action potential bursting in the absence (left) and presence (right) of paxilline. Paxilline caused a prolongation of the bursts of action potentials. Reprinted from Neurogastroenterology & Motility, volume 24, France et al., Impaired propulsive motility in the distal but not proximal colon of BK channel β1-subunit knockout mice, p e450-9, copyright (2012).

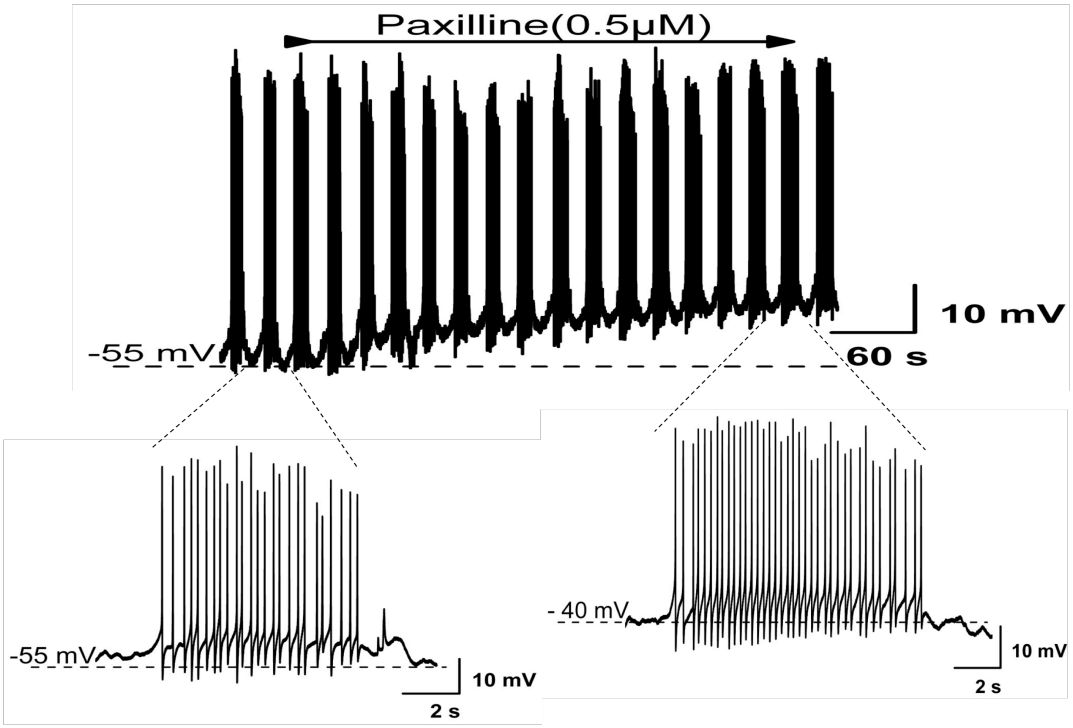

Figure 3.8 Effect of paxilline on smooth muscle membrane potential. Paxilline caused a significant depolarization in distal colon smooth muscle cells from WT mice (recordings from 9 cells from 3 mice) (*p<0.05). Paxilline also caused an increase in the number of action potentials per burst (*p<0.05). Reprinted from Neurogastroenterology & Motility, volume 24, France et al., Impaired propulsive motility in the distal but not proximal colon of BK channel β1-subunit knockout mice, p e450-9, copyright (2012).

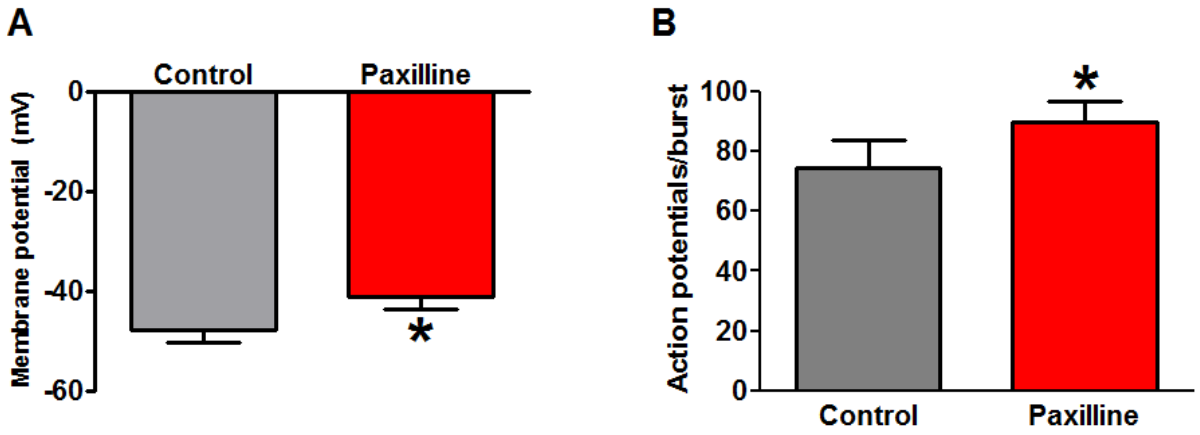

3.5 Discussion

My *in vitro* data indicate that although β1BK channel function is not important to maintain inhibitory neuromuscular communication, it is crucial to maintain the resting membrane potential and rhythmic action potential firing in the mouse distal colonic smooth muscles.

I tested if β1Bk channel plays a role in mediating inhibitory neuromuscular communication and smooth muscle excitability in the distal colon by measuring IJPs and action potential activity in WT and β1-subunit KO. Mouse distal colon was the tissue of interest because unlike small intestine and proximal colon whose function is to absorb nutrients and water from the gut lumen, distal colon is primarily a storage organ, hence, the greater need for smooth muscle relaxation (which would be facilitated by BK channel activity).

Nifedipine was applied to prevent spontaneous smooth muscle contraction and obtain stable impalements. I measured IJPs from WT and β1-subunit KOs but could detect any difference in either the amplitude or the area of IJPs. Since nifedipine blocks L-type voltage gated calcium channels and prevents Ca^{2+} entry to the cells, it is possible that application of nifedipine drops intracellular calcium level below the threshold needed for β1BK channel function (1-10μM). In order to address this issue, the amplitude and the area of IJPs were measured in absence of nifedipine. However, no significant difference between WT and β1-subunit KOs were found. This suggests inhibitory neuromuscular transmission is not impaired in β1-subunit KOs. Next I applied paxilline in order to study if the α subunit of BK channel plays a role in mediating inhibitory neuromuscular transmission. Paxilline did not disrupt IJPs in both WT and β1-subunit KOs, however, apamin a SK channel blocker significantly disrupted IJPs in both tissues. This suggests that unlike SK channels, β1BK channel does not participate in mediating inhibitory neuromuscular communication in the mouse distal colon.

Next I tested if the β1BK channel regulates smooth muscle excitability. Since β1BK channels are activated by Ca^{2+} induced Ca^{2+} release from intracellular stores and the β1-subunit modulates channel function by increasing Ca^{2+} sensitivity (Ohi *et al.*, 2001; Qian & Magleby, 2003; Sweet & Cox, 2009), absence of the β1-subunit would reduce Ca^{2+} sensitivity and therefore reduce channel opening. Reductions in outward K^+ currents would increase smooth muscle excitability (Petkov *et al.*, 2001; Semenov *et al.*, 2011). This theory is supported by my electrophysiological data where I found that action potential firing is increased in β1-subunit KO mice as seen by continuous action potential firing in distal colon smooth muscle cells from these mice. Conversely, action potentials occurred in short bursts with an interburst interval of ~10 s in WT mice.

Action potentials in all smooth muscle cells were Na^+ independent and Ca^{2+}-dependent because the L-type Ca2+ channel antagonist, nifedipine, blocked action potentials while TTX could not. Bursting behavior in WT cells would result from Ca^{2+} entry during action potential generation subsequently activating BK channels and bringing the membrane potential below action potential threshold. Firing would cease until intracellular Ca^{2+} levels fell below those needed to activate BK channels allowing the membrane to depolarize again leading to another burst of action potentials. In β1-subunit KO cells, the BK channel would be less sensitive to Ca^{2+} and would not open during intracellular Ca^{2+} increases that would occur during action potential bursts. Post-burst hyperpolarization would be absent and therefore smooth muscle cells could fire action potentials continuously. Continuous firing would also be driven by the depolarized membrane potential as measured in β1-subunit KO smooth muscle cells. The BK channel blocker, paxilline partially mimicked the effects of β1-subunit KO. Paxilline caused a depolarization in smooth muscle membrane potential supporting the role of the BK channel in

regulating membrane potential of the smooth muscle cells. However, paxilline did not change the action potential firing pattern from bursting to continuous in WT tissues. In the presence of paxilline, bursting behavior was sustained but the duration of each burst was prolonged. These data suggest that blocking the BK channel has different effects on smooth muscle activity compared with deletion of a molecular component of the channel. Alternatively, there may be other molecular changes in the mechanisms controlling smooth muscle excitability in response to β1-subunit KO that are not mimicked by acute pharmacological blockade of the BK channel.

Nifedipine caused a depolarization in distal colon smooth muscle cells from WT, but not β1-subunit KO mice. This is consistent with Ca^{2+} entry through L-type Ca^{2+} channels driving BK channel activation and hyperpolarization of the membrane potential. In the absence of the β1-subunit, the α-subunit is less sensitive to Ca^{2+} activation and therefore the membrane potential of smooth muscle cells is less polarized. As stated above, nifedipine was able to block action potentials in both WT and β1-subunit KO cells. In β1-subunit KO cells, action potentials occur continuously until the addition of nifedipine. Nifedipine acts to reduce gradually the action potential firing frequency as nifedipine concentrations slowly reached a steady state level. Firing frequency decreased but I did not detect bursting in β1-subunit KO cells as action potentials fired continuously, but at a progressively lower frequency.

In conclusion these data suggests that while β1BK channel do not play a major role in mediating inhibitory neuromuscular transmission, it is imperative to maintain smooth muscle excitability in the mouse distal colon. Genetic KO of β1-subunit could therefore lead to disrupted colonic propulsive motility patterns (France *et al.*, 2012).

BIBLIOGRAPHY

BIBLIOGRAPHY

Bolton TB & Imaizumi Y. (1996). Spontaneous transient outward currents in smooth muscle cells. *Cell Calcium* **20,** 141-152.

Braun M, Ramracheya R, Bengtsson M, Zhang Q, Karanauskaite J, Partridge C, Johnson PR & Rorsman P. (2008). Voltage-gated ion channels in human pancreatic beta-cells: electrophysiological characterization and role in insulin secretion. *Diabetes* **57,** 1618-1628.

Brenner R, Jegla TJ, Wickenden A, Liu Y & Aldrich RW. (2000a). Cloning and functional characterization of novel large conductance calcium-activated potassium channel beta subunits, hKCNMB3 and hKCNMB4. *J Biol Chem* **275,** 6453-6461.

Brenner R, Peréz GJ, Bonev AD, Eckman DM, Kosek JC, Wiler SW, Patterson AJ, Nelson MT & Aldrich RW. (2000b). Vasoregulation by the beta1 subunit of the calcium-activated potassium channel. *Nature* **407,** 870-876.

Chang T, Wu L & Wang R. (2006). Altered expression of BK channel beta1 subunit in vascular tissues from spontaneously hypertensive rats. *Am J Hypertens* **19,** 678-685.

Cox DH & Aldrich RW. (2000). Role of the beta1 subunit in large-conductance Ca(2+)-activated K(+) channel gating energetics. Mechanisms of enhanced Ca(2+) sensitivity. *J Gen Physiol* **116,** 411-432.

Evseev AI, Semenov I, Archer CR, Medina JL, Dube PH, Shapiro MS & Brenner R. (2013). Functional effects of KCNQ K(+) channels in airway smooth muscle. *Front Physiol* **4,** 277.

France M, Bhattarai Y, Galligan JJ & Xu H. (2012). Impaired propulsive motility in the distal but not proximal colon of BK channel β1-subunit knockout mice. *Neurogastroenterol Motil* **24,** e450-459.

Hagen BM, Bayguinov O & Sanders KM. (2003). Beta 1-subunits are required for regulation of coupling between Ca2+ transients and Ca2+-activated K+ (BK) channels by protein kinase C. *Am J Physiol Cell Physiol* **285,** C1270-1280.

Leo MD, Bannister JP, Narayanan D, Nair A, Grubbs JE, Gabrick KS, Boop FA & Jaggar JH. (2014). Dynamic regulation of β1 subunit trafficking controls vascular contractility. *Proc Natl Acad Sci U S A* **111,** 2361-2366.

Meera P, Wallner M & Toro L. (2000). A neuronal beta subunit (KCNMB4) makes the large conductance, voltage- and Ca2+-activated K+ channel resistant to charybdotoxin and iberiotoxin. *Proc Natl Acad Sci U S A* **97,** 5562-5567.

Nelson MT, Cheng H, Rubart M, Santana LF, Bonev AD, Knot HJ & Lederer WJ. (1995). Relaxation of arterial smooth muscle by calcium sparks. *Science* **270,** 633-637.

Ohi Y, Yamamura H, Nagano N, Ohya S, Muraki K, Watanabe M & Imaizumi Y. (2001). Local Ca(2+) transients and distribution of BK channels and ryanodine receptors in smooth muscle cells of guinea-pig vas deferens and urinary bladder. *J Physiol* **534,** 313-326.

Pabbidi MR, Mazur O, Fan F, Farley JM, Gebremedhin D, Harder DR & Roman RJ. (2014). Enhanced large conductance K+ channel activity contributes to the impaired myogenic response in the cerebral vasculature of Fawn Hooded Hypertensive rats. *Am J Physiol Heart Circ Physiol* **306,** H989-H1000.

Petkov GV, Bonev AD, Heppner TJ, Brenner R, Aldrich RW & Nelson MT. (2001). Beta1-subunit of the Ca2+-activated K+ channel regulates contractile activity of mouse urinary bladder smooth muscle. *J Physiol* **537,** 443-452.

Plüger S, Faulhaber J, Fürstenau M, Löhn M, Waldschütz R, Gollasch M, Haller H, Luft FC, Ehmke H & Pongs O. (2000). Mice with disrupted BK channel beta1 subunit gene feature abnormal Ca(2+) spark/STOC coupling and elevated blood pressure. *Circ Res* **87,** E53-60.

Qian X & Magleby KL. (2003). Beta1 subunits facilitate gating of BK channels by acting through the Ca2+, but not the Mg2+, activating mechanisms. *Proc Natl Acad Sci U S A* **100,** 10061-10066.

Rueda A, Fernández-Velasco M, Benitah JP & Gómez AM. (2013). Abnormal Ca2+ spark/STOC coupling in cerebral artery smooth muscle cells of obese type 2 diabetic mice. *PLoS One* **8,** e53321.

Semenov I, Wang B, Herlihy JT & Brenner R. (2006). BK channel beta1-subunit regulation of calcium handling and constriction in tracheal smooth muscle. *Am J Physiol Lung Cell Mol Physiol* **291,** L802-810.

Semenov I, Wang B, Herlihy JT & Brenner R. (2011). BK channel β1 subunits regulate airway contraction secondary to M2 muscarinic acetylcholine receptor mediated depolarization. *J Physiol* **589,** 1803-1817.

Shi L, Liu B, Li N, Xue Z & Liu X. (2013). Aerobic exercise increases BK(Ca) channel contribution to regulation of mesenteric arterial tone by upregulating β1-subunit. *Exp Physiol* **98,** 326-336.

Sweet TB & Cox DH. (2009). Measuring the influence of the BKCa {beta}1 subunit on Ca2+ binding to the BKCa channel. *J Gen Physiol* **133,** 139-150.

Tricarico D, Mele A & Conte Camerino D. (2005). Phenotype-dependent functional and pharmacological properties of BK channels in skeletal muscle: effects of microgravity. *Neurobiol Dis* **20,** 296-302.

Wan E, Kushner JS, Zakharov S, Nui XW, Chudasama N, Kelly C, Waase M, Doshi D, Liu G, Iwata S, Shiomi T, Katchman A, D'Armiento J, Homma S & Marx SO. (2013). Reduced vascular smooth muscle BK channel current underlies heart failure-induced vasoconstriction in mice. *FASEB J* **27,** 1859-1867.

Wang ZW, Saifee O, Nonet ML & Salkoff L. (2001). SLO-1 potassium channels control quantal content of neurotransmitter release at the C. elegans neuromuscular junction. *Neuron* **32,** 867-881.

Yang Y, Li PY, Cheng J, Mao L, Wen J, Tan XQ, Liu ZF & Zeng XR. (2013). Function of BKCa channels is reduced in human vascular smooth muscle cells from Han Chinese patients with hypertension. *Hypertension* **61,** 519-525.

Zheng YM, Park SW, Stokes L, Tang Q, Xiao JH & Wang YX. (2013). Distinct activity of BK channel β1-subunit in cerebral and pulmonary artery smooth muscle cells. *Am J Physiol Cell Physiol* **304,** C780-789.

CHAPTER 4

HIGH FAT DIET DISRUPTS INHIBITORY NEUROMUSCULAR TRANSMISSION AND SMOOTH MUSCLE EXCITABILITY IN THE MOUSE DISTAL COLON

4.1 Abstract

High fat (HF) diet disrupts gastrointestinal (GI) motility by unclear mechanisms. We studied the effect of HF diet on nitrergic neurons, neuromuscular transmission, smooth muscle cell (SMC) excitability and colonic motility in wild type (WT; C57BL/6J) and β1-subunit knockout (KO) mice. HF diet caused increased myenteric plexus oxidative stress, a 28% decrease in nitrergic myenteric neurons and a 20% decrease in basal NO levels in the myenteric plexus. Circular muscle inhibitory junction potentials (IJPs) were smaller in the colon of WT HF fed mice. NLA (NOS inhibitor) was less effective at inhibiting relaxations in HF fed compared to control fed WT mice (11% vs 37%). SMCs in HF fed WT mice exhibited depolarized membrane potential (-47 ± 2 mV, n=6) and continuous action potential firing compared to control fed WT mice (-53 ± 2 mV n=6, $p<0.05$), which showed rhythmic firing. SMCs from control and HF fed β1BK KO mice exhibited continuous action potential firing. NLA depolarized colonic SMC membrane potential and caused continuous firing in SMCs from control fed WT mice. Sodium nitroprusside (NO donor) hyperpolarized membrane potential and changed continuous to rhythmic action potential firing in colonic tissues from WT HF fed and β1BK KO mice. Colonic migrating motor complexes were disrupted in β1BK KO mice and HF fed WT mice. Diet did not change BK α-subunit protein or mRNA expression or β1BK-subunit mRNA expression. We conclude that HF diet disrupts IJPs, SMC excitability and GI motility by promoting oxidative stress, loss of nitrergic neurons and disruption of SMC β1BK channel function.

4.2 Introduction

Obesity in humans is mostly caused by the consumption of high fat (HF) diet (Y Lee, 2013) and leads to Type 2 diabetes (T2D) (Colditz *et al.*, 1995), heart disease (Huang *et al.*, 1998), arthritis (Heliövaara *et al.*, 1993) and cancer (Kopelman, 2000; Farag & Gaballa, 2011). Obesity and HF diet are also associated with increased risk of gastrointestinal (GI) motility disorders (Delgado-Aros *et al.*, 2004; Xing & Chen, 2004; Mushref & Srinivasan, 2013; Y Lee, 2013). GI motility is controlled largely by interactions between enteric neurons, interstitial cells of Cajal (ICC), and smooth muscle cells (SMCs) but how obesity-induced changes in these cell types contribute to GI dysmotility is poorly understood.

Animal models of obesity show an increase in oxidative stress followed by altered function of some myenteric neurons (Chandrasekharan *et al.*, 2011a; Voukali *et al.*, 2011; Voss *et al.*, 2013). The neuropathological changes that cause GI dysmotility vary among animal models and location in the GI tract (Chandrasekharan & Srinivasan, 2007). Inhibitory nitric oxide (NO) motor neurons are most susceptible to damage caused by obesity (Chandrasekharan *et al.*, 2011a; Beraldi *et al.*, 2014). Since activation of NO motor neurons cause smooth muscle (SM) relaxation (Murr *et al.*, 1999; Grasa *et al.*, 2009), it is crucial to determine if myenteric NO neurons are lost in obesity and how this contributes to disrupted GI motility.

GI SMC function also plays a crucial role producing propulsive motility. GI SMCs have rhythmic electrical activity (slow waves), initiated by ICCs and slow waves control contraction frequency. The large conductance Ca^{2+} activated K^{+} channel (BK channel) helps to regulate membrane potential and excitability of GI SMCs (Vergara *et al.*, 1998; France *et al.*, 2012). The SMC BK channel is composed of an α subunit and the SM specific $\beta1$ subunit. The BK $\beta1$ subunit enhances Ca^{2+} sensitivity of the pore forming α subunit (Cox & Aldrich, 2000; Qian &

Magleby, 2003). Down-regulation of BK β1-subunit expression reduces the calcium sensitivity of the α subunit and causes increased SM contractility (Brenner *et al.*, 2000b; Plüger *et al.*, 2000). This leads to various disorders that include hypertension (Yang *et al.*, 2013), heart failure (Wan *et al.*, 2013) and urinary bladder over activity (Petkov *et al.*, 2001). Although obesity (Howitt *et al.*, 2011), oxidative stress (Santarelli *et al.*, 2004; Tang *et al.*, 2004) and NO availability (Leo *et al.*, 2014) all modulate the function/expression of β1 subunit in vascular SMCs, it is unclear is similar modulation occurs in the gut.

The etiology of obesity induced GI motility disorders is multifactorial and includes alterations to multiple cell types. My aim in the present study was to address how inhibitory neuromuscular transmission is affected by obesity. I hypothesized that in obesity, oxidative stress causes loss of inhibitory nitrergic motor neurons and disrupts β1BK channel function/expression leading to impaired inhibitory neuromuscular transmission and increased SMC excitability. I tested my hypothesis using colonic tissues from wild type (WT) and β1BK KO mouse models placed either on control or HF diet. My findings show that HF diet causes oxidative stress induced loss of NO motor neurons, which disrupts inhibitory neuromuscular transmission and SM excitability causing impaired colonic motility.

4.3 Materials and methods

4.3.1 Ethics Statement

All studies were conducted in accordance with the National Institutes of Health Guide for the Care and Use of Laboratory Animals (NIH Publication No. 85-23, revised 1996) and approved by Institutional Animal Care and Use Committee of Michigan State University.

4.3.2 Animals

Wild type (WT) 18-24 weeks old male C57BL/6J mice maintained either on control (10 kcal% fat; D12450B) or HF diet (60 kcal% fat; D12492), were obtained from Jackson laboratories (Bar Harbor, Maine, USA) *(http://jaxmice.jax.org/diomice/diets.html),* while β1BK KO mice were obtained as a gift from Dr. Robert Brenner (University of Texas Health Science Center, San Antonio). β1BK KO mice were maintained as homozygous lines at Michigan State University (Xu *et al.*, 2011; France *et al.*, 2012; Xu *et al.*, 2012; Xu *et al.*, 2014). Pups of β1BK KO mice were weaned at 3 weeks. After 3 weeks, mice were placed either on control or a HF diet. Animals were kept in 12/12 hr light/dark cycle, and had access to food and water *ad libitum*. WT and β1BK KO mice were age matched for the study. WT mice were maintained in our animal facility for 1-week prior to use in any experiments. Euthanasia was carried out by isoflurane anesthesia followed by cervical dislocation.

4.3.3 Oxidative stress measurements

Whole colon segments from control or HF WT mice were cut open along the mesenteric border, washed, and stretched using fine pins (0.1mm) (Fine Science Tools, Foster City, CA) in a silastic elastomer-lined (VWR, Buffalo Grove, IL) petri dish. Tissues were dissected to expose the longitudinal muscle myenteric plexus (LMMP). Reduced thiols were labeled with Alexa fluor 680-conjugated C_2 maleimide (1 μM; Life Technologies, Grand Island, NY) in 4% paraformaldehyde (PFA), 0.02% Triton X-100 and 1 mM N-ethylmaleimide (NEM, E3876;

Sigma-Aldrich, St. Louis, MO) in 1 M PBS for 20 min at room temperature. Tissues were rinsed with PBS. In order to visualize oxidized thiols, LMMP preparations were then treated with 5 mM tris (2-carboxyethyl) phosphine hydrochloride (TCEP) (Catalog #C4706; Sigma-Aldrich, St. Louis, MO) for 20 min. TCEP chemically reacts with oxidized thiol to form reduced free thiols. The newly formed reduced thiols were labeled with 1 μM Alexa fluor 546 C_5 maleimide in 1 mM NEM in PBS for another 20 min at room temperature. Finally, the ratio of 546-maleimide (oxidized thiol) /680-maleimide (reduced thiol) (SS/SH ratio) fluorescence intensity was calculated using Image J (Version 1.44 g, National Institute of Health, USA) software. Higher ratios indicate increased oxidative stress.

4.3.4 Immunohistochemistry for nitric oxide synthase (NOS) containing neurons

Mucosa, submucosa and the circular muscle were dissected away to expose myenteric ganglia from control and HF mice. Whole-mount LMMP preparations were fixed in 4% PFA for 1 hour at room temperature. The tissues were then washed (3 x 10 min) with 0.1M PBS prior to incubation in 0.5% Triton X-100 and 4% normal donkey serum. Tissues were incubated overnight in sheep anti nNOS primaries (Cat #AB1529, Millipore, USA; 1:200 dilution). After washing the tissues (3 x 15 min) in PBS the following day, the antibody staining was visualized using fluorescein isothiocyanate (FITC)-conjugated donkey anti sheep antibody (Cat # 713-486-147, Jackson Lab, West Grove, PA; 1:100 dilution). Fluorescent images were obtained through 40X (PlanFluor, 0.75 numerical aperture) objective of an upright epiflourescence microscope (Nikon Eclipse, Melville, NY) equipped with a Retiga 2000R camera (QImaging, Surrey, BC, Canada) controlled by QCapture Pro 7.0 (QImaging) software. Primary and secondary only controls were run and showed no labeling. NO positive neurons number and ganglionic area

were obtained from five random locations on the tissues. Images were analyzed using Image J (Version 1.44g, National Institute of Health, USA) software.

4.3.5 Nitric oxide (NO) measurements

Freshly dissected LMMP preparations from either control or HF mice were treated with collagenase type II (156μg/ml) (Cat #17101-015; Gibco, Grand Island, NY) and dispase (1μg/ml) (Cat #17105-041; Gibco, Grand Island, NY) dissolved in DMEM/F-12 media (Life technologies, USA) for 15min. The tissues were then loaded with diaminofluorophore 4-amino-5-methylamino-2′-7′-difluorofluorescein diacetate (DAF-FM-DA; 4μM; Catalog # D-2321, Life Technologies, Grand Island, NY; 1:1000) dissolved in DMEM/F-12 supplemented with 0.08% probenecid for 30 min. Tissues were washed (3 x 1 min) with DMEM/F12 and allowed to de-esterify for 20 min in presence of 200 μM probenecid. DAF-FM fluorescence in myenteric ganglia was captured through the 40X water-immersion objective of an upright Olympus BX51WI fixed-stage microscope (Olympus, Center Valley, PA) equipped with a Neo sCMOS digital camera (Andor, South Windsor, CT) controlled by Andor IQ3 software. Images were analyzed offline using Image J software.

4.3.6 Electrophysiological recordings from colonic circular muscle SMCs

Distal colon segments were removed from euthanized mice and placed in carboxygenated (95% O_2 and 5% CO_2 mixture) Krebs solution containing (mM) 11 glucose, 117 NaCl, 25 $NaHCO_3$, 4.7 KCl, 1.2 $NaH_2PO_4.H_2O$, 2.5 $CaCl_2.2H_2O$, and 1.2 $MgCl_2$ $6H_2O$, (pH 7.3–7.4). The mesenteric fat was removed and the segment was opened along the mesenteric border. The tissue segment was stretched and pinned flat on a silastic elastomer lined petri dish with stainless steel pins. Mucosa and submucosa were removed using fine forceps. A small tissue section (~3 x 1 cm) with intact myenteric plexus and circular muscle was cut out and transferred to a silastic

elastomer lined recording chamber. The chamber was then placed on the stage of an inverted microscope (Nikon Eclipse TS100). Warm carboxygenated Krebs solution (37°C) was continuously perfused through the chamber at 3-4 ml/min. Circular SMCs were impaled with a glass microelectrode filled with 2M KCl (50 - 80MΩ tip resistance). Membrane potential was recorded using an Axoclamp 2A amplifier, a Digidata 1332A analog-digital converter and axoscope 9.2 software (all from Molecular Devices, Sunnyvale, CA). Resting membrane potential of the SMC and the spontaneous action potential activity was recorded in absence of nifedipine. Individual recordings that lasted ≥ 2 min were later used for data analysis.

Inhibitory junction potentials (IJPs) were evoked using electrical field stimulation (train duration, 200-1000 ms; frequency, 10 Hz; pulse duration 0.8 ms; voltages 60-120V) was applied using two parallel silver chloride wires placed 3.5 cm apart (Ø=0.03", A-M systems, Carlsberg, WA). The wires were placed perpendicular to the longitudinal axis of the preparation. The L-type Ca^{2+} channel blocker, nifedipine (1 μM) was added to abolish spontaneous muscle contractions.

4.3.7 Isometric tension measurement of muscle relaxation *in-vitro*

Experiments were designed to assess the contribution of β1BK channels in mediating SM relaxation. One-centimeter segments of distal colon from WT and β1BK KO mice fed a control and HF diets were used. Tissues were attached horizontally (in the axis of the circular muscle) to the tissue holder and connected to a force-displacement transducer (FT03C; Grass Instruments, Quincy, MA) using silk thread. Preparations were suspended horizontally and placed under 1 g of passive tension in 20 ml of glass organ baths containing warm carboxygenated Krebs solution (37°C). Tissues were then allowed to equilibrate for 40 min prior to the start of experiments. During this time Krebs solution was changed every 10 min. Electrical field stimulation (EFS; 20

mA, 10 – 40 Hz) was applied using concentric platinum wire electrodes to elicit neurogenic relaxation in the presence of $PGF_{2\alpha}$ (5 μM, to increase muscle tone) and scopolamine (1 μM to block muscarinic receptors). The amplitude and area of the relaxation were measured. Data were analyzed using Labscribe software (Iworx, Dover, NH). The Na^+ channel blocker tetrodotoxin (TTX, 1 μM) was used to confirm that stimulation evoked relaxations were neurogenic.

4.3.8 *In-vitro* assessment of colonic motility

Whole colons were harvested from WT and β1BK KO mice, and luminal contents were flushed with Krebs buffer. A stainless-steel rod was then inserted into the lumen. The tissue was secured at each end (~1.5 cm apart) with small needles that were attached to surgical silk thread. The silk threads were then attached to two force transducers. The rod holding the tissue was placed in a 60 ml reservoir filled with warm carboxygenated krebs solution and stretched to an initial tension of 0.5 g. The tissues were then allowed to equilibrate for 30 min. After regular colonic migrating contractions (CMMC) were established, CMMC activity was recorded from control fed and HF tissue for an hour. Recordings were obtained using two strain gauge amplifiers (Grass Instruments CP122A) attached to an analog/digital converter (Minidigi 1A, Molecular Devices) and finally analyzed with axoscope 9.2 software (Molecular Devices). Retrograde (anal to oral), anterograde (oral to anal) and simultaneous (oral and anal occurring at the same time) contractions were identified and recorded. Velocity of anterograde CMMC propagation was obtained by dividing the distance between the clips (1.5 cm) with the time delay for oral contraction to reach the anal end.

4.3.9 *In-vivo* assessment of colonic motility

WT and β1BK KO mice placed on control and HF diet were individually housed in clean cages where food and water were removed for 1 h between 11 AM and 12 PM. Fecal pellets

collected from each mouse during this time and were counted and the wet weight measured. Fecal pellets were later stored in a warm (40°C) oven for 24 hours and the dry weight was measured the next day. This protocol was repeated for four consecutive days. Fecal pellet number, wet weight and dry weight were all normalized to the body weight of the animal over the four-day period.

4.3.10 Western blot for α subunit protein expression

Colon samples from WT control and HF mice were collected. Mucosa and submucosal layers were quickly removed in cold Krebs solution containing protease inhibitor cocktail (P8340; Sigma-Aldrich, St. Louis, MO) 10 mmol/L sodium fluoride (S7920; Sigma - Aldrich), and 1 mmol/L sodium orthovanadate (S6508; Sigma-Aldrich) to prevent protein degradation. Tissues were stored at -80° C until ready to be processed and later homogenized with a mortar and pestle that had been pre-cooled with liquid nitrogen. Homogenized tissues were lysed with 1X lysis buffer (12.5 ml 0.5M Tris HCl, 20 ml 10% SDS, 10 ml Glycerol, 57.5 ml dH_2O) that contained protease inhibitor cocktail. Protein (5 mg) was loaded for SDS-PAGE along with the full-range rainbow molecular weight marker (GE Healthcare, RPN800E). Proteins were separated at 100 V on a 10-12% gel, and electro-transferred overnight onto a 0.45 mm PVDF at 30 V (Milipore, IPVH00010). Ponceau S was used to verify efficient protein transfer. The following day membranes were blocked for 1 hour at room temperature in 5% milk-TBS-T to prevent non-specific binding. Membranes were blocked for 2hrs, with BK α-subunit primary antibodies (Alomone labs, APC-107; 1:20,000). Membranes were then washed (3 X 10 minutes) with TBS-T, and blotted with the appropriate HRP-conjugated secondary antibodies (1:4000) for 1 hour at room temperature in blocking solution. Blots were imaged with ECL Plus Western Blotting Detection System (GE Healthcare).

4.3.11 Real time rt-PCR for α and β1 subunits mRNA expression

I used rt-PCR to detect if there were HF diet-induced changes in α and β1 mRNA expression in WT mice. Mucosa and submucosa layers were dissected and colonic SMs were collected. SMs were stored in All Protect Reagent (Qiagen, 76405) until ready to be processed. RNA was isolated using the MELT Total Nucleic Acid Isolation System kit (Ambion, no. AM1983). RNA isolates were reverse-transcribed to cDNA using High Capacity RNA to cDNA kits (Applied Biosystems, 4387406). Resultant cDNA was used for real-time PCR assays. Applied Biosystems TaqMan Fast Advanced master mix (Applied Biosystems, 4444556) was used to prepare reactions (20 µl). Reactions were assayed with TaqMan Gene Expression assays (KCNMA1-no Mm00516078_m1, Gapdh – no. Rn01775763_g1). Samples were analyzed in duplicate.

4.3.12 Statistics

Potential differences between treatment groups were tested using either two-way ANOVA with Bonferroni post-hoc test or Student's t-test. Data are mean ± SEM. Differences were considered significant when $p < 0.05$. Analysis was done in Graph Pad Prism 4.0 software (San Diego, CA).

4.4 Results

4.4.1 HF diet increases body weight and abdominal fat pad weight

I tested if mice develop obesity after consuming a HF diet for 18-22 weeks and found that HF fed mice had a significant increase in body weight (41.7 ± 1.4 g, n=21) compared to control fed mice (28.3 ± 0.47 g, n=21; $p<0.05$). HF fed mice also had a significant increase in abdominal fat pad weight compared to control fed groups (0.4 ± 0.04g, n=9 Vs 1.7 ± 0.2g, n=9; $p<0.05$).

4.4.2 WT HF mice exhibit increased neuronal oxidative stress, decreased NOS neuron density and lower NO availability.

I measured neuronal thiol oxidation to determine if consumption of a HF diet drives oxidative stress in myenteric NO neurons. I observed an increase in the GSSG/GSH fluorescence ratio in NOS and non NOS neurons of HF fed mice compared to control fed mice (Figure 4.1).

Figure 4.1 Glutathione fluorescence in the myenteric plexus of the mouse distal colon. Representative images of (A) oxidized and (B) reduced glutathione fluorescence intensity. (C) nNOS positive neurons were co-localized with glutathione fluorescence measurements to measure oxidative stress (increased oxidized glutathione) in these neurons. (D) Fluorescence intensity measurements show 17 ± 2% increase in oxidized/reduced glutathione ratio in myenteric nitric oxide neurons of HF (n=6) compared to control fed mice (n=6). (E) Increase in oxidized/ reduced GSH ratio was also seen in non-nNOS positive neurons from HF fed (n=13) compared to control fed mice (n=14). *p<0.05.

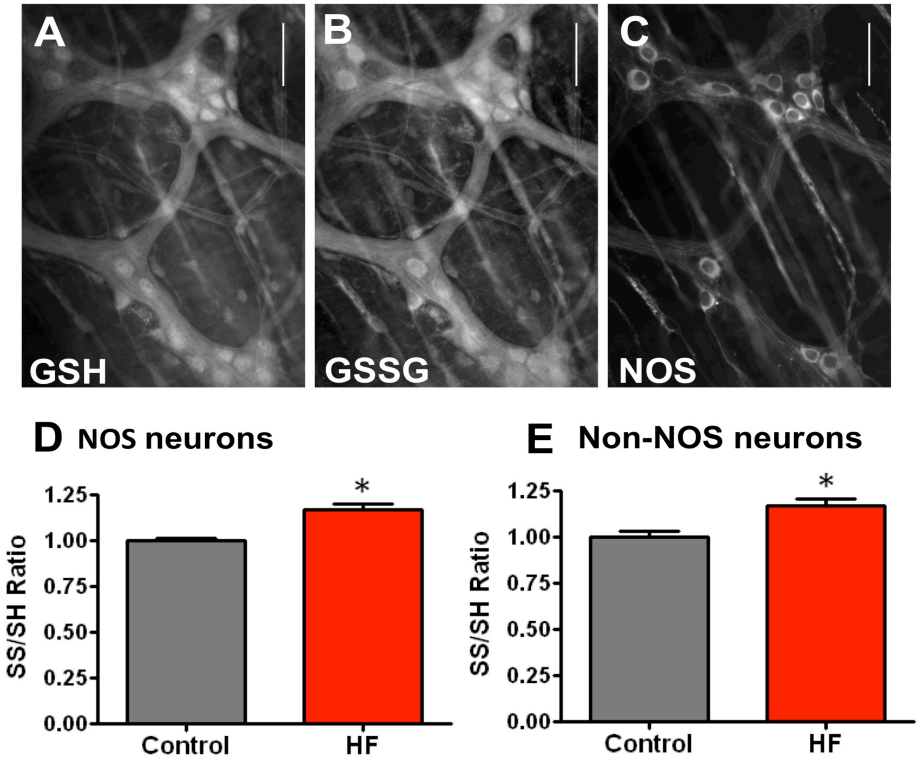

I tested to see if an increase in oxidative stress is accompanied by loss of NOS neurons in HF fed mice. nNOS positive neurons were detected in the myenteric plexus of control fed and HF mice but nNOS neuron density was significantly lower in the myenteric plexus of HF fed compared to control fed mice (Figure 4.2C). Given the lower frequency of neurons containing nNOS in mice fed a HF diet, I reasoned that myenteric ganglia in these animals would contain lower levels of NO availability. Therefore, I assessed NO levels within myenteric ganglia using the fluorescent NO indicator dye, DAF-FM-DA. DAF-FM-DA reliably detects NO levels in vertebrates (Hong et al., 2009) and does not fluoresce in the absence of NO. In the presence of

NO, DAF-FM-DA is converted into fluorescent benzotriazole molecules whose intensity is directly correlated to bioavailability of NO in the tissue (Hong et al., 2009). I measured the fluorescence intensity of benzotriazole derivative as an indirect measure of basal NO availability. The fluorescence intensity of the benzotriazole derivative was greater in control mice suggesting lower NO availability in the myenteric ganglia of HF mice (Figure 4.2D)

Figure 4.2 Immunohistochemical labeling for neuronal nitric oxide synthase (nNOS) containing neurons from control and high fat (HF) mice. (C) Number of nNOS positive neurons per ganglionic area was higher in control fed (n=6) compared to HF fed mice (n=6). (D) Fluorescence intensity of DAF-FM-DA derived benzotriazole derivative is greater in HF fed (n=6) compared to control fed mice (n=6). *p<0.05.

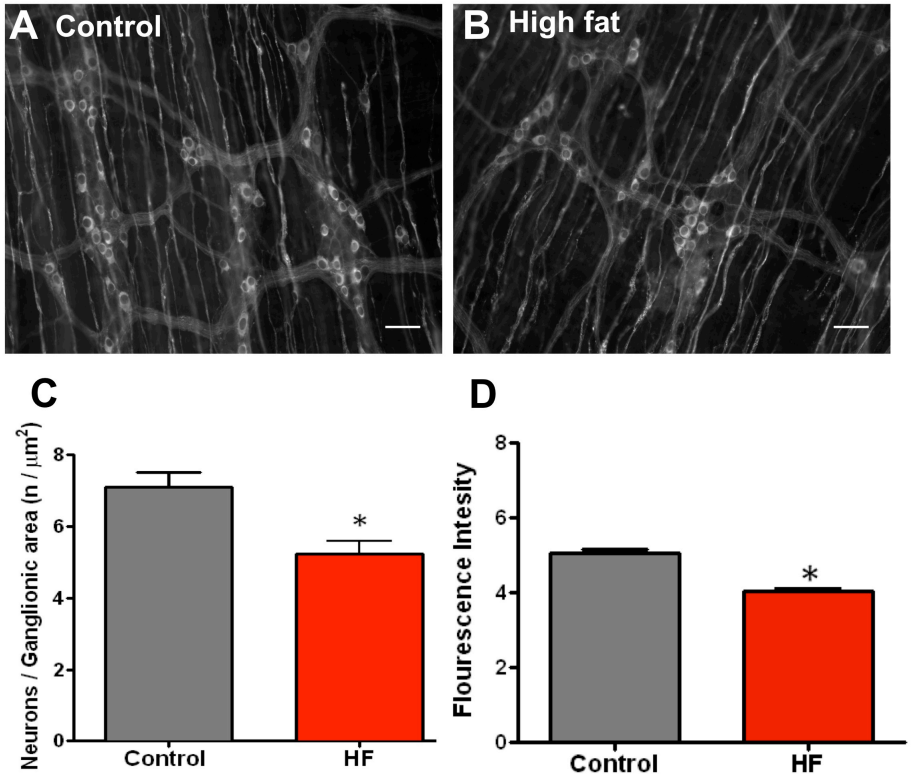

4.4.3 HF diet impairs inhibitory nitrergic neuromuscular transmission

Inhibitory neuromuscular transmission in the gut involves purinergic and nitrergic signaling (Murr *et al.*, 1999; Gallego *et al.*, 2008; Grasa *et al.*, 2009). A purine mediates fast inhibitory junction potentials (IJPs) and fast relaxation while NO mediates slowly developing but

longer lasting IJPs and relaxations. I used intracellular microelectrode recording to measure IJPs at varying train duration (200-1000 ms) and measured amplitude (indicative of fast purinergic IJP) and the area (indicative of nitrergic slow IJP) in control and HF fed mice. At higher train duration (800 ms), the area of IJP but not the amplitude was significantly smaller (52% 100 V, $p<0.05$) in HF mice compared to controls (Figure 4.3).

Figure 4.3 IJP recordings from control and HF fed mice. (A) Representative recording of IJPs in mouse distal colon (EFS: 100 V, 10 Hz and 0.2-1 s train duration) from control and HF tissues. (B) IJP area was reduced only at the 0.8 s train duration in tissues from HF fed mice. (C) IJP amplitude was similar in tissues from control and HF fed mice. *$p<0.05$.

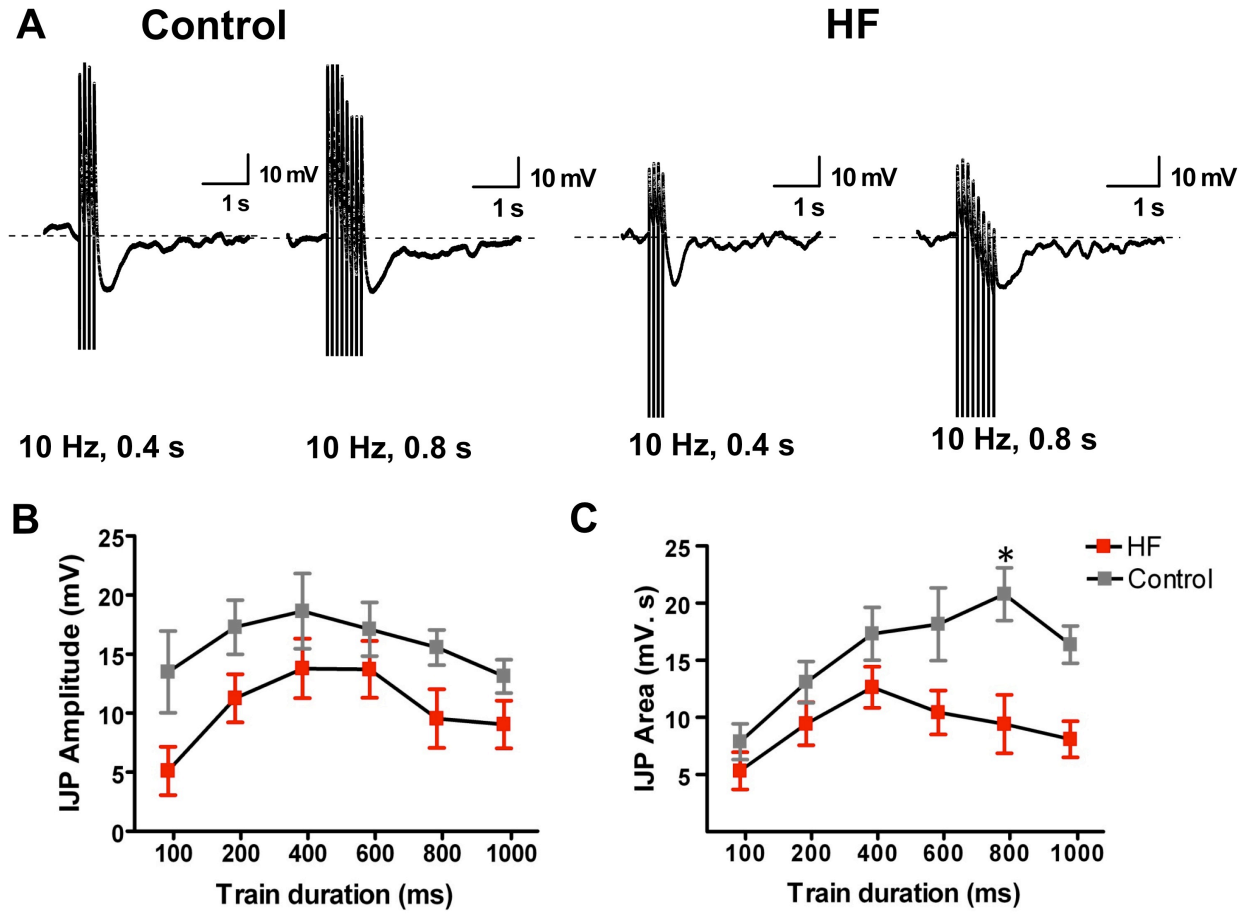

4.4.4 HF diet impairs neurogenic smooth muscle relaxation

To test if disrupted inhibitory neuromuscular transmission can lead to impairment in neurogenic SM relaxation, I measured the force of relaxation generated by the colonic circular

smooth muscle (Figure 4.4A). We found that neurogenic relaxations in tissues from WT HF fed were smaller than in tissues from control fed mice ($p<0.05$, *two-way* ANOVA), however no such differences were observed in β1BK KOs (Figure 4.4B). NLA (100 μM) also caused a smaller inhibition of neurogenic relaxation in tissues from HF fed mice (11 ± 3%) compared to control fed mice (37 ± 6%, $p<0.05$) (Figure 4.4C).

Figure 4.4 Measurement of neurogenic smooth muscle relaxation in the mouse distal colon. (A) Neurogenic smooth muscle relaxation in control and HF groups in presence of prostaglandin (5 μM) and scopolamine (10 μM). (B) HF mice showed significantly impaired neurogenic smooth muscle relaxation across varying frequencies compared to control groups. (C) Application of NLA (100 μM; Nitric oxide synthase inhibitor) significantly decreased neurogenic relaxation in both groups. However, the percentage inhibition of relaxation in presence of NLA was significantly greater in controls than in HF. *$p<0.05$. All tissues were pre-contracted with PGF_{2a} (5 mM) and muscarinic receptors were blocked with scopolamine (1 mM).

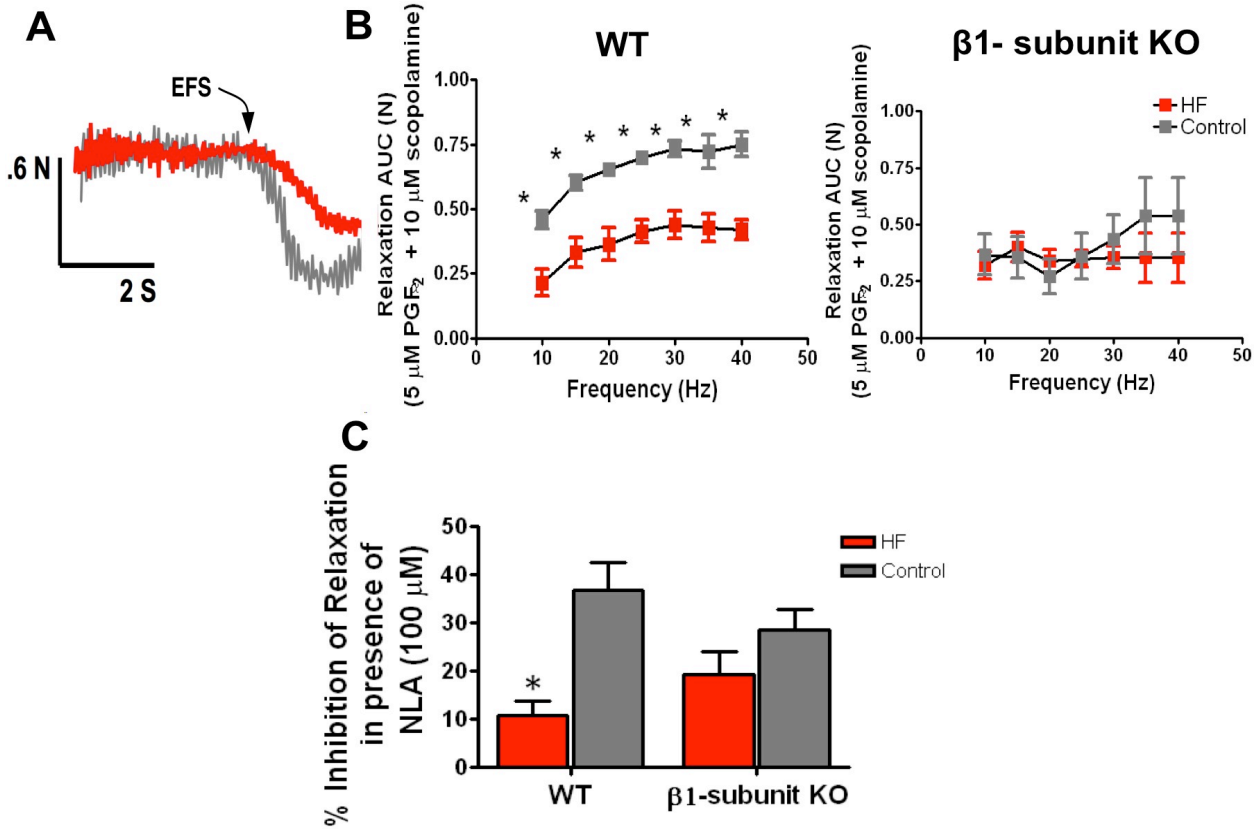

4.4.5 HF diet mimics the effect of β1BK KO on SM electrical activity

I tested the hypothesis that HF diet dependent increase in oxidative stress alters smooth muscle electrical activity by impairing β1BK channel function. Intracellular recording were obtained from colonic circular SMCs from control and HF fed mice. Colon SMCs from HF fed mice had a depolarized membrane potential (-47 ± 1.9 mV n=16) compared to control fed mice (-53 ± 1.7 mV n=13; $p<0.05$). SMCs in WT control fed mice showed rhythmic action potential firing, while SMCs in tissues from HF fed mice showed continuous action potential firing activity. 13 out of 17 cells from 7 WT HF mice exhibited continuous action potential firing behavior while 11 out of 13 cells impaled in 6 WT controls exhibited bursting behavior. ($p<0.05$, Fischer exact test, n=6) (Figure 4.5). SMCs from β1BK KO mice showed continuous action potential firing independent of diet. Only 4 out of 11 cells recorded from 6 control fed β1BK KO mice showed bursting action potential firing while remaining 7 cells showed continuous firing. Only 3 out of 18 cells from 7 β1BK KO HF mice showed bursting action potential firing while remaining 15 cells showed continuous firing ($p<0.05$, Fischer exact test).

4.4.6 NO availability affects SM excitability in WT and β1BK KO mice

NO modulates BK channel activity in vascular SMCs (Mistry & Garland, 1998; L'Heureux *et al.*, 2010). To test if NO availability alters GI SM excitability, I applied NLA (100 μM) and SNP (10 mM) to WT and β1BK KO tissues. NLA depolarized (-50 ± 2.4 mV Vs -46 ± 2.5 mV n=4; $p<0.05$, paired t-test) SMCs and changed the action potential firing from a rhythmic pattern to continuous firing in tissues from control fed WT mice. NLA did not change membrane potential or action potential firing in SMCs from HF WT mice. SNP hyperpolarized (-51 ± 0.7 mV Vs -67 ± 1.8 mV n=3; $p<0.05$, paired t-test) the membrane potential and stopped action potential firing in colonic SMCs from WT HF. In β1BKKOs, SNP did not significantly

(p>0.05) hyperpolarize the membrane potential but changed action potential firing from continuous to bursting pattern in both β1BKKO control and β1BKKO HF tissues (Figure 4.5).

Figure 4.5 NO modulates smooth muscle excitability. Effects of L-NNA (A and B) and SNP (C, D and E) on smooth muscle excitability. (A) WT HF mice show continuous action potential firing compared to WT on control diet which shows bursting like action potential firing behavior *p<0.05. (A) In WT controls, L-NNA depolarizes the membrane and increases the firing frequency (*p<0.05, paired t-test, n=3) (B) Application of L-NNA in WT HF does not depolarize the cell membrane. (C) Application of SNP in WT HF mice hyperpolarized the membrane and stopped action potential firing in a reversible manner. (D and E) BK KO mice irrespective of the diet had continuous action potential firing. Application of SNP on BK KO mice changed action potential firing to bursting like firing with no apparent change in RMP. (E) Application of SNP on BK KO mice fed a control diet changed action potential firing to a greater extent than HF tissues.

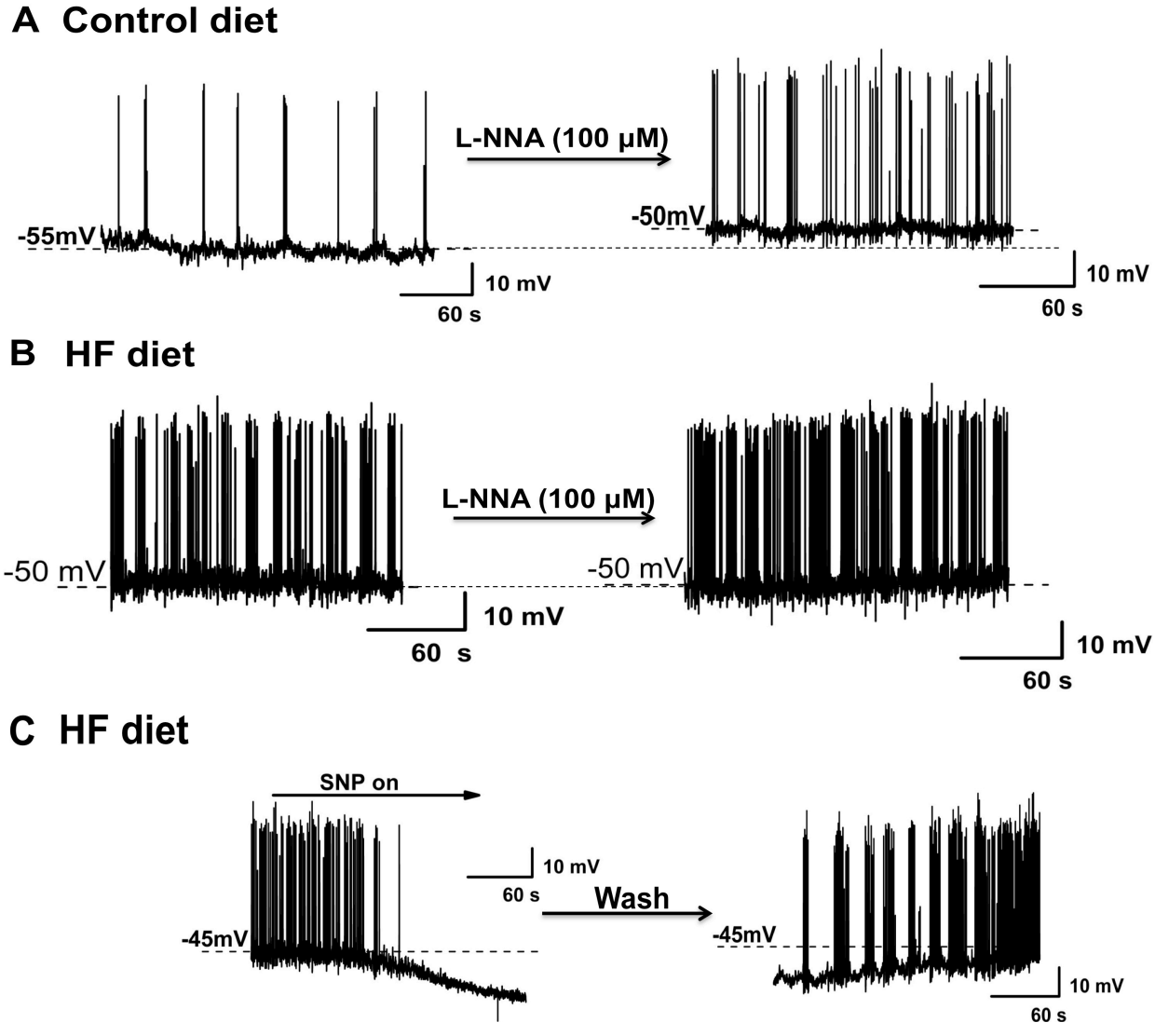

Figure 4.5 (cont'd)

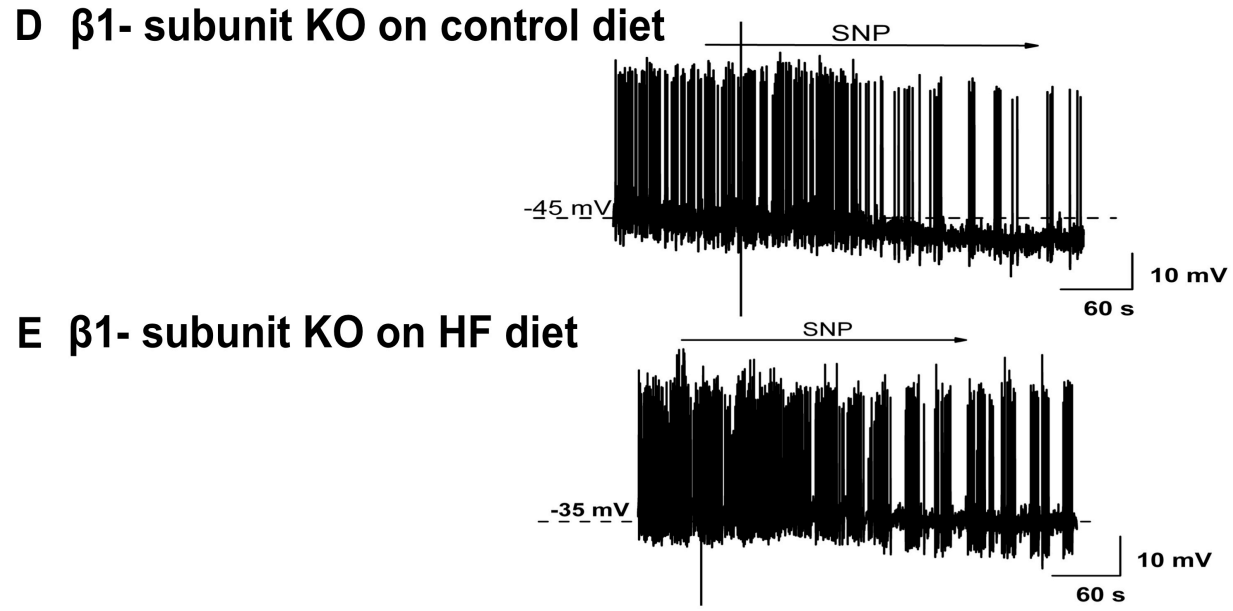

4.4.7 WT HF mice exhibit disruptions in colonic migrating motor complex (CMMC) activity and CMMCs are disrupted in β1BK KO mice regardless of diet

In order to test the hypothesis that HF diet disrupts *in-vitro* colonic motility, CMMCs were examined (Figure 4.6). I found that colonic contractions from control mice propagated aborally (anterograde) in all cases (100% anterograde). However, in HF mice only 64 ± 10% of contractions recorded at the oral end propagated anterogradely while 17 ± 8% of the contractions propagated retrogradely (anal to oral) and 6 ± 4% of contraction occurred simultaneously. The remaining (15 ± 10%) contractions did not propagate at all (i.e. they were seen either only in the oral segment or in the anal segment) (Figure 4.6B). The CMMC pattern was also disrupted in the colon from control and HF fed β1BK KO mice (Figure 4.6C). Oral and aboral contraction area was greater in WT HF than WT controls while no such difference were observed among KOs (Figure 4.6D and 4.6E). I found that the velocity of CMMC propagation was significantly faster in WT HF diet fed mice compared to WT controls (Figure 4.6F) ($p<0.05$).

Figure 4.6 *In vitro* recordings of colonic migrating motor complex (CMMC) in colonic segments from WT and β1-subunit KO mice placed on control and HF diet. (A) Representative recording of CMMC in the colon from a control fed mouse. Recording shows contractions propagate regularly in an oral to anal direction. (B) Summary of propagation patterns in colon segments from control (n=6) and HF fed (n=9) mice. Almost all of CMMCs propagate in anterograde direction in tissues from WT control fed mice while only 64% of CMMC propagate anterogradely in colon segments from WT HF fed mice. There was a significant increase in the percentage of retrogradely propagated contractions, and contractions that either occurred simultaneously or only at one recording site in the colon from HF mice (*p < 0.05). (C) CMMC propagation disrupted in β1-subunit KOs irrespective of the diet. Contraction area was greater in segments from WT HF compared to WT control fed mice at oral (D) aboral (E) ends of the segments, however no differences were detected among β1-subunit KOs. (F) CMMC velocity was faster (*p < 0.05) in colon segments from WT HF mice (AUC: Area under the curve) *p<0.05.

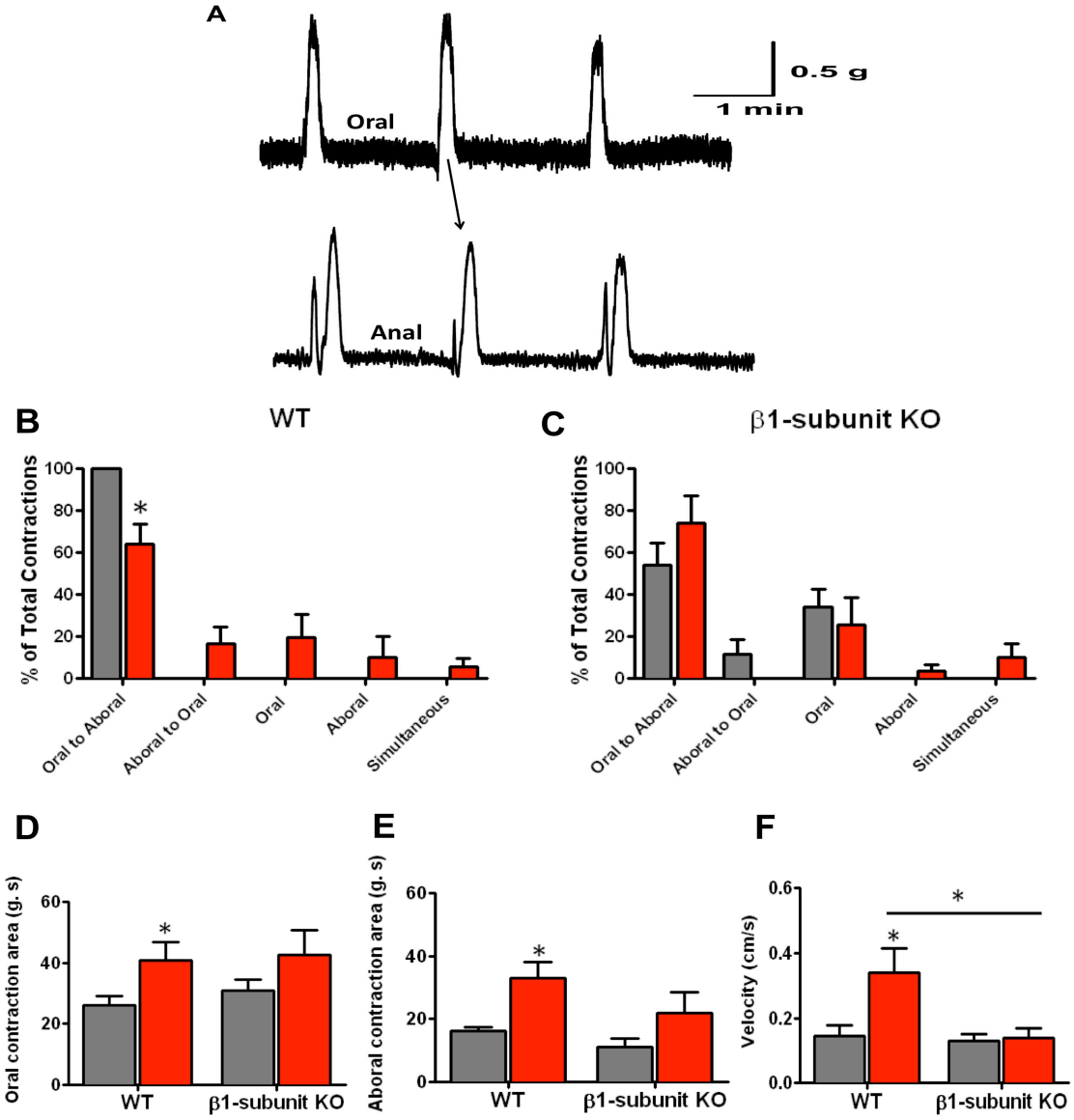

4.4.8 Consumption of a HF diet increases fecal pellet output in WT mice

WT mice show significantly higher fecal pellet output per gram of body weight compared to β1BK KOs (Figure 4.7). Among WTs, mice fed a HF diet exhibit greater fecal pellet output compared to control fed. However, there was no difference in either the dry weight or the wet weight of the pellet among WTs and β1BK KOs. I also did not detect any diet dependent difference in either fecal pellet output, wet weight or the dry weight between β1BK KO mice fed a control and β1BK KO fed a HF diet.

Figure 4.7 *In vivo* colonic motility measurements from WT and β1-subunit KO mice. WT mice had increased fecal output than β1BK KOs. Among WTs, mice fed a HF diet have increased fecal pellet output per gram of body weight than controls (n=5; *p < 0.05).

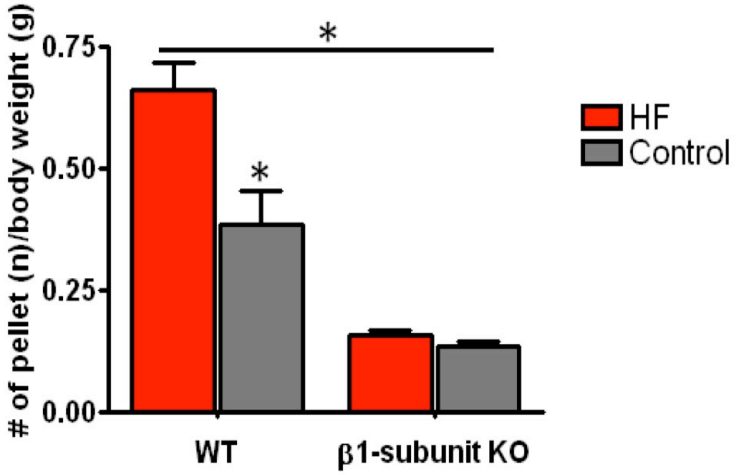

4.4.9 α-subunit protein expression of a β1BK channel is not altered in HF mice

I did not find any difference in BKα subunit expression between WT control and HF mice. Although I had hypothesized that expression of β1subunit is altered in HF mice, I was unable to study the expression of β1subunit using western blot due to the lack of commercially available specific antibody for β1subunit (Bhattarai *et al.*, 2014).

Figure 4.8 BK channel α-subunit western blot. (A) The BK α-subunit antibody detected a protein band at ~110 kDa from the mouse distal colonic smooth muscle cell preparations. Antibody binding was blocked pre-incubating the primary antibody with its competing peptide and using secondary only controls. (B) Representative blot of BK_{Ca} α subunit and β-actin expression in colonic SMs of mice placed on control and HF diet. (C) No significant difference in BK_{Ca} α subunit / β-actin subunit protein expression was observed between WT controls and WT HFs.

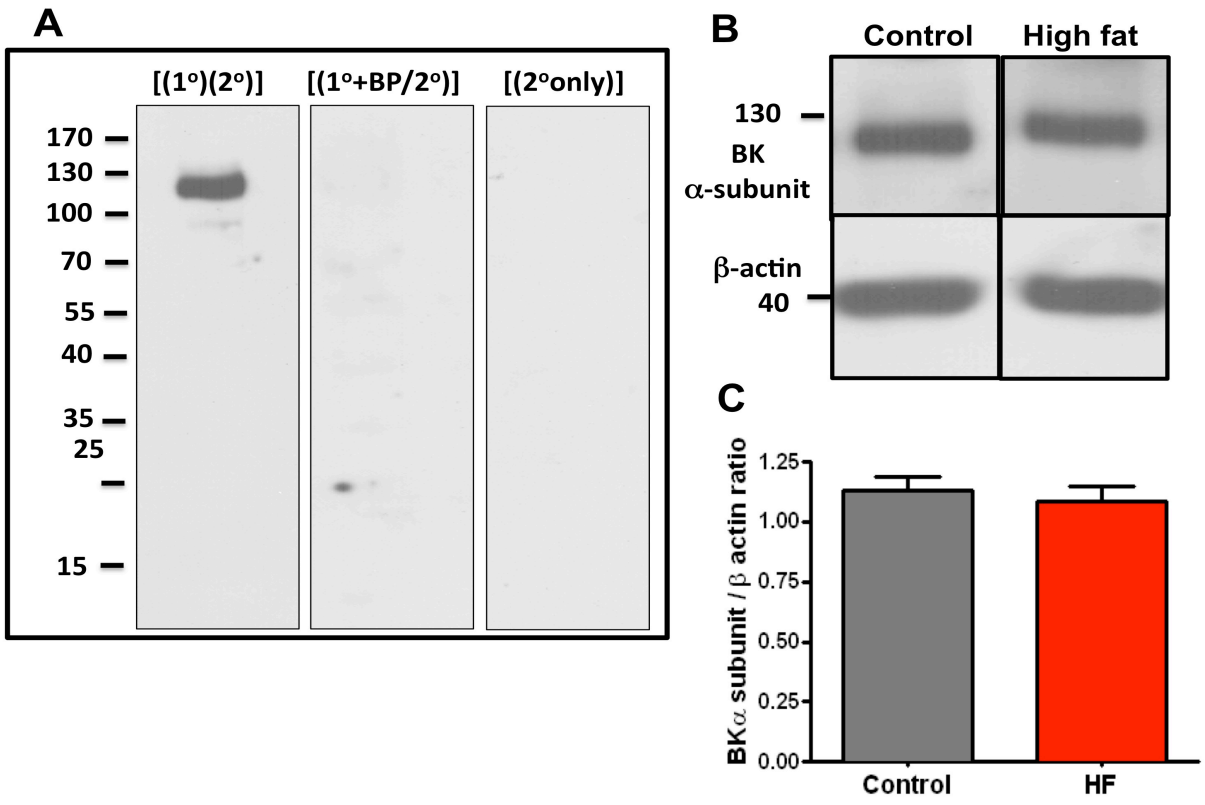

4.4.10 β1-subunit mRNA expression is not changed in HF mice

I used rt-PCR to detect changes in β1subunit gene expression between control and HF mice. However, I did not detect any significant change in the expression of either the α or the β1-subunit mRNA

Figure 4.9 rt-PCR measurements for the α and the β1subunit mRNA expression. rt-PCR showed no difference in either (A) the α or (B) the β1 subunit expression between HF and controls

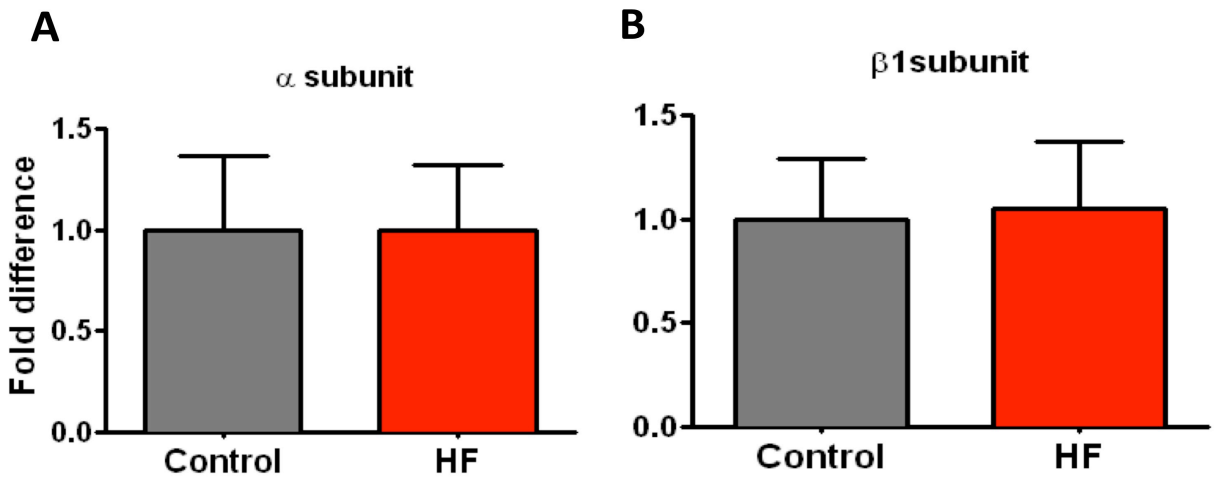

4.5 Discussion

The aim of this study was to identify the pathogenesis of HF associated enteric neuron loss and altered SM electrical activity that contributes to GI dysmotility in obesity. My results show that HF diet disrupts inhibitory neuromuscular transmission, SM relaxation and excitability in WT but not β1BK KO mice. This effect is due to oxidative stress induced loss of NO neurons, which ultimately leads to impaired i*n-vitro* and *in-vivo* colonic propulsive motility. Electrophysiological studies suggest that compromised BK channel β1-subunit function might play a role in mediating these disruptions.

Consumption of a free fatty acid rich diet increases reactive oxygen species (ROS) generation via increased mitochondrial uncoupling and β-oxidation (Evans *et al.*, 2002). NO neurons are susceptible to oxidative damage because NO reacts with superoxide anion to produce peroxynitrite ($ONOO^-$), a highly reactive oxidizing agent (Murphy *et al.*, 1998; Rivera *et al.*, 2011). Since peroxynitrite reacts with reduced glutathione (GSH) to produce oxidized glutathione disulphide (GSSG), I quantified the ratio of oxidized/reduced (SS/SH) GSH as an indicator of oxidative stress (Murphy *et al.*, 1998). I found that myenteric neurons in the colon of HF fed mice have an increased GSSG/GSH ratio suggesting increased oxidative stress. Increased in oxidative stress was associated with a decrease in the number of myenteric NOS neurons. Since, NOS neurons constitute ~25-40% of total myenteric neuron population (Bagyánszki *et al.*, 2000; Bódi *et al.*, 2009; Bagyánszki & Bódi, 2012), I tested to see if loss of NOS neurons reduced NO availability in the myenteric ganglia of HF mice. I found that mice placed on HF diet showed significant decreased benzotriazole product fluorescence intensity compared to control fed WT mice, suggesting lower NO bioavailability myenteric ganglia of HF fed mice.

I tested to see if oxidative stress, reduced NOS neurons and NO bioavailability disrupted inhibitory neuromuscular transmission and smooth muscle relaxation. Stimulation of enteric neurons at lower frequencies produced purinergic IJPs while higher stimulation frequencies causes mixed purinergic/nitrergic IJPs (Gallego *et al.*, 2008). SMCs in the colon of HF fed mice had reduced IJP area but not peak amplitude indicating impairment of nitrergic but not purinergic signaling. I also found that impairment in nitrergic signaling is sufficient to cause disruptions in neurogenic SM relaxation in WT HF mice. Inhibition of neurogenic relaxation in the presence of NLA was also lower in HF fed WT mice compared to control fed WT mice suggesting lower NO availability.

NO mediated relaxation occurs through activation of β1BK channel either via cyclic GMP-dependent pathway or via S-nitrosylation of cysteine residues (George & Shibata, 1995; Mistry & Garland, 1998; Jaffrey *et al.*, 2001; Hess *et al.*, 2005). I therefore tested to see if loss of β1 subunit in itself is sufficient to disrupt SM relaxation in GI tissues. I measured neurogenic relaxation from β1BK KO mice fed either a control or a HF diet. I found that in contrast to wild type mice, β1BK KO mice showed no diet dependent difference in the colonic SM relaxation and NLA dependent inhibition of relaxation was similar in both mice irrespective of the diet. These data suggest that NO possibly mediates SM relaxation by activating β1BK channel function in colonic smooth muscle.

In vascular SMCs, oxidative stress decreases BK channel open probability in a dose dependent fashion by preferentially attacking calcium sensing cysteine residues (Brzezinska *et al.*, 2000), which disrupts calcium sensing mechanism and causes channel to behave as if the β1 subunit had been deleted (Tang *et al.*, 2004). However, the effect is reversible with addition of antioxidant, GSH (Brzezinska *et al.*, 2000). I therefore hypothesized that HF diet dependent

oxidative stress contributes to changes in SM excitability via altered β1BK channel function. Using intracellular recordings, I found out that while control diet fed mice had significantly hyperpolarized SM membrane potential and fired action potentials in bursts, HF mice showed depolarized membrane potential and fired action potential continuously. Previous study done in our lab has shown that β1BK KO mice are constipated (France *et al.*, 2012) and exhibit depolarized RMP and continuous action potential firing similar to WT HF mice. This suggests that HF diet might alter SM excitability in such a way that the HF tissues behaves as β1BK KO. Since HF diet has also been associated with lower NO availability I tested to see if NO availability contributes to colonic SM excitability. I found out that application of NLA in control diet fed mice depolarized the resting membrane potential of colonic SM (by ~3-5 mV) and increased action potential firing. This caused control mice to behave as HF. Application of SNP to tissues from HF fed mice hyperpolarized SMCs in a reversible manner. This results suggests that NO modulates SM excitability. Continuous action potential firing in colonic SMCs from HF fed mice are possibly due to loss of NO availability leading to subsequent SM depolarization and increased SM excitability. I repeated these experiment in β1BK KO mice to test if loss of the β1 subunit is sufficient to increase SMC excitability. Although I did not see any diet dependent difference (action potential firing were continuous in both cases), application of SNP restored bursting like action potential firing in β1BK KO. I also observed that in β1BK KO HF tissues, the number of action potentials that remained after SNP application were greater compared to control tissues suggesting greater excitability in these tissues compared to WT. These results are similar to studies carried in rat hippocampus where application of SNP restored the activity of BK channels in the NO deficient neurons caused by intermittent hypoxia (Tjong *et al.*, 2008) suggesting that although that NO and β1BK channel share a common pathway to modulate the

SM excitability, application of NO is sufficient to reverse the changes caused by abnormal BK channel function.

To assess if alterations in NO dependent neurogenic relaxation and impairment in SM excitability leads to disrupted colonic motility *in-vitro*, I measured CMMC activities in WT and β1BK KO mice fed a control and a HF diet. CMMCs are waves of contractile activity that occurs at regular interval in fasting state. I found that the velocity, directionality and the force of contraction were all disrupted in WT HF fed mice and β1BK KO (irrespective of diet) compared to WT control. Application of NLA disrupted the frequency, the tone, and the directionality of the contraction in both controls and HF WT mice suggesting that loss of endogenous NO in WT HF mice disrupts *in-vitro* motility (Powell & Bywater, 2001). The changes that I saw in CMMC activity in WT and β1BK KO mice correspond to changes in *in-vivo* colonic motility. This was evident by the fact that the fecal pellet output in WT mice was significantly greater than β1BK KOs. Among WTs, mice placed on HF diet had greater fecal output than controls while no such difference was observed among β1BK KO.

NO is involved in rapid anterograde trafficking of β1 subunit from the endosomes to the cell membrane and helps β1 subunit to associate with BKα subunit elevating channel Ca^{2+} sensitivity in myocytes and inducing vasodilation in vascular SMCs (Leo *et al.*, 2014). Since I have shown that NO levels are lower in HF mice, it is possible that mechanisms that lead to the trafficking of β1 subunit to cell membrane are disrupted leading to disruptions in SMC excitability. Besides this, decreased BK channel β1/α subunit ratio, and altered Ca^{2+} spark generation has been observed in cerebral arteries of *db/db* mice (Rueda *et al.*, 2013). I therefore hypothesized that HF diet dependent oxidative stress and lower NO availability leads to changes in β1 subunit protein expression of BK channel ultimately causing altered colonic SM

excitability. Although I showed no change in expression of the BK α-subunit, I was unable to study the expression of β1subunit using western blot analysis due to the lack of specificity in commercially available antibodies for β1subunit (Bhattarai *et al.*, 2014). I did not find any diet-induced changes in β1subunit gene expression using rt-PCR. This suggests that if there is any diet dependent changes that occurs in β1subunit, they are downstream of mRNA transcription (i.e. disruptions in β1 trafficking, changes in post translational modification). These studies indicate that HF diet alters colonic motility via oxidative stress induced loss of NO motor neurons, and by causing changes in SM excitability. Although the results of this study insinuate that β1BK channel might play a crucial role in modulating these changes, measurement of β1BK protein expression is necessary to conclusively validate this point.

BIBLIOGRAPHY

BIBLIOGRAPHY

Bagyánszki M & Bódi N. (2012). Diabetes-related alterations in the enteric nervous system and its microenvironment. *World J Diabetes* **3,** 80-93.

Bagyánszki M, Román V & Fekete E. (2000). Quantitative distribution of NADPH-diaphorase-positive myenteric neurons in different segments of the developing chicken small intestine and colon. *Histochem J* **32,** 679-684.

Beraldi EJ, Soares A, Borges SC, de Souza AC, Natali MR, Bazotte RB & Buttow NC. (2014). High-Fat Diet Promotes Neuronal Loss in the Myenteric Plexus of the Large Intestine in Mice. *Dig Dis Sci*.

Bhattarai Y, Fernandes R, Kadrofske MM, Lockwood LR, Galligan JJ & Xu H. (2014). Western blot analysis of BK channel β1-subunit expression should be interpreted cautiously when using commercially available antibodies. *Physiol Rep* **2**.

Brenner R, Peréz GJ, Bonev AD, Eckman DM, Kosek JC, Wiler SW, Patterson AJ, Nelson MT & Aldrich RW. (2000). Vasoregulation by the beta1 subunit of the calcium-activated potassium channel. *Nature* **407,** 870-876.

Brzezinska AK, Gebremedhin D, Chilian WM, Kalyanaraman B & Elliott SJ. (2000). Peroxynitrite reversibly inhibits Ca(2+)-activated K(+) channels in rat cerebral artery smooth muscle cells. *Am J Physiol Heart Circ Physiol* **278,** H1883-1890.

Bódi N, Battonyai I, Talapka P, Fekete E & Bagyánszki M. (2009). Spatial pattern analysis of nitrergic neurons in the myenteric plexus of the duodenum of different mammalian species. *Acta Biol Hung* **60,** 347-358.

Chandrasekharan B, Anitha M, Blatt R, Shahnavaz N, Kooby D, Staley C, Mwangi S, Jones DP, Sitaraman SV & Srinivasan S. (2011). Colonic motor dysfunction in human diabetes is associated with enteric neuronal loss and increased oxidative stress. *Neurogastroenterology and Motility* **23**.

Chandrasekharan B & Srinivasan S. (2007). Diabetes and the enteric nervous system. *Neurogastroenterol Motil* **19,** 951-960.

Colditz GA, Willett WC, Rotnitzky A & Manson JE. (1995). Weight gain as a risk factor for clinical diabetes mellitus in women. *Ann Intern Med* **122,** 481-486.

Cox DH & Aldrich RW. (2000). Role of the beta1 subunit in large-conductance Ca(2+)-activated K(+) channel gating energetics. Mechanisms of enhanced Ca(2+) sensitivity. *J Gen Physiol* **116,** 411-432.

Delgado-Aros S, Locke GR, Camilleri M, Talley NJ, Fett S, Zinsmeister AR & Melton LJ. (2004). Obesity is associated with increased risk of gastrointestinal symptoms: a population-based study. *Am J Gastroenterol* **99,** 1801-1806.

Evans JL, Goldfine ID, Maddux BA & Grodsky GM. (2002). Oxidative stress and stress-activated signaling pathways: a unifying hypothesis of type 2 diabetes. *Endocr Rev* **23,** 599-622.

Farag YMK & Gaballa MR. (2011). Diabesity: an overview of a rising epidemic. *Nephrology Dialysis Transplantation* **26,** 28-35.

France M, Bhattarai Y, Galligan JJ & Xu H. (2012). Impaired propulsive motility in the distal but not proximal colon of BK channel β1-subunit knockout mice. *Neurogastroenterol Motil* **24,** e450-459.

Gallego D, Gil V, Aleu J, Aulí M, Clavé P & Jiménez M. (2008). Purinergic and nitrergic junction potential in the human colon. *Am J Physiol Gastrointest Liver Physiol* **295,** G522-533.

George MJ & Shibata EF. (1995). Regulation of calcium-activated potassium channels by S-nitrosothiol compounds and cyclic guanosine monophosphate in rabbit coronary artery myocytes. *J Investig Med* **43,** 451-458.

Grasa L, Gil V, Gallego D, Martín MT & Jiménez M. (2009). P2Y(1) receptors mediate inhibitory neuromuscular transmission in the rat colon. *Br J Pharmacol* **158,** 1641-1652.

Heliövaara M, Mäkelä M, Impivaara O, Knekt P, Aromaa A & Sievers K. (1993). Association of overweight, trauma and workload with coxarthrosis. A health survey of 7,217 persons. *Acta Orthop Scand* **64,** 513-518.

Hess DT, Matsumoto A, Kim SO, Marshall HE & Stamler JS. (2005). Protein S-nitrosylation: purview and parameters. *Nat Rev Mol Cell Biol* **6,** 150-166.

Howitt L, Sandow SL, Grayson TH, Ellis ZE, Morris MJ & Murphy TV. (2011). Differential effects of diet-induced obesity on BKCa {beta}1-subunit expression and function in rat

skeletal muscle arterioles and small cerebral arteries. *Am J Physiol Heart Circ Physiol* **301,** H29-40.

Huang Z, Willett WC, Manson JE, Rosner B, Stampfer MJ, Speizer FE & Colditz GA. (1998). Body weight, weight change, and risk for hypertension in women. *Ann Intern Med* **128,** 81-88.

Jaffrey SR, Erdjument-Bromage H, Ferris CD, Tempst P & Snyder SH. (2001). Protein S-nitrosylation: a physiological signal for neuronal nitric oxide. *Nat Cell Biol* **3,** 193-197.

Kopelman PG. (2000). Obesity as a medical problem. *Nature* **404,** 635-643.

L'Heureux MC, Muinuddin A, Gaisano HY & Diamant NE. (2010). Nitric oxide activation of a potassium channel (BK(Ca)) in feline lower esophageal sphincter. *World J Gastroenterol* **16,** 5852-5860.

Leo MD, Bannister JP, Narayanan D, Nair A, Grubbs JE, Gabrick KS, Boop FA & Jaggar JH. (2014). Dynamic regulation of β1 subunit trafficking controls vascular contractility. *Proc Natl Acad Sci U S A* **111,** 2361-2366.

Mistry DK & Garland CJ. (1998). Nitric oxide (NO)-induced activation of large conductance Ca2+-dependent K+ channels (BK(Ca)) in smooth muscle cells isolated from the rat mesenteric artery. *Br J Pharmacol* **124,** 1131-1140.

Murphy MP, Packer MA, Scarlett JL & Martin SW. (1998). Peroxynitrite: a biologically significant oxidant. *Gen Pharmacol* **31,** 179-186.

Murr MM, Balsiger BM, Farrugia G & Sarr MG. (1999). Role of nitric oxide, vasoactive intestinal polypeptide, and ATP in inhibitory neurotransmission in human jejunum. *J Surg Res* **84,** 8-12.

Mushref MA & Srinivasan S. (2013). Effect of high fat-diet and obesity on gastrointestinal motility. *Ann Transl Med* **1,** 14.

Petkov GV, Bonev AD, Heppner TJ, Brenner R, Aldrich RW & Nelson MT. (2001). Beta1-subunit of the Ca2+-activated K+ channel regulates contractile activity of mouse urinary bladder smooth muscle. *J Physiol* **537,** 443-452.

Plüger S, Faulhaber J, Fürstenau M, Löhn M, Waldschütz R, Gollasch M, Haller H, Luft FC, Ehmke H & Pongs O. (2000). Mice with disrupted BK channel beta1 subunit gene feature

abnormal Ca(2+) spark/STOC coupling and elevated blood pressure. *Circ Res* **87,** E53-60.

Powell AK & Bywater RA. (2001). Endogenous nitric oxide release modulates the direction and frequency of colonic migrating motor complexes in the isolated mouse colon. *Neurogastroenterol Motil* **13,** 221-228.

Qian X & Magleby KL. (2003). Beta1 subunits facilitate gating of BK channels by acting through the Ca2+, but not the Mg2+, activating mechanisms. *Proc Natl Acad Sci U S A* **100,** 10061-10066.

Rivera LR, Poole DP, Thacker M & Furness JB. (2011). The involvement of nitric oxide synthase neurons in enteric neuropathies. *Neurogastroenterol Motil* **23,** 980-988.

Rueda A, Fernández-Velasco M, Benitah JP & Gómez AM. (2013). Abnormal Ca2+ spark/STOC coupling in cerebral artery smooth muscle cells of obese type 2 diabetic mice. *PLoS One* **8,** e53321.

Santarelli LC, Chen J, Heinemann SH & Hoshi T. (2004). The beta1 subunit enhances oxidative regulation of large-conductance calcium-activated K+ channels. *J Gen Physiol* **124,** 357-370.

Tang XD, Garcia ML, Heinemann SH & Hoshi T. (2004). Reactive oxygen species impair Slo1 BK channel function by altering cysteine-mediated calcium sensing. *Nat Struct Mol Biol* **11,** 171-178.

Tjong YW, Li M, Hung MW, Wang K & Fung ML. (2008). Nitric oxide deficit in chronic intermittent hypoxia impairs large conductance calcium-activated potassium channel activity in rat hippocampal neurons. *Free Radic Biol Med* **44,** 547-557.

Vergara C, Latorre R, Marrion NV & Adelman JP. (1998). Calcium-activated potassium channels. *Curr Opin Neurobiol* **8,** 321-329.

Voss U, Sand E, Olde B & Ekblad E. (2013). Enteric neuropathy can be induced by high fat diet in vivo and palmitic acid exposure in vitro. *PLoS One* **8,** e81413.

Voukali E, Shotton HR & Lincoln J. (2011). Selective responses of myenteric neurons to oxidative stress and diabetic stimuli. *Neurogastroenterol Motil* **23,** 964-e411.

Wan E, Kushner JS, Zakharov S, Nui XW, Chudasama N, Kelly C, Waase M, Doshi D, Liu G, Iwata S, Shiomi T, Katchman A, D'Armiento J, Homma S & Marx SO. (2013). Reduced vascular smooth muscle BK channel current underlies heart failure-induced vasoconstriction in mice. *FASEB J* **27,** 1859-1867.

Xing J & Chen JD. (2004). Alterations of gastrointestinal motility in obesity. *Obes Res* **12,** 1723-1732.

Xu H, Garver H, Fernandes R, Galligan JJ & Fink GD. (2014). Altered L-type Ca2+ channel activity contributes to exacerbated hypoperfusion and mortality in smooth muscle cell BK channel deficient septic mice. *Am J Physiol Regul Integr Comp Physiol*.

Xu H, Garver H, Galligan JJ & Fink GD. (2011). Large-conductance Ca2+-activated K+ channel beta1-subunit knockout mice are not hypertensive. *Am J Physiol Heart Circ Physiol* **300,** H476-485.

Xu H, Wang Y, Garver H, Galligan JJ & Fink GD. (2012). Vascular BK channel deficiency exacerbates organ damage and mortality in endotoxemic mice. *J Cardiovasc Pharmacol* **59,** 207-214.

Y Lee C. (2013). The Effect of High-Fat Diet-Induced Pathophysiological Changes in the Gut on Obesity: What Should be the Ideal Treatment? *Clin Transl Gastroenterol* **4,** e39.

Yang Y, Li PY, Cheng J, Mao L, Wen J, Tan XQ, Liu ZF & Zeng XR. (2013). Function of BKCa channels is reduced in human vascular smooth muscle cells from Han Chinese patients with hypertension. *Hypertension* **61,** 519-525.

CHAPTER 5

WESTERN BLOT ANALYSIS OF BK CHANNEL β1-SUBUNIT EXPRESSION SHOULD BE INTERPRETED CAUTIOUSLY WHEN USING COMMERCIALLY AVAILABLE ANTIBODIES

5.1 Abstract

Large conductance Ca^{2+} activated K^+ (BK) channels consist of pore forming α- and accessory β-subunits. There are 4 β-subunit subtypes (β1-β4), and the BK β1-subunit is specific for smooth muscle cells (SMC). Reduced BK β1-subunit expression is associated with SMC dysfunction in animal models of human disease, since down-regulation of BK β1-subunit reduces channel activity and increases SMC contractility. Several anti-BK β1-subunit antibodies are commercially available. However, the specificity and the sensitivity of most antibodies have not been tested or confirmed in the tissues from BK β1-subunit knockout (KO) mice. In this study, I tested the specificity and sensitivity of six commercially available antibodies from five manufacturers. I performed western blot analysis on BK β1-subunit enriched tissues (mesenteric arteries and colons) and non-SM tissue (cortex of kidney) from wild-type (WT) and BK β1-KO mice. I found that all tested antibodies lack specificity for BK β1-subunits in murine tissues. Antibodies either detected protein bands of the appropriate molecular weight in tissues from both WT and BK β1-KO mice, or failed to detect protein bands at the appropriate molecular weight in tissues from WT mice. The absence of BK β1-subunit mRNA expression in arteries, and colons from BK β1-KO mice was confirmed by RT-PCR analysis. I conclude that these commercially available antibodies are not reliable tools for studying BK β1-subunit expression in murine tissues. Data obtained using these antibodies should be interpreted cautiously. Developing a highly specific BK β1-subunit antibody is needed for future studies of BK channel murine models of human disease.

5.2 Introduction

BK (large conductance Ca^{2+}-activated K^{+}) channels are expressed in many mammalian cell types and BK channel activity is an important regulator of cell excitability. BK channels are composed of pore forming α-subunits and accessory β-subunits that modulate α-subunit Ca^{2+} sensitivity and channel activity (Nelson *et al.*, 1995; Brenner *et al.*, 2000b). There are 4 subtypes (β1-β4) of BK channel β-subunits. The BK β1-subunit is largely smooth muscle cell (SMC) specific, although it has been found in the distal nephron of murine kidney (Grimm *et al.*, 2007), BK β2- and β3-subunits are expressed in endocrine cells (Xia *et al.*, 1999; Braun *et al.*, 2008), while BK β4-subunits are expressed in neurons (Meera *et al.*, 2000) and in the distal nephron of the kidney (Grimm *et al.*, 2007). In SMCs, BK channels stabilize membrane potential and excitability through negative-feedback modulation. Activation of BK channels causes SMC hyperpolarization, L-type Ca^{2+} channel closure and SMC relaxation (Nelson *et al.*, 1995). Down-regulation of BK β1-subunit expression may contribute to human diseases including metabolic disorders (Zhang *et al.*, 2010a), hypertension (Yang *et al.*, 2013), heart failure (Wan *et al.*, 2013), asthma (Semenov *et al.*, 2011), maladaption of uteroplacental circulation (Hu *et al.*, 2012), urinary bladder over activity (Petkov *et al.*, 2001) and gastrointestinal motility disorders (France *et al.*, 2012). Down-regulation of BK β1-subunit expression reduces α-subunit Ca^{2+} sensitivity, therefore, causing SMC membrane depolarization and increased muscle contractility (Brenner *et al.*, 2000b; Plüger *et al.*, 2000; Xu *et al.*, 2011). BK β1-subunit expression in pathological situations is mainly affected by signaling at the post-transcriptional level where protein synthesis is reduced (Nelson *et al.*, 1995; Grimm *et al.*, 2009; Xu *et al.*, 2011; Shi *et al.*, 2013a; Shi *et al.*, 2013b) or protein degradation is accelerated (Zhang *et al.*, 2010a; Lu *et al.*,

2012). Therefore, accurate measurement of BK β1-subunit protein expression is crucial in studies of BK channel dysfunction in diseases.

The anti-BK β1-subunit antibodies used in published studies are either custom made (Lu *et al.*, 2012; Yi *et al.*, 2014) or purchased commercially. BK β1-subunit protein expression is typically measured using western blot analysis. Importantly, the specificity and sensitivity of commercially available BK β1-subunit antibodies has not been tested or confirmed in tissues from BK β1-subunit knockout (KO) mice, although BK β1-KO mice have been generated by two research groups (Brenner *et al.*, 2000b; Plüger *et al.*, 2000). BK β1-KO mice have been widely used as an animal model to study the contribution of BK channel dysfunction in hypertension (Grimm *et al.*, 2007; Xu *et al.*, 2011), septic shock (Xu *et al.*, 2012; Xu *et al.*, 2014), heart failure (Wan *et al.*, 2013), asthma (Evseev *et al.*, 2013), metabolic disorders (Lynch *et al.*, 2013), irritable bowel syndrome (France *et al.*, 2012) and urinary bladder over activity (Petkov *et al.*, 2001). Conclusions about the physiological significance of BK β1-subunits in health and disease have been based in part on studies in mice.

I used western blot analysis to test the specificity and sensitivity of six commercially available BK β1-subunit antibodies from five manufacturers in BK β1-subnuit enriched SM tissues (mesenteric arteries, MA, and colons) from wild-type (WT) and BK β1-KO mice (Brenner *et al.*, 2000b; Grimm *et al.*, 2007). I confirmed that BK β1-KO mice lack β1-subunit mRNA using RT-PCR analysis.

5.3 Materials and Methods

5.3.1 Ethics Statement

All studies were conducted in accordance with the National Institutes of Health Guide for the Care and Use of Laboratory Animals (NIH Publication No. 85-23, revised 1996) and approved by the Michigan State University Institutional Animal Care and Use Committee.

5.3.2 Animals

Homozygous breeder male and female BK β1-KO mice were a gift from Dr. Robert Brenner (University of Texas Health Science Center, San Antonio). BK β1-KO mice are congenic as a result of seven generations of inbreeding to the C57BL/6 line and maintained originally as homozygous lines at Michigan State University (Xu *et al.*, 2011; France *et al.*, 2012; Xu *et al.*, 2012; Xu *et al.*, 2014). Pups of BK β1-KO mice were weaned at 3 weeks. Age matched WT (C57BL/6) mice were purchased from Jackson Laboratories (Bar Harbor, Maine, USA). All mice were fed a normal diet. Mice used in our studies were at 20-24 weeks of age (male).

5.3.3 Western blot

Colons and MA from WT and BK β1-KO mice were homogenized and lysed with 1X lysis buffer (12.5 ml 0.5M Tris HCl, 20 ml 10% SDS, 10 ml Glycerol, 57.5 ml dH_2O) along with a protease inhibitor cocktail (P8340, Sigma), sodium fluoride (S7920, Sigma), and sodium orthovanadate (S6508, Sigma). Protein levels were quantified with Sigma's *Bicinchoninic* Assay (BCA1 and B9643). Samples were reduced with Laemmli Buffer (Bio-Rad 161-0737) and β-mercaptoethanol and boiled for 5 minutes at 95 - 100 °C. Protein (30-100 mg for MA and colons, 500 mg for kidney) were loaded on SDS-PAGE (10-12%) gel along with the full-range rainbow molecular weight marker (RPN800E, GE Healthcare); separated at 100-120 V with

Laemmli running buffer (6 g Tris base, 28.8 g glycine, 1 g SDS, 1L dH_20), and electrotransferred overnight at 30 V onto Nitrocellulose membranes (RPN68D, Amersham Hybond-ECL, USA) or PVDF (IPVH00010, Milipore, USA) overnight, or at 100 V for 1 hour, with transfer buffer (3 g Tris base, 14.4 g glycine, 200 ml methanol, 800 ml dH_2O). Ponceau S was used to verify efficient protein transfer. Samples were blocked for 1 hour at room temperature in 5% milk-TBS-T, 5% BSA-TBS-T, or 4% chicken ovalbumin-TBS-T.

I tested six commercially available BK β1-subunit antibodies from five manufacturers (Table 5.1).

Table 5.1 List of commercially available anti-BK β1-subunit antibodies. Reprinted from Physiological reports, Volume 2, Bhattarai et.al., Western blot analysis of BK channel β1-subunit expression should be interpreted cautiously when using commercially available antibodies, copyright (2014).

Manufacturer	Catalog #	Immunogen	MW (kDa)	Reactivity	Concentration	Secondary Ab
Alomone	APC-036	2-17	28	H, R, M	1:100-1000	Anti-Rabbit 1:2000 (sc-2313; 7074S)
Abcam	Ab3587	90-103	35	H, R, M	1:500	Anti-Rabbit 1:2000 (#7074S)
Pierce	PA1-924	90-103	28	H, R, M	1:100-1000	Anti-Rabbit 1:2000 (sc-2313; 7074S)
Pierce	PA5-28284	1-191	28	H, M	1:100-1000	Anti-Rabbit 1:2000 (sc-2313)
Santa Cruz	sc-14749	1-191	28	H, R, M	1:200	Anti-Goat 1:500 (sc-2056)
Biorbyt	orb-101774	10-80	21	H, R, M	1:100-500	Anti-Rabbit 1:2000 (sc-2313; 7074S)

MW, manufacturer recommended molecular weight; H, human; R, rat; M, mouse; sc-1213, donkey anti-rabbit IgG-conjugated to horseradish peroxidase, Santa Cruz Biotechnology; sc-2056, donkey anti-goat IgG-conjugated to horseradish peroxidase, Santa Cruz Biotechnology; 7074S, goat anti-rabbit IgG-conjugated to horseradish peroxidase, Cell Signaling.

I also tested an anti-BK α-subunit antibody (APC-107, anti-*KCa1.1*, 1:500, Alomone Labs) in protein extracts from colons and MA to confirm BK channel expression in these tissues. Protein loading and transfer were confirmed by re-blotting for β-actin (A228, Anti-β-Actin, 1:1000, Sigma) on each membrane after the BK β1-subunit antibody was stripped. Membranes were blotted overnight at 4°C or 2 hours at room temperature, with anti BK α- or β1-subunit primary antibodies used at the manufacturers' suggested dilutions and after primary antibody incubation with antigen peptide (1:100) overnight (Table 5.1). The following day membranes were washed 3 X 10 minute intervals with TBS-T, and blotted with the appropriate HRP-conjugated secondary antibodies (Table 5.1) for 1 hour at room temperature in blocking solution. Membranes were then washed with TBS-T for 3 X 10 minutes. Blots were imaged with Super Signal West Dura Extended Duration Substrate (34076, Pierce) using a LICOR-FC imager, or using the Enhanced Chemiluminescence (ECL) Plus Western Blotting Detection System (RPN2133, GE Healthcare).

5.3.4 Real time RT-PCR

Samples were collected and stored in All Protect Reagent (76405, Qiagen, USA) until ready to be processed. Total RNA was isolated with the MELT Total Nucleic Acid Isolation System kit (AM1983, Ambion, USA) following the manufacturer's instructions. RNA isolates were reverse-transcribed using High Capacity RNA to cDNA kits (4387406, Applied Biosystems, USA), following the manufacturer's protocols. As a control for genomic DNA contamination, all cDNA synthesis reactions were set up with additional samples lacking reverse transcriptase. Resultant cDNA was used for real-time PCR assays. Reactions (20 ml) were prepared with TaqMan Fast Advanced master mix (4444556, Applied Biosystems, USA) and inventoried with TaqMan Gene Expression assays (Mm00466621_m1 for KCNMB1,

Rn01775763_g1 for Gapdh, Applied Biosystems, USA). Samples were analyzed in duplicate. Real time RT-PCR products at 40 cycles were also determined by agarose gel analysis (1.5% TBE agarose gel at 100V for 1 hour).

5.4 Results

5.4.1 Western blots in MA and colons from WT and BK β1-KO mice

In SM tissues, APC-036 (Alomone Labs) and PA5-28284 (Thermo Scientific-Pierce) anti-BK β1-subunit antibodies detected protein bands at ~28 kDa (manufacturer suggested molecular weight of BK β1-subunit protein) in MA and colonic tissues from WT and BK β1-KO mice, (Figure 5.1A, 5.1B). Ab3587 (Abcam) anti-BK β1-subunit antibody detected a protein band at ~38 kDa (manufacturer's suggested molecular weight of BK β1-subnit protein) in MA and colons from WT and BK β1-KO mice (Figure 5.1C). Signals were blocked after pre-incubation of the Ab3587 antibody with its competing peptide (Ab5023) (Figure 5.1C). PA1-924 (Thermo Scientific-Pierce) anti-BK β1-subunit antibodies detected a protein band at ~40 kDa in MA and colons from WT and BK β1-KO mice, but not at ~28 kDa (manufacturer suggested molecular weight of BK β1-subunit protein) (Figure 5.1D). The sc-14749 (Santa Cruz Biotechnology) and Orb-101774 (Biorbyt) antibodies detected multiple protein bands in MA and colonic tissues from WT and BK β1-KO mice. However, none of these protein bands corresponded to a protein with a molecular weights of ~28 kDa or ~21 kDa (the manufacturer's suggested molecular weight of BK β1-subunit protein) in tissues from WT mice, even when gels were loaded with 80 mg of protein and incubated with high concentration of primary antibody (1:100) (Figure 5.1E, 5.1F). Protein loading and transfer were confirmed by β-actin immune blot (Figure 5.1E). I repeated sc-14749 and Orb-101774 immunoblotting using a variety of protocols (See Methods). Results obtained using modified approaches were similar to the results described above. Tissues from 6-8 animals were tested in each group.

Figure 5.1 Representative western blot obtained using commercially available anti-BK β1subunit antibodies. (A) Alomone Labs (APC-036), (B) Pierce (PA5-28284), and (C) Abcam (Ab3587) antibodies detected a protein band at ~28 kDa or ~38 kDa in colons or MA from both WT and BK β1-KO mice. The bands in Abcam sets were diminished after preincubation of the primary antibody with the competing peptide. (D) Pierce (PA1-924), (E) Santa Cruz (sc-14749), and (F) Biorbyt (orb-101774) antibodies did not detect any band at ~28 kDa or ~21 kDa in MA or colons from WT mice. Arrows indicate the manufacturer's recommended molecular weight of BK β1-subunit protein. Reprinted from Physiological reports, Volume 2, Bhattarai et.al., Western blot analysis of BK channel β1-subunit expression should be interpreted cautiously when using commercially available antibodies, copyright (2014).

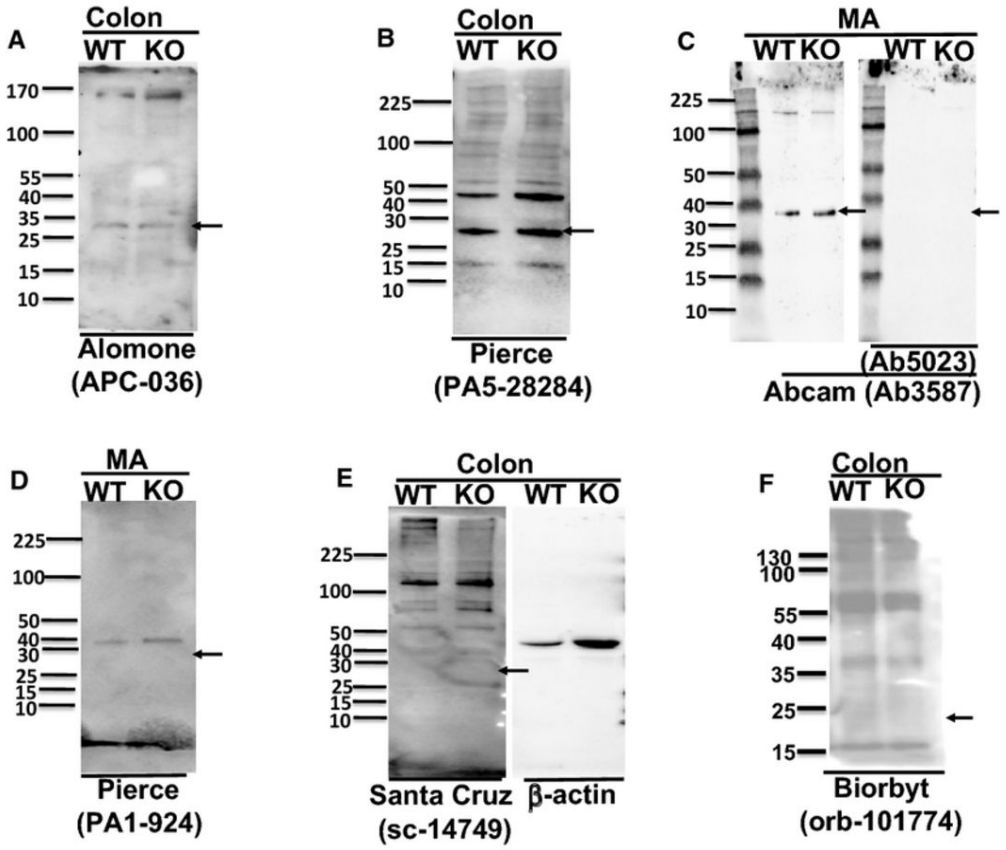

5.4.2 BK β1-subunit mRNA expression in tissues from BK β1-KO mice

To confirm the BK β1-subunit gene has been deleted in BK β1-KO mice, I measured expression of BK β1-subunit mRNA levels in MA and colons from WT and BK β1-KO mice using real time RT-PCR. After 40 PCR cycles, the Ct values of BK β1-subunit mRNA levels in MA and colon from WT mice were ~25 and ~24 respectively (Figure 5.2A, 5.2B) but BK β1-

subunit mRNA was undetectable in tissues from BK β1-KO mice (Figure 5.2C). Tissues from 6-8 animals were tested in each group.

Figure 5.2 Real-time RT-PCR analysis of BK β1-subunit and GAPDH in MA and colons from WT and BK β1-KO mice. (A and B) The expression threshold was set at 0.22 for amplification plots, a level above background fluorescence but within the linear phase of the amplification plot. The intersection between the threshold level and the amplification plot is the Ct value, which correlates with the amount of template in the sample. Ct values over 35 are excluded, as these values approach the sensitivity limits of the Taqman assay. (C) Agarose gel separation of RT-PCR products. Amplification of real-time RT-PCR products was seen at 75 bp in tissues from WT animals only. Reprinted from Physiological reports, Volume 2, Bhattarai et.al., Western blot analysis of BK channel β1-subunit expression should be interpreted cautiously when using commercially available antibodies, copyright (2014). Abbreviation: Con, non-template control.

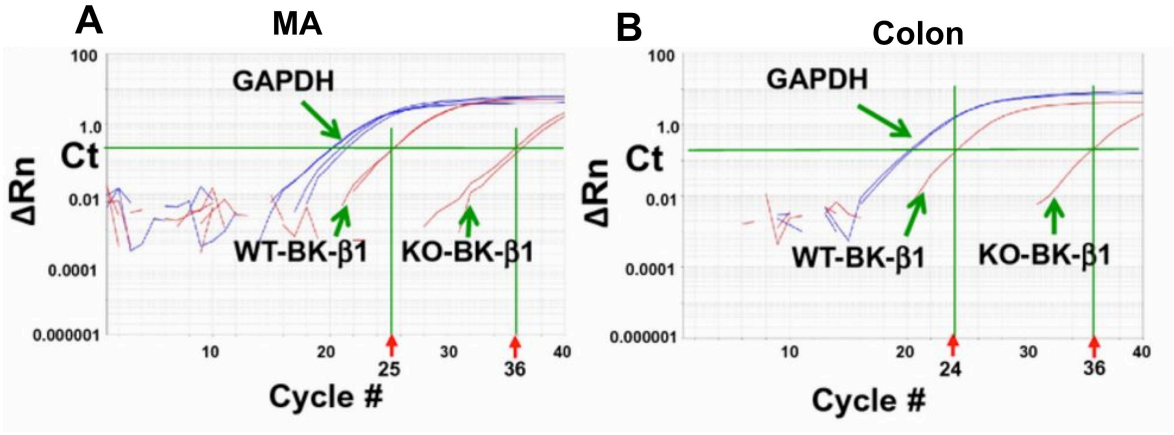

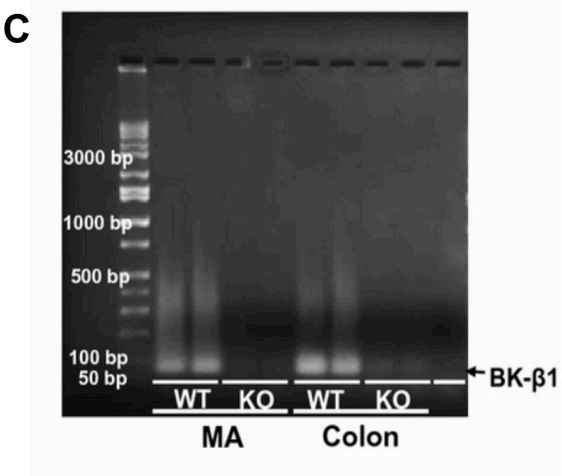

5.4.3 Expression of BK α-subunit in the colons

APC-107 anti BK α-subunit detected a protein band at ~100 kDa (manufacturer suggested molecular weight) in colonic tissues from WT and BK β1-KO mice. Western blot

signals were blocked after pre-incubation of the APC-107 antibody with its competing peptide (Figure 5.3).

Figure 5.3 BK α-subunit western blot in colonic tissues from WT and BK β1-KO mice. Antibody detected a protein band at ~100 kDa in all tissues from WT and BK β1-KO mice. The signals are blocked by pre-incubation with the antibody competing peptide (CP). Arrows indicate the manufacturer's recommended molecular weight of BK α-subunit protein. Reprinted from Physiological reports, Volume 2, Bhattarai et.al., Western blot analysis of BK channel β1-subunit expression should be interpreted cautiously when using commercially available antibodies, copyright (2014).

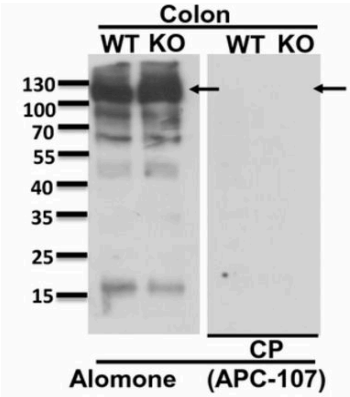

5.5 Discussion

I tested the specificity and sensitivity of commercially available BK β1-subunit antibodies using tissues from WT and BK β1-KO mice, and found that each antibody lacked specificity and the sensitivity for BK β1-subunit in BK β1-subunit enriched tissues from C57BL/6 mice. The antibodies evaluated in this paper have been used extensively in published work (Table 5.2). However, this study is the first to determine their specificity for detection of the BK β1-subunit using BK β1-subunit KO mice.

Table 5.2 Publications that performed BK β1-subunit western blot analysis using commercially available antibodies.

Antibody	References #	Model	Tissue Type	Reported MW	Used BK β1 KO mice
Alomone APC-037	(Zheng *et al.*, 2013),(Shi *et al.*, 2013a),(Zhang *et al.*, 2010a),(Shi *et al.*, 2013b),(Kunduri *et al.*, 2013),(Rueda *et al.*, 2013),(Pabbidi *et al.*, 2014)	H, R, M	Blood Vessel	24-28 kDa	NO
Abcam Ab-3587	(Leo *et al.*, 2014),(Nystoriak *et al.*, 2014), (Evanson *et al.*, 2014)	M	Blood Vessel	35-45	NO
Santa Cruz SC-14749	(Grimm *et al.*, 2007),(Ahn *et al.*, 2012), (Xie *et al.*, 2010),(Loot *et al.*, 2012),(Grimm *et al.*, 2009)	H, R, M	Blood Vessel, Adrenal Gland	22-28 kDa	Yes (Grimm *et al.*, 2007), (Loot *et al.*, 2012), (Grimm *et al.*, 2009)
Pierce, PA1-924	(Chang *et al.*, 2006),(Evseev *et al.*, 2013),(Yang *et al.*, 2013),(Albarwani *et al.*, 2010)	H, R, M	Blood Vessel, SMC from Tracheal	37 kDa	NO
Customer Made	(Yi *et al.*, 2014),(Lu *et al.*, 2012)	H, M	Blood Vessel	32kDa	NO
Merck	(Yang *et al.*, 2009),(Howitt *et al.*, 2011),(Matharoo-Ball *et al.*, 2003),	H, R	Blood vessel, Myometrium	32-36	NO

H, human; R, rat; M, mouse.

The BK β1-KO mice used in our study were generated by using a viral vector (pPNT) to completely delete exon 2 of gene 27, which also includes a transcriptional terminator after the lacZ gene to prevent downstream expression of β1-subunits (Brenner *et al.*, 2000b). Absence of BK β1-subunit expression in the BK β1-KO mice has been confirmed by RT-PCR previously (Brenner *et al.*, 2000b) and in this study. BK β1-subunit specific antibodies should identify a protein band with a molecular weight of 21 - 35 kDa (depending on the supplier's recommended molecular weight) in BK β1-subunit enriched tissues obtained from WT mice. BK β1-subunit protein expression should either be absent, or it would be detected as a truncated lower molecular weight protein in tissues from BK β1-KO mice, if the terminator is not fully functional, and the immunogenic site for each antibody was expressed. However, all tested antibodies either failed to detect proteins at the appropriate molecular weight in tissues from WT mice, or the antibodies detected identical protein bands in tissues from WT and BK β1-KO mice. These results suggest that the proteins detected by these antibodies are not specific for the BK β1-subunit; even though some of bands could be blocked by pre-incubation of the primary antibodies with its competing peptide.

I tested six antibodies not only in BK β1-subunit specific SM tissues (arteries and colons), but also tested in kidneys, a BK β1-subunit enriched non-SM tissue (Grimm *et al.*, 2007). Results from all tissues indicate that none of antibodies can reliably detect the BK β1-subunit. I confirmed protein loading and transfer performance on these blots by detection of β-actin on the same membrane. I also reliably detected the BK a-subunit protein in these tissues by western blot. Finally I confirmed BK β1-subunit gene deletion in the BK β1-KO mice using real time RT-PCR on the same tissue samples used for western blot analysis.

Two groups previously western blot data using the sc-14749 antibody in tissues from BK β1-KO mice. Loot et al. studied BK β1-subunit expression in cultured pulmonary arterial SMCs from WT and BK β1-KO mice (Loot *et al.*, 2012). However, the mouse strain used to generate the BK β1-KO mice used in their study differs from ours (Brenner *et al.*, 2000b; Plüger *et al.*, 2000). Those BK β1-KI mice were generated on B6CBAF1/J (female) and deleted exon 1 of BK β1-subunit gene. In addition, the protein bands obtained from extracts of SMCs from WT mice were not well resolved, and molecular weight of the protein detected was lower than the manufacturer's recommendation (<25 kDa). Grimm et al. reported a ~28 kDa protein band in extracts from kidney cortex and adrenal glands from WT mice, which was absent in tissues from BK β1-KO mice (Grimm *et al.*, 2007; Grimm *et al.*, 2009). The BK β1-KO mice used in this study were generated from the same mouse strain used in our studies. When I used the Sc-14749 antibody I failed to detect a protein band at the predicted molecular weight (~28 kDa) in protein extracts from MA or colons from WT mice.

Studies have been done using custom-made antibodies (Lu *et al.*, 2012; Yi *et al.*, 2014) or an antibody produced by the Merck pharmaceutical company (Matharoo-Ball *et al.*, 2003; Yang *et al.*, 2009; Howitt *et al.*, 2011) (also see Table 5.2). The antibody from Merck is no longer available and I was unable to test this antibody.

My data indicate that several commercially available BK β1-subunit antibodies lack specificity and sensitivity in western blot protocols. Data obtained using these reagents should be interpreted cautiously. There is a continuing need for the development of specific and sensitive BK β1-subunit antibodies for studies of BK channel expression and function (Bhattarai *et al.*, 2014).

BIBLIOGRAPHY

BIBLIOGRAPHY

Ahn YT, Kim YM, Adams E, Lyu SC, Alvira CM & Cornfield DN. (2012). Hypoxia-inducible factor-1α regulates KCNMB1 expression in human pulmonary artery smooth muscle cells. *Am J Physiol Lung Cell Mol Physiol* **302,** L352-359.

Albarwani S, Al-Siyabi S, Baomar H & Hassan MO. (2010). Exercise training attenuates ageing-induced BKCa channel downregulation in rat coronary arteries. *Exp Physiol* **95,** 746-755.

Bhattarai Y, Fernandes R, Kadrofske MM, Lockwood LR, Galligan JJ & Xu H. (2014). Western blot analysis of BK channel β1-subunit expression should be interpreted cautiously when using commercially available antibodies. *Physiol Rep* **2**.

Braun M, Ramracheya R, Bengtsson M, Zhang Q, Karanauskaite J, Partridge C, Johnson PR & Rorsman P. (2008). Voltage-gated ion channels in human pancreatic beta-cells: electrophysiological characterization and role in insulin secretion. *Diabetes* **57,** 1618-1628.

Brenner R, Peréz GJ, Bonev AD, Eckman DM, Kosek JC, Wiler SW, Patterson AJ, Nelson MT & Aldrich RW. (2000). Vasoregulation by the beta1 subunit of the calcium-activated potassium channel. *Nature* **407,** 870-876.

Chang T, Wu L & Wang R. (2006). Altered expression of BK channel beta1 subunit in vascular tissues from spontaneously hypertensive rats. *Am J Hypertens* **19,** 678-685.

Evanson K, Bannister JP, Leo MD & Jaggar JH. (2014). LRRC26 is a Functional BK Channel Auxiliary γ Subunit in Arterial Smooth Muscle Cells. *Circ Res*.

Evseev AI, Semenov I, Archer CR, Medina JL, Dube PH, Shapiro MS & Brenner R. (2013). Functional effects of KCNQ K(+) channels in airway smooth muscle. *Front Physiol* **4,** 277.

France M, Bhattarai Y, Galligan JJ & Xu H. (2012). Impaired propulsive motility in the distal but not proximal colon of BK channel β1-subunit knockout mice. *Neurogastroenterol Motil* **24,** e450-459.

Grimm PR, Foutz RM, Brenner R & Sansom SC. (2007). Identification and localization of BK-beta subunits in the distal nephron of the mouse kidney. *Am J Physiol Renal Physiol* **293,** F350-359.

Grimm PR, Irsik DL, Settles DC, Holtzclaw JD & Sansom SC. (2009). Hypertension of Kcnmb1-/- is linked to deficient K secretion and aldosteronism. *Proc Natl Acad Sci U S A* **106,** 11800-11805.

Howitt L, Sandow SL, Grayson TH, Ellis ZE, Morris MJ & Murphy TV. (2011). Differential effects of diet-induced obesity on BKCa {beta}1-subunit expression and function in rat skeletal muscle arterioles and small cerebral arteries. *Am J Physiol Heart Circ Physiol* **301,** H29-40.

Hu XQ, Xiao D, Zhu R, Huang X, Yang S, Wilson SM & Zhang L. (2012). Chronic hypoxia suppresses pregnancy-induced upregulation of large-conductance Ca2+-activated K+ channel activity in uterine arteries. *Hypertension* **60,** 214-222.

Kunduri S, Dick G, Nayeem M & Mustafa S. (2013). Adenosine A1 receptor signaling inhibits BK channels through a PKCα-dependent mechanism in mouse aortic smooth muscle. *Physiol Rep* **1**.

Leo MD, Bannister JP, Narayanan D, Nair A, Grubbs JE, Gabrick KS, Boop FA & Jaggar JH. (2014). Dynamic regulation of β1 subunit trafficking controls vascular contractility. *Proc Natl Acad Sci U S A* **111,** 2361-2366.

Loot AE, Moneke I, Keserü B, Oelze M, Syzonenko T, Daiber A & Fleming I. (2012). 11,12-EET stimulates the association of BK channel α and β(1) subunits in mitochondria to induce pulmonary vasoconstriction. *PLoS One* **7,** e46065.

Lu T, Chai Q, Yu L, d'Uscio LV, Katusic ZS, He T & Lee HC. (2012). Reactive oxygen species signaling facilitates FOXO-3a/FBXO-dependent vascular BK channel β1 subunit degradation in diabetic mice. *Diabetes* **61,** 1860-1868.

Lynch FM, Withers SB, Yao Z, Werner ME, Edwards G, Weston AH & Heagerty AM. (2013). Perivascular adipose tissue-derived adiponectin activates BK(Ca) channels to induce anticontractile responses. *Am J Physiol Heart Circ Physiol* **304,** H786-795.

Matharoo-Ball B, Ashford ML, Arulkumaran S & Khan RN. (2003). Down-regulation of the alpha- and beta-subunits of the calcium-activated potassium channel in human myometrium with parturition. *Biol Reprod* **68,** 2135-2141.

Meera P, Wallner M & Toro L. (2000). A neuronal beta subunit (KCNMB4) makes the large conductance, voltage- and Ca2+-activated K+ channel resistant to charybdotoxin and iberiotoxin. *Proc Natl Acad Sci U S A* **97,** 5562-5567.

Nelson MT, Cheng H, Rubart M, Santana LF, Bonev AD, Knot HJ & Lederer WJ. (1995). Relaxation of arterial smooth muscle by calcium sparks. *Science* **270,** 633-637.

Nystoriak MA, Nieves-Cintrón M, Nygren PJ, Hinke SA, Nichols CB, Chen CY, Puglisi JL, Izu LT, Bers DM, Dell'acqua ML, Scott JD, Santana LF & Navedo MF. (2014). AKAP150 contributes to enhanced vascular tone by facilitating large-conductance Ca2+-activated K+ channel remodeling in hyperglycemia and diabetes mellitus. *Circ Res* **114,** 607-615.

Pabbidi MR, Mazur O, Fan F, Farley JM, Gebremedhin D, Harder DR & Roman RJ. (2014). Enhanced large conductance K+ channel activity contributes to the impaired myogenic response in the cerebral vasculature of Fawn Hooded Hypertensive rats. *Am J Physiol Heart Circ Physiol* **306,** H989-H1000.

Petkov GV, Bonev AD, Heppner TJ, Brenner R, Aldrich RW & Nelson MT. (2001). Beta1-subunit of the Ca2+-activated K+ channel regulates contractile activity of mouse urinary bladder smooth muscle. *J Physiol* **537,** 443-452.

Plüger S, Faulhaber J, Fürstenau M, Löhn M, Waldschütz R, Gollasch M, Haller H, Luft FC, Ehmke H & Pongs O. (2000). Mice with disrupted BK channel beta1 subunit gene feature abnormal Ca(2+) spark/STOC coupling and elevated blood pressure. *Circ Res* **87,** E53-60.

Rueda A, Fernández-Velasco M, Benitah JP & Gómez AM. (2013). Abnormal Ca2+ spark/STOC coupling in cerebral artery smooth muscle cells of obese type 2 diabetic mice. *PLoS One* **8,** e53321.

Semenov I, Wang B, Herlihy JT & Brenner R. (2011). BK channel β1 subunits regulate airway contraction secondary to M2 muscarinic acetylcholine receptor mediated depolarization. *J Physiol* **589,** 1803-1817.

Shi L, Liu B, Li N, Xue Z & Liu X. (2013a). Aerobic exercise increases BK(Ca) channel contribution to regulation of mesenteric arterial tone by upregulating β1-subunit. *Exp Physiol* **98,** 326-336.

Shi L, Liu X, Li N, Liu B & Liu Y. (2013b). Aging decreases the contribution of MaxiK channel in regulating vascular tone in mesenteric artery by unparallel downregulation of α- and β1-subunit expression. *Mech Ageing Dev* **134,** 416-425.

Wan E, Kushner JS, Zakharov S, Nui XW, Chudasama N, Kelly C, Waase M, Doshi D, Liu G, Iwata S, Shiomi T, Katchman A, D'Armiento J, Homma S & Marx SO. (2013). Reduced vascular smooth muscle BK channel current underlies heart failure-induced vasoconstriction in mice. *FASEB J* **27,** 1859-1867.

Xia XM, Ding JP & Lingle CJ. (1999). Molecular basis for the inactivation of Ca2+- and voltage-dependent BK channels in adrenal chromaffin cells and rat insulinoma tumor cells. *J Neurosci* **19,** 5255-5264.

Xie MJ, Ma YG, Gao F, Bai YG, Cheng JH, Chang YM, Yu ZB & Ma J. (2010). Activation of BKCa channel is associated with increased apoptosis of cerebrovascular smooth muscle cells in simulated microgravity rats. *Am J Physiol Cell Physiol* **298,** C1489-1500.

Xu H, Garver H, Fernandes R, Galligan JJ & Fink GD. (2014). Altered L-type Ca2+ channel activity contributes to exacerbated hypoperfusion and mortality in smooth muscle cell BK channel deficient septic mice. *Am J Physiol Regul Integr Comp Physiol*.

Xu H, Garver H, Galligan JJ & Fink GD. (2011). Large-conductance Ca2+-activated K+ channel beta1-subunit knockout mice are not hypertensive. *Am J Physiol Heart Circ Physiol* **300,** H476-485.

Xu H, Wang Y, Garver H, Galligan JJ & Fink GD. (2012). Vascular BK channel deficiency exacerbates organ damage and mortality in endotoxemic mice. *J Cardiovasc Pharmacol* **59,** 207-214.

Yang Y, Li PY, Cheng J, Mao L, Wen J, Tan XQ, Liu ZF & Zeng XR. (2013). Function of BKCa channels is reduced in human vascular smooth muscle cells from Han Chinese patients with hypertension. *Hypertension* **61,** 519-525.

Yang Y, Murphy TV, Ella SR, Grayson TH, Haddock R, Hwang YT, Braun AP, Peichun G, Korthuis RJ, Davis MJ & Hill MA. (2009). Heterogeneity in function of small artery smooth muscle BKCa: involvement of the beta1-subunit. *J Physiol* **587,** 3025-3044.

Yi F, Wang H, Chai Q, Wang X, Shen WK, Willis MS, Lee HC & Lu T. (2014). Regulation of Large Conductance Ca2+-activated K+ (BK) Channel β1 Subunit Expression by Muscle RING Finger Protein 1 in Diabetic Vessels. *J Biol Chem* **289,** 10853-10864.

Zhang DM, He T, Katusic ZS, Lee HC & Lu T. (2010). Muscle-specific f-box only proteins facilitate bk channel β(1) subunit downregulation in vascular smooth muscle cells of diabetes mellitus. *Circ Res* **107,** 1454-1459.

Zheng YM, Park SW, Stokes L, Tang Q, Xiao JH & Wang YX. (2013). Distinct activity of BK channel β1-subunit in cerebral and pulmonary artery smooth muscle cells. *Am J Physiol Cell Physiol* **304,** C780-789.

CHAPTER 6

KEY FINDINGS, SIGNIFICANCE AND FUTURE DIRECTIONS

Key findings

In the first part of my dissertation I advanced the field by identifying neurotransmitters, receptors, and ion channels involved in mediating IJPs in the mouse distal colon. I found that ATP and NO ultimately act on SK channels and CaCCs to mediate inhibitory neuromuscular transmission in the mouse distal colon. The opposing effect of K^+ and Cl^- ion regulates both the IJP and the membrane potential of the smooth muscle.

Figure 6.1 Mechanism of IJP production in the mouse distal colon. ATP acts on GQ coupled P2Y1 receptors to increase intracellular Ca^{2+}concentration $[Ca^{2+}{}_i]$ while NO mediates PKG activation. Increase in $[Ca^{2+}{}_i]$ and PKG activation causes opening of SK channels and closure of CaCCs to produce IJPs.

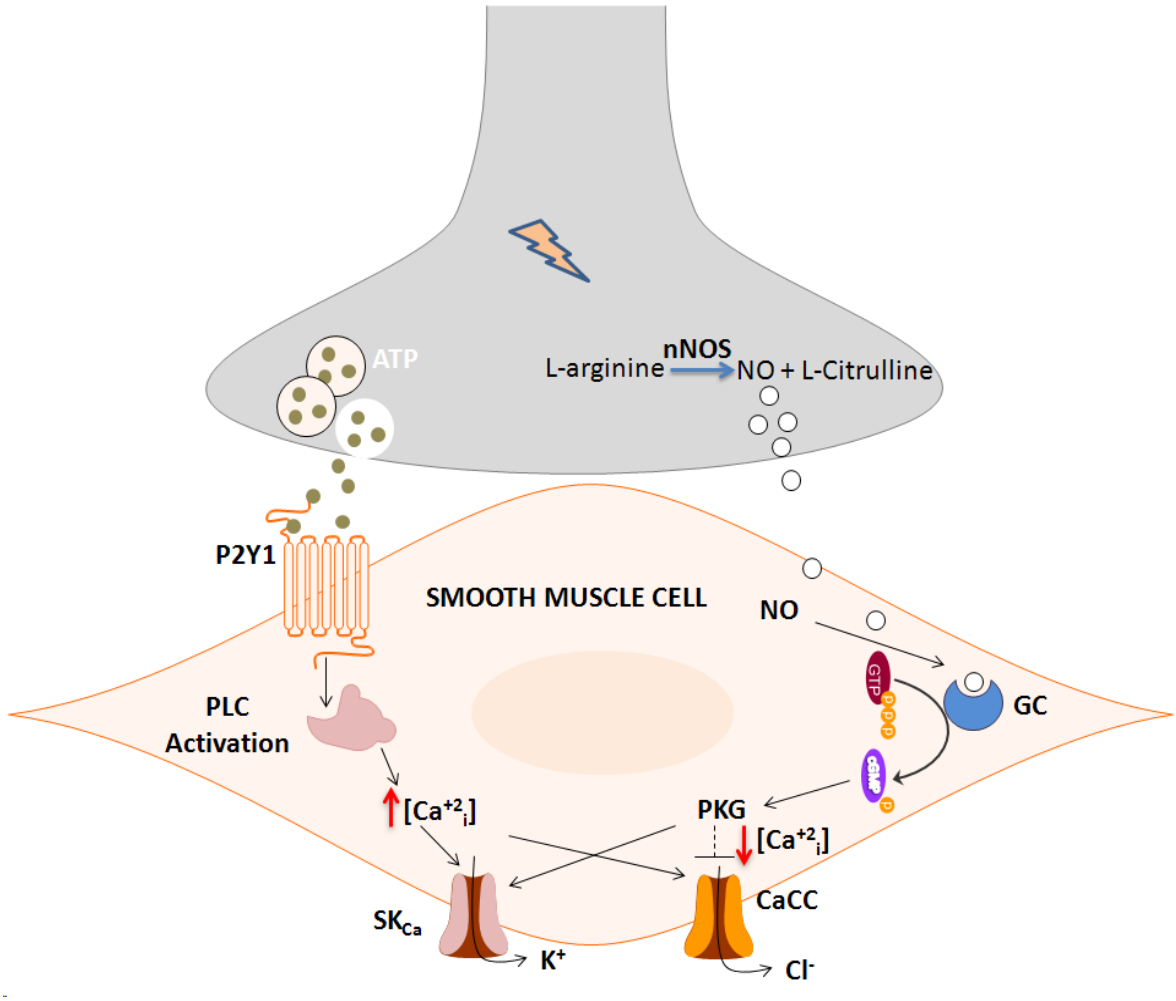

In the second part of the study, I found that β1BK channel regulates the RMP and the action potential firing in the mouse distal colon. Disruption or genetic manipulation leading to loss of β1 subunit increases smooth muscle excitability and impairs colonic motility (France *et al.*, 2012).

Figure 6.2 Regulation of colonic smooth muscle excitability via β1BK channel function. Depolarizing stimulus in the smooth muscle activate voltage gated Ca^{2+} channels. (1) Influx of Ca^{2+} into the cell and efflux of K^+ from the cell causes smooth muscle action potential generation. Continuous influx of Ca^{2+} in the cell activates ryanodine receptors in the SER to produce Ca^{2+} sparks thereby increasing subplasmalemmal Ca^{2+} concentration above ≥ 1μM. Such increase in Ca^{2+} concentration activates β1BK channels. (3) β1BK channels activation causes quick efflux of K^+ out of the cell causing membrane hyperpolarization. Membrane hyperpolarization leads to closure of voltage gated Ca^{2+} channels and abolishes action potential generation causing cessation of burst in WT DC.

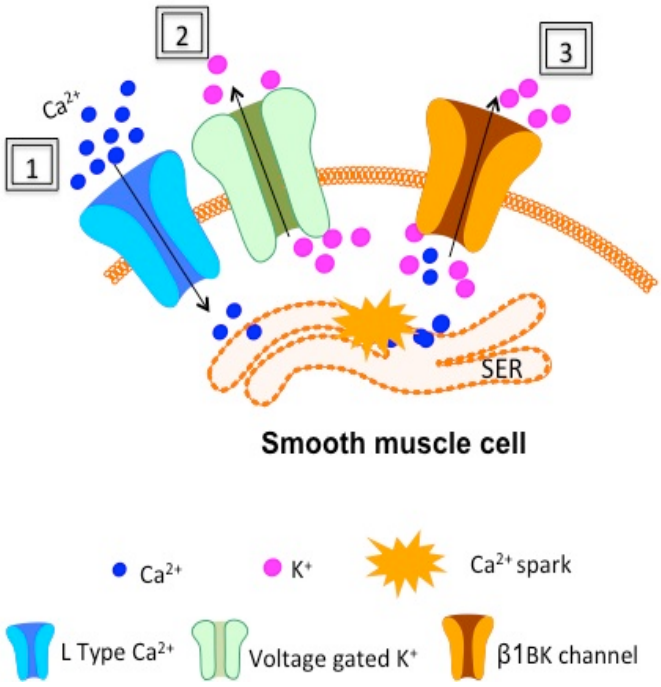

In the third part of my dissertation I investigated in detail the etiology of colonic dysmotility caused by HF diet. I found that HF diet causes oxidative stress, loss of inhibitory NOS neurons, and decreases basal NO availability in the mouse colonic myenteric ganglia. This causes disruption in neuromuscular transmission, impairment in colonic smooth muscle relaxation and alterations in colonic smooth muscle excitability. NOS neuron loss in HF fed mice alters mouse colonic smooth muscle excitability in such a way that it recapitulates changes in smooth muscle excitability seen in β1BK KO mice. This suggests that HF diet might affect β1BK channel function. However, I could not detect whether β1 subunit expression is down regulated in HF diet fed mice due to lack of commercially available β1 subunit specific antibodies. Figure below summarizes the details of the investigation.

Figure 6.3 Mechanisms of colonic dysmotility due to HF diet consumption. Dotted line indicates that β1BK channel function/expression might be altered in HF diet fed mice.

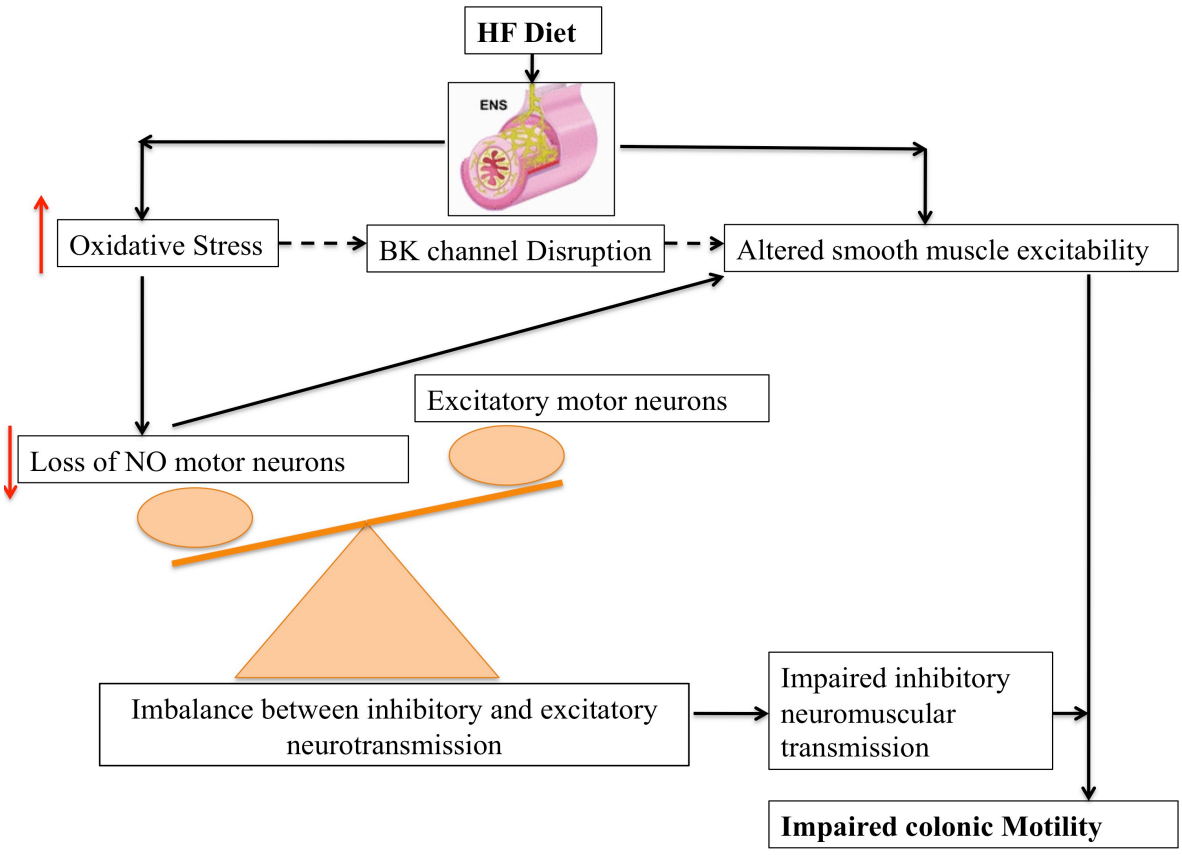

Significance

My study provides a comprehensive overview how IJPs are regulated in the mouse distal colon. Using a novel ectoneuclotidase, POM-1, I verified that ATP is the primary neurotransmitter involved in mediating IJP. My study also suggests that development of drugs that target CaCCs could benefit patients with impaired colonic motility.

My study demonstrates that β1BK channels and NO regulate smooth muscle excitability by regulating the RMP and action potential firing activity in the mouse distal colon. I show HF diet causes oxidative stress induced loss of NOS neurons and lower NO availability in mouse colonic myenteric ganglia. Loss of NOS neurons contributes to impaired inhibitory neuromuscular transmission, disrupted smooth muscle relaxation and alterations in smooth muscle excitability. This suggests that antioxidants or drugs that target the NO synthesis pathway might have beneficial effects on patients with colonic motility complications. I also show that disruption in smooth muscle relaxation, electrical activity and colonic dysmotility seen in HF fed mice is similar to β1BK KO mice. These results suggest that β1BK KO mice could serve as an excellent model for testing of prokinetic drugs for obese patients with altered colonic motility.

Finally, my study cautions investigators to use appropriate positive and negative controls when using commercially available antibodies in western blot experiments to avoid erroneous conclusion. I highlight that identifying protein bands at manufacturers recommended molecular weight and using blocking peptide is not sufficient to conclude that a protein of interest has been detected. Using β1BK KO mice I emphasized that, appropriate negative control such as a KO animal models must be used to test the specificity of the commercially available antibodies. This is especially important in study of diseases where altered protein expression might have a pronounced effect.

Future directions

In the first part of the dissertation, I concluded that the CaCCs and the SK channels mediate inhibitory neuromuscular communication and smooth muscle RMP in the mouse distal colon. These conclusions are based on results obtained from electrophysiolgical studies where pharmacologic application of apamin and NFA blocked IJPs and disrupted the RMP in the colonic smooth muscles. Although NFA is a CaCC blocker, some studies suggests that it also blocks nonspecific cation channels (Gögelein *et al.*, 1990), L type Ca^{2+} channels (Doughty *et al.*, 1998) and can activate Ca^{2+} activated K^{+} channels (Toma *et al.*, 1996; Cruickshank *et al.*, 2003). Thus it is possible that results obtained from NFA could be due to an indirect effect on cation or Ca^{2+} activated K^{+} channels. It would therefore be necessary to see how modulation of extracellular Cl^{-} concentration in the presence of NFA impacts the IJPs and the membrane potential of the colonic smooth muscle in order to verify that disruption in IJPs and the RMP are due to closure of CaCCs.

My studies show that HF diet causes oxidative stress concomitant with nNOS neuron loss, disrupted neuromuscular communication and altered smooth muscle excitability. However, it is important to investigate if feeding HF mice with antioxidants can reverse NO neuron loss and disrupted neuromuscular transmission to conclusively verify if oxidative stress causes NO neuron loss. It would also be interesting to investigate whether neuromuscular transmission and smooth muscle excitability in nNOS KO mice replicates our HF mice model. Besides smooth muscle, NO also acts on interstitial cells of Cajal (ICC) to modulate IJPs (Lies *et al.*, 2014). Therefore, it is possible that disruptions in function/expression of the ICCs, but not the NOS neurons causes impairment in neuromuscular transmission seen in HF mice. One way to tackle this issue is by measuring Anoctamin-1 (Ano1, ICC specific CaCCs protein) protein expression and by recording IJPs from HF mice in presence of NFA.

Lastly, most of my conclusions on the role of β1BK channels are based on electrophysiological studies. These data needs to be verified using proper expression studies such as rt-PCR and western blot before important conclusions can be drawn. Continued development and exploration of β1BK antibodies for studies of β1BK channel expression and function is therefore crucial.

BIBLIOGRAPHY

BIBLIOGRAPHY

Cruickshank SF, Baxter LM & Drummond RM. (2003). The Cl(-) channel blocker niflumic acid releases Ca(2+) from an intracellular store in rat pulmonary artery smooth muscle cells. *Br J Pharmacol* **140,** 1442-1450.

Doughty JM, Miller AL & Langton PD. (1998). Non-specificity of chloride channel blockers in rat cerebral arteries: block of the L-type calcium channel. *J Physiol* **507 (Pt 2),** 433-439.

France M, Bhattarai Y, Galligan JJ & Xu H. (2012). Impaired propulsive motility in the distal but not proximal colon of BK channel β1-subunit knockout mice. *Neurogastroenterol Motil* **24,** e450-459.

Gögelein H, Dahlem D, Englert HC & Lang HJ. (1990). Flufenamic acid, mefenamic acid and niflumic acid inhibit single nonselective cation channels in the rat exocrine pancreas. *FEBS Lett* **268,** 79-82.

Lies B, Gil V, Groneberg D, Seidler B, Saur D, Wischmeyer E, Jiménez M & Friebe A. (2014). Interstitial cells of Cajal mediate nitrergic inhibitory neurotransmission in the murine gastrointestinal tract. *Am J Physiol Gastrointest Liver Physiol* **307,** G98-106.

Toma C, Greenwood IA, Helliwell RM & Large WA. (1996). Activation of potassium currents by inhibitors of calcium-activated chloride conductance in rabbit portal vein smooth muscle cells. *Br J Pharmacol* **118,** 513-520.